Forschungszentrum Karlsruhe
in der Helmholtz-Gemeinschaft

Wissenschaftliche Berichte
FZKA 7285

Analysis of the Molecular Basis Underlying Signal-regulated Splicing via the RNA-binding Protein Sam68

A. Tisserant

Institut für Toxikologie und Genetik

Januar 2007

Forschungszentrum Karlsruhe
in der Helmholtz-Gemeinschaft
Wissenschaftliche Berichte
FZKA 7285

Analysis of the molecular basis underlying signal-regulated splicing via the RNA-binding protein Sam68

Anne Tisserant
Institut für Toxikologie und Genetik

Von der Fakultät für Chemie und Biowissenschaften
der Universität Karlsruhe (TH)
genehmigte Dissertation

Forschungszentrum Karlsruhe GmbH, Karlsruhe
2007

Forschungszentrum Karlsruhe GmbH
Postfach 3640, 76021 Karlsruhe

Mitglied der Hermann von Helmholtz-Gemeinschaft
Deutscher Forschungszentren (HGF)

ISSN 0947-8620

urn:nbn:de:0005-072858

Analysis of the molecular basis underlying signal-regulated splicing via the RNA-binding protein Sam68.

Zur Erlangung des akademischen Grades eines

DOKTORS DER NATURWISSENSCHAFTEN

(Dr. rer. nat.)

von der Fakultät für Chemie und Biowissenschaften der Universität Karlsruhe (TH) genehmigte

DISSERTATION

von

Anne Tisserant

aus Epinal, Frankreich

Dekan: Prof. Dr. Holger Puchta

Referent: Dr. Harald König

Korreferent: Prof. Dr. Margot Zöller

Tag der mündlichen Prüfung: 17/07/06

Analyse der molekularen Grundlagen für signal-reguliertes Spleißen durch das RNA-Bindeprotein Sam68

ZUSAMMENFASSUNG

Die Evolution höherer Organismen ausgehend von einer überraschend kleinen Zahl an Genen wird vorwiegend durch Mechanismen erklärt, durch die aus einem Gen mehrere Proteine hervorgehen können. Der häufigste dieser Mechanismen ist das alternative Spleißen von prä-mRNA. Um Spleißvarianten räumlich und zeitlich richtig zu exprimieren muß die Spleißmaschinerie durch extrazelluläre Signale gesteuert werden. Das RNA-Bindeprotein Sam68 repräsentiert einen ersten Spleißregulator, der an Signaltransduktionsprozesse gekoppelt ist. Nach Aktivierung des Ras-Signalweges vermittelt Sam68 über seine Phosphorylierung durch die Extrazelluläre-Signal-Regulierte Kinase (ERK) den Einschluß eines varianten CD44-Exons, v5, in die mRNA. Diese Exonsequenz wird häufig nach der Aktivierung von Immunzellen und bei der Tumorentstehung gefunden.

Ziel meiner Arbeit war es zu verstehen wie Sam68 an den Spleißapparat gekoppelt ist und wie die signalabhängige Modifikation durch ERK die Auswahl von Exons steuern kann. Ich zeige hier, daß, zusätzlich zu dem bekannten RNA-Element innerhalb des CD44-Exon v5, ein zweites Element im davorliegenden Intron existiert, das Sam68 *in vitro* bindet, und daß beide Elemente das Ausmaß des Exon-Einschlusses bestimmen. Über die Etablierung einer Immunpräzipitations-Methode für prä-mRNA konnte ich zeigen, daß Sam68 die diese Elemente enthaltende Region der prä-mRNA auch *in vivo* bindet und daß die verstärkte Expression von Sam68 zu einer verstärkten Bindung der generellen Spleißosomkomponente U2AF65, einem wichtigen Faktor für die Spleißosombildung, an die prä-mRNA führt. Ras-Aktivierung führte zu keiner weiteren Steigerung der U2AF-Bindung. Co-immunpräzipitationen zeigten zudem die Interaktion von Sam68 mit U2AF und mit hnRNP A1, einem Exon-Silencer-Faktor, der an das v5-Exon bindet. Interessanterweise erfolgte die signalabhängige Aktivierung des Spleißens unabhängig von der RNA-Bindungsfähigkeit von

Sam68 und die Aktivierung des Ras-Signalweges reduzierte die Bindung von Sam68 an die prä-mRNA *in vivo*. Weiterhin hemmte die Phosphorylierung von rekombinantem Sam68-Protein mit ERK dessen RNA-Bindung.

Die Ergebnisse legen nahe, daß Sam68 Teil eines Multiproteinkomplexes an der v5-Exon-Region ist und den Spleißosomfaktor U2AF rekrutieren kann, wodurch Sam68 an den Aufbau von Spleißosomen gekoppelt ist. Dies scheint signalunabhängig zu erfolgen und führt zu vorgeformten spleißkompetenten Komplexen. Weiterhin sprechen die Daten dafür, daß ein Schritt in der Aktivierung des Spleißens die Hemmung der RNA-Bindung von Sam68 über dessen Phosphorylierung durch ERK ist. Dieser Schritt könnte die Umbildung der Komplexe initieren und den weiteren Zusammenbau der Spleissosomen erlauben und somit erklären wie die signal-induzierte Modifikation von Sam68 Spleißen steuern kann.

SUMMARY

Evolution of higher organisms from a surprisingly small number of genes is mainly explained by mechanisms generating multiple proteins from a single gene, the most prevalent of which is alternative pre-mRNA splicing. To ensure an appropriate spatial and temporal expression of splice variants, the splicing machinery must be instructed by extracellular cues. The RNA-binding protein Sam68 represents a first splice regulator that is linked to signal transduction. Through phosphorylation by extracellular signal-regulated kinase (ERK) it mediates Ras-pathway dependent inclusion in CD44 pre-mRNA of a variant exon, v5, often found during immune-cell activation and tumorigenesis.

The aim of my work was to understand how the Sam68 protein is connected to the splicing machinery and how its signal-dependent modification by ERK may affect exon choice. I show here that, beside the known RNA element within exon v5, there is a second element upstream of the CD44 v5 exon that binds Sam68 *in vitro* and that both sites determine the general level of v5 exon inclusion in mRNA. Establishing a pre-mRNA immunoprecipitation technique, I could show that Sam68 binds to the pre-mRNA region carrying these sequences also *in vivo,* and that forced expression of Sam68 enhances binding to pre-mRNA of the general spliceosome component U2AF65, a critical factor for spliceosome assembly. Ras-activation did not further enhance U2AF binding. By co-immunoprecipitations I showed that Sam68 interacts with U2AF65, and with hnRNPA1, an exon silencing factor, previously shown to bind the v5 exon. Intriguingly, the signalling-dependent activation of v5 exon splicing was independent of the RNA-binding ability and Ras-signalling reduced Sam68 binding to the v5 pre-mRNA region *in vivo*. Similarly, phosphorylation of recombinant Sam68 by ERK impaired its binding to RNA.

The results suggest that Sam68 is part of a multiprotein complex over the v5 exon region and can recruit the spliceosomal factor U2AF65, thus linking Sam68 to spliceosome assembly. This step appears to be independent from cell signalling and leads to pre-formed splice-competent complexes. The data further suggest that one step in the splicing activation process involves a weakening or loss of Sam68 binding to RNA via its phosphorylation by ERK. This step might initiate the remodeling of the complex allowing further spliceosome assembly and may explain how the signalling-induced modification of Sam68 can affect splicing.

CONTENTS PAGE

Introduction

During evolution, organisms have displayed a broad spectrum of functional and behavioural complexity. An increase in the number of components that constitute organisms, and/or the elaboration of new relationships and networks between these components could be the origin of higher complexity. Among the mechanisms which can expand the size of the proteome (the complete set of proteins expressed by the genome during the life of an organism), alternative pre-mRNA splicing is considered to be the primary source of protein diversity in vertebrates (Black, 2000; Graveley, 2001; Faustino et al., 2003). Alternative pre-mRNA splicing, occurring during the expression of 35 to 75% of human genes (Modrek et al. 2001; Modrek et al., 2002; Johnson et al., 2003), allows the production of structurally and functionally distinct proteins from a single gene.

1. Pre-mRNA splicing

1.1 Molecular mechanisms in pre-mRNA splicing

The pre-mRNA splicing reaction is a maturation process carried out by the spliceosomes, ribonucleoprotein complexes containing five uridine-rich small nuclear RNAs (U1, U2, and U4, U5 and U6 snRNAs) and a large number of associated proteins (Reed, 2000; Stevens et al., 2002; Zhou et al., 2002). The spliceosome recognizes the intron/exon boundaries (splice sites), and performs the catalysis that removes introns from the pre-mRNA and joins exons, to produce mature mRNA.

At the early stage in spliceosome assembly, the U1snRNP is tightly associated with the 5'splice site (GU). The heterodimer U2AF (U2 snRNP auxiliary factor) which contains a large (U2AF65) and a small (U2AF35) subunit, binds to the polypyrimidine tract and to the 3'splice site (AG). In addition, U1snRNP is associated with the branch point binding protein mBBP/SF1 and members of the SR protein family (Staknis et al., 1994; Reed, 1996) through protein-protein interactions with their RS (Arginine-Serine-rich) domain, to promote subsequent steps in spliceosome assembly (Berglund et al., 1997; Merendino et al., 1999; Staknis et al., 1994; Wu et al., 1999; Zamore et al., 1992; Zorio et al., 1999) (Figure 1A).

U2AF was identified as an activity required for recruitment of the U2 snRNP to the branch point (Wu et al., 1999), and recognition of the polypyrimidine tract by U2AF65 is central to splice site selection and spliceosomal formation for the major class of introns in higher eukaryotes (Reed, 1989; Coolidge et al., 1997). Following the assembly of U2 snRNP-containing pre-splicing complex on the 3' splice site, U4/U6 and U5 snRNPs enter the assembly pathway as a pre-formed tri-snRNP particle (see Figure 1A) which, together with additional protein factors, forms an assembled spliceosome.

1.2 Exon definition in alternative splicing

In alternative splicing, certain exons can be included or excised from the pre-mRNA. The exon definition, the process by which exons are distinguished from introns, is a critical step. In higher eukaryotes, the sequences of surrounding splice sites and the branch site of alternatively spliced exons usually diverge from the consensus sequences (Berget, 1995; Reed, 1996), resulting in a weak affinity for the spliceosome factors. Specific RNA sequence elements called splicing enhancers interact mainly with SR proteins (Figure 1A) and help to recruit and stabilize the splicing machinery on the flanking weak 3' and 5' splice sites.

In contrast, some RNA sequences called splicing silencers, known to interact mainly with the heterogeneous nuclear ribonucleoprotein (hnRNP) family, can repress splice-site selection (Figure 1B). Among the best characterized members of the hnRNP family is hnRNPA1. HnRNP A1 (an abundant nuclear protein which can shuttle between nucleus and cytoplasm) was shown to be implicated in many cellular processes, such as mRNA transport (Dreyfuss et al., 1993; Swanson, 1995) and splicing (Mayeda et al., 1992; Dreyfuss et al., 1993; Swanson, 1995; Del Gatto et al., 1999; Tange et al., 2001). HnRNP A1 is a concentration-dependent antagonist of the SR protein SF2-ASF (Mayeda et al., 1992), it can thus function as an exonic splicing repressor (Del Gatto et al., 1999; Matter et al., 2000). Furthermore, it was reported to act through an intronic splicing silencer to inhibit U2 snRNP association to a 3'splice site (Tange et al., 2001) or to reduce the binding of U1 snRNP to the 5' splice site (Eperon et al., 2000).

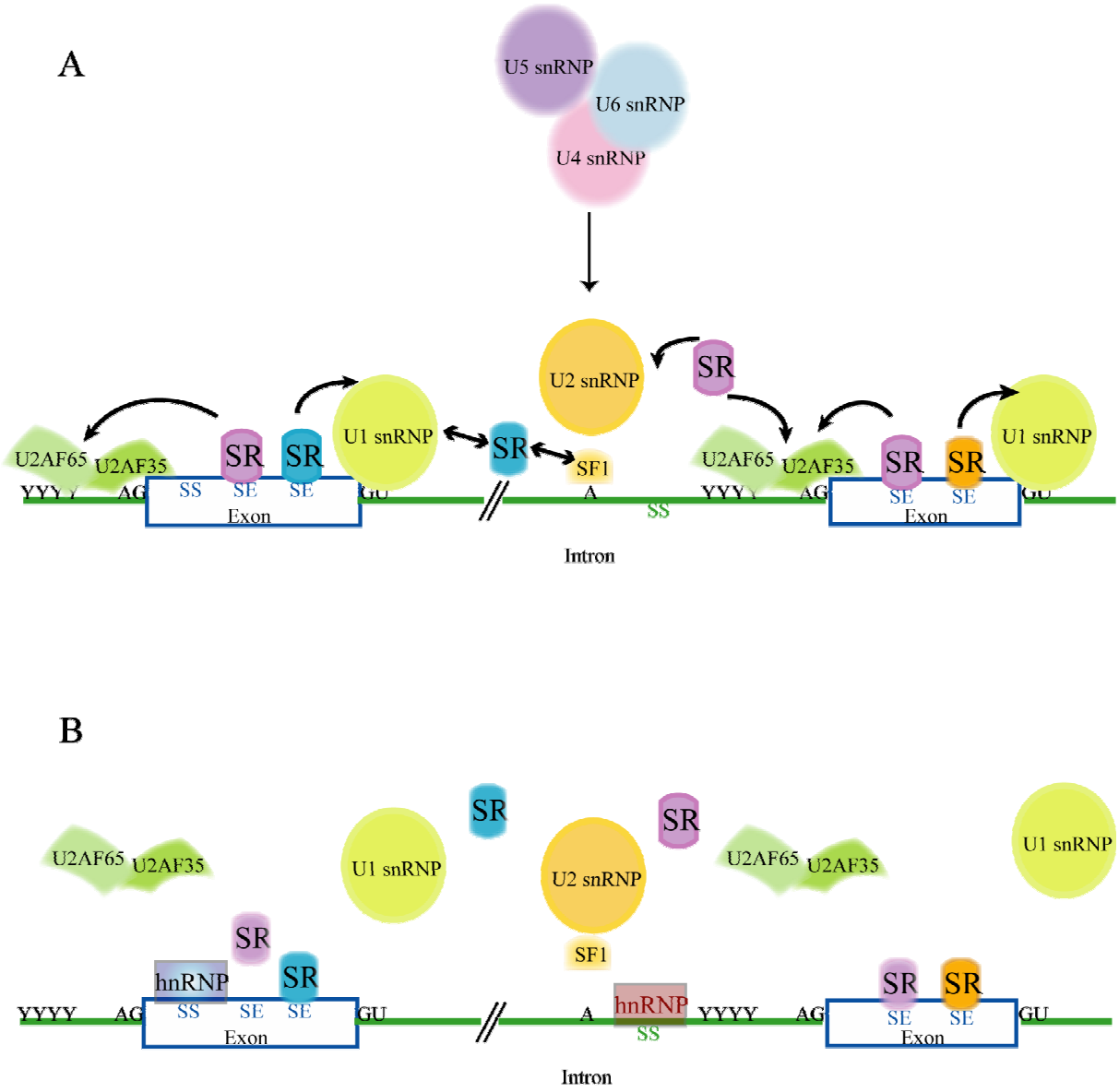

Figure 1: Exon definition.
A: The 5' splice site (GU) , the branch point (A), the polypyrimidine tract (YYY) and 3' splice site (AG) are recognized by U1 snRNP, SF1mBBP, and U2AF 65 and 35 kDa subunits respectively. The assembly is promoted by SR proteins which bind splicing enhancer sequences (SE). U4/U6 and U5 snRNPs enter the assembly pathway as a pre-formed tri-snRNP particle giving rise to an assembled spliceosome. **B:** Some RNA sequences called splicing silencers (SS) known to interact mainly with the heterogeneous nuclear ribonucleoprotein (hnRNP) family, can repress splice-site selection.

1.3 Alternative splicing regulation

Changes in splice site choice leading to inclusion or skipping of exon sequences, can have diverse effects on the encoded protein, like altered ligand binding, enzymatic activity or protein localization (Naor et al., 1997; Skelton et al., 1998; Yao et al., 2005; Blanco et al., 2006).

The selection of alternative splice sites can be regulated dependent on tissue or cell type (Sharp, 1994), developmental stage (Rio, 1993), physiological state, sex (Baker, 1989) and in response to various stress factors. Extracellular signals including stimulation of receptors by growth factors (Scotet et al., 1998), cytokines or hormones, membrane depolarization, antigenic stimulation of the T-cell receptor (Screaton et al., 1997; König et al., 1998; Lynch et al., 2000; Weg-Remers et al., 2001) and cellular stresses like heat shock and change of pH, have been shown to induce changes in the selection of splice sites (Stamm, 2002; Faustino et al., 2003). These extracellular cues are thought to act through a network of signalling cascades, with different level of complexity, that pass the information to the nucleus. As a result the relative abundance, activation state, or localization of the splicing activating (for instance SR proteins) and repressing (for instance hnRNPs) factors may be changed, leading to a repression or a promotion of exon inclusion in the mRNA (Xu et al., 2003).

1.4 The Ras signalling cascade: a highly conserved link between extracellular cues and alternative splicing

Among the signalling cascades, the highly conserved Ras signalling pathway was shown to regulate alternative splicing (Fichter et al., 1997; Smith et al., 1997; König et al., 1998; Lynch et al., 2000; Weg-Remers et al., 2001). Ras is a 21kda GTP-binding protein with GTPase activity. Its activity was shown to be required for a proper alternative splicing of Agrin mRNA. Agrin is an extracellular matrix protein that plays a key role in directing the formation and the maintenance of the post-synaptique apparatus of the neuromuscular junction. In response to Nerve Growth Factor (NGF), the Ras signalling pathway induces the inclusion of 2 inserts required for further clustering of acethylcholine receptors, in motorneurons (Smith et al., 1997).

Moreover, activation of T lymphocytes, through the T cell Receptor (TCR), or B lymphocytes, through BCR, leads to the activation of signalling cascades, including the Ras pathway, which ultimately results in a number of morphological and functional changes in the cell, depending on alternative splicing events (Downward et al., 1990; Downward et al., 1992;

Weiss et al., 1994; Lynch et al., 2000). TCR/BRC-induced Ras activation is basically the result of the activation of guanine nucleotide exchange factors (GEFs) and the inhibition of GTPase activating proteins (GAP) (Genot and Cantrell, 2000) (Figure 2). Antigen receptors activate tyrosine kinases including src family kinases, Tec family kinases and the specific antigen receptor associated kinases. The coordinated action of these tyrosine kinases phosphorylates adapter proteins, notably LAT (linker for activated T cells; Zhang et al., 1998), which then recruits Phospholipase C (PLC) (Finco et al., 1998). This results in increased hydrolysis of inositol lipid and the production of diacylglycerol (DG) which can regulate the GEF, Ras GRP (Ebinu et al., 1998). Tyrosine-phosphorylated LAT also recruits Grb2 and the GEF, Sos, to the plasma membrane (McCormick, 1993). In addition, sequestration of Ras GAPs by adaptaters such as p62DOK inhibits GAPs activity and promotes Ras accumulation in the active GTP bound state (Yamanashi and Baltimore, 1997).

Ras interacts directly with the serine/threonine kinase Raf-1, which regulates the activity of a kinase cascade that includes MAP Kinase Kinases (MEKs) and Mitogen-Activated Protein (MAPs) kinases, also called Extracellular signal-regulated kinases (ERK) (Weiss, et al., 1994; Crews et al., 1993). The serine-threonine protein kinases ERK1 and ERK2 are the best-characterized family members. ERKs play important roles in the control of key cellular processes such as differentiation, apoptosis, and proliferation (Screaton et al., 1997; Smith et al., 1997) (Figure 2). In T-lymphoma cells, but not in primary T-cells, Ras through interaction with the small GTPase Rac and via signalling to different MEKs also activates c-Jun NH(2)-terminal kinases (JNKs) and p38 kinase (Izquierdo et al., 1993; Genot et al., 1996; Genot et al., 1998; Zhang et al., 1999; Dong et al., 2000; Weiss et al., 2000) (Figure 2).

Many isoforms of the protein tyrosine phosphatase CD45 are expressed on the surface of human T cells. The expression of these isoforms has been shown to vary upon T-cell activation. It was shown that activation of the exclusion of variable exons from CD45 mRNA was mediated via a PKC-dependent signalling pathway, which can be mimicked by constitutive activation of Ras (Lynch et al., 2000).

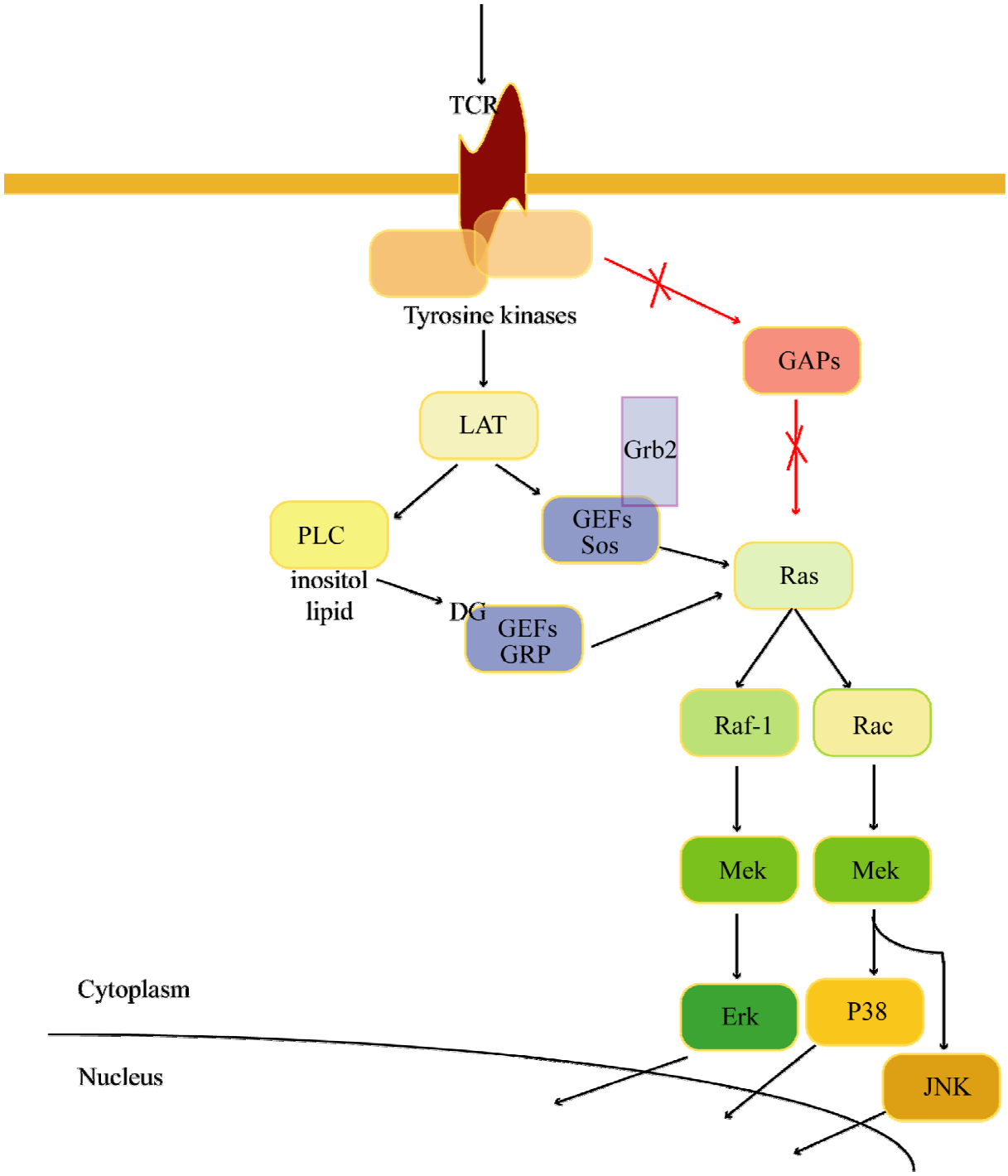

Figure 2: Ras-pathway activation following T cell receptor (TCR) stimulation.
TCR activates Tyrosine kinases which phosphorylate LAT (linker for activated T cells) which then recruits phospholipase C (PLC) responsible for the activation of the GEF (guanine nucleotide exchange factor) GRP, after hydrolysis of inositol lipid in diacylglycerol (DG). LAT activates also the GEF, Sos which associates to Grb2. The tyrosine kinases are also responsible for GAPs (GTPase-activating protein) inactivation. Ras activation is then the cumulated effect of activation of GEFs and inhibition of GAPs (Genot and Cantrell, 2000). The dowstream effectors of Ras will bring the signal to the nucleus which will ultimately results in a number of morphological and functional changes in the cell.

1.5 splicing and diseases

Mutations that interfere with proper exon recognition result in a large number of human genetic diseases (Faustino et al., 2003; Cartegni et al., 2002). At least 15 % of the single base-pair mutations that cause human genetic diseases result in pre-mRNA splicing defects (Krawczak et al., 1992; Maniatis et al., 2002). Misregulation of alternative splicing has been implicated in neurodegenerative disorders (Kar et al., 2005) and cancer. Aberrant transcripts seem, actually, to be an intrinsic property of cancer cells. In Xu et al. (2003), 316 human genes were shown to have cancer-specific splice variants. The best known example of genes linking alternative splicing and cancer is the cell surface protein CD44

2. CD44

CD44 are class I transmembrane glycoproteins present on the surface of most vertebrate cells (Naor et al., 1997). It was first described in 1980 by Dalchau *et al.*, as a human molecule present on lymphocytes, granulocytes, and cortical thymocytes which reacted with the monoclonal antibody F10-44-2. All the CD44 proteins are encoded by a single, highly conserved gene composed of 20 exons (Screaton et al., 1992). The members share N-terminal and C-terminal sequences but differ in the extracellular domain due to alternative splicing of ten variant exons which can be completely excised all or used in various combinations (Screaton et al., 1992; Tolg et al., 1993) (Figure 3). This heterogeneity generated by alternative splicing and which is further enhanced by differential glycosylation (posttranslational modifications) of the resulting polypeptide isoforms and/or addition of heparan sulphate, (Stamenkovic et al., 1991; Gunthert et al., 1991; Borland et al., 1998) suggests a wide spectrum of physiological functions.

2.1 Protein structure of CD44 (Figure 3)

The amino-terminal hyaluronan-binding domain is encoded by the first five exons of CD44 which are constitutively included in the mRNA. This domain contains motifs that function as docking sites for extracellular matrix (ECM) components like hyaluronan (a high-molecular-weight polysaccharide).

The amino-terminal globular domain of the smallest CD44 isoform (the standard isoform or CD44s) is separated from the plasma membrane by a short stem structure. The

stem structure can be enlarged by sequences that are encoded by the alternatively spliced, variant (v1 to v10) exons of CD44. The inclusion of these variant exons is dependent, at least in part, on mitogenic signals that regulate alternative splicing (König et al., 1998; Weg-Remers et al., 2001; Matter et al., 2002).

The hydrophobic transmembrane region of CD44 seems to participate in the formation of CD44 oligomers. The cytoplasmic-tail-region and the intracellular protein partners of CD44 contain motifs important for CD44 subcellular localisation (Naor et al., 1997). ERM (ezrin, radixin and moesin) proteins, implicated in the regulation of cell migration and cell shape, were shown to interact with the cytoplasmic tail of CD44 (Tsukita et al., 1994). They crosslink the actin cytoskeleton to CD44 and to other proteins (Legg et al., 2002).

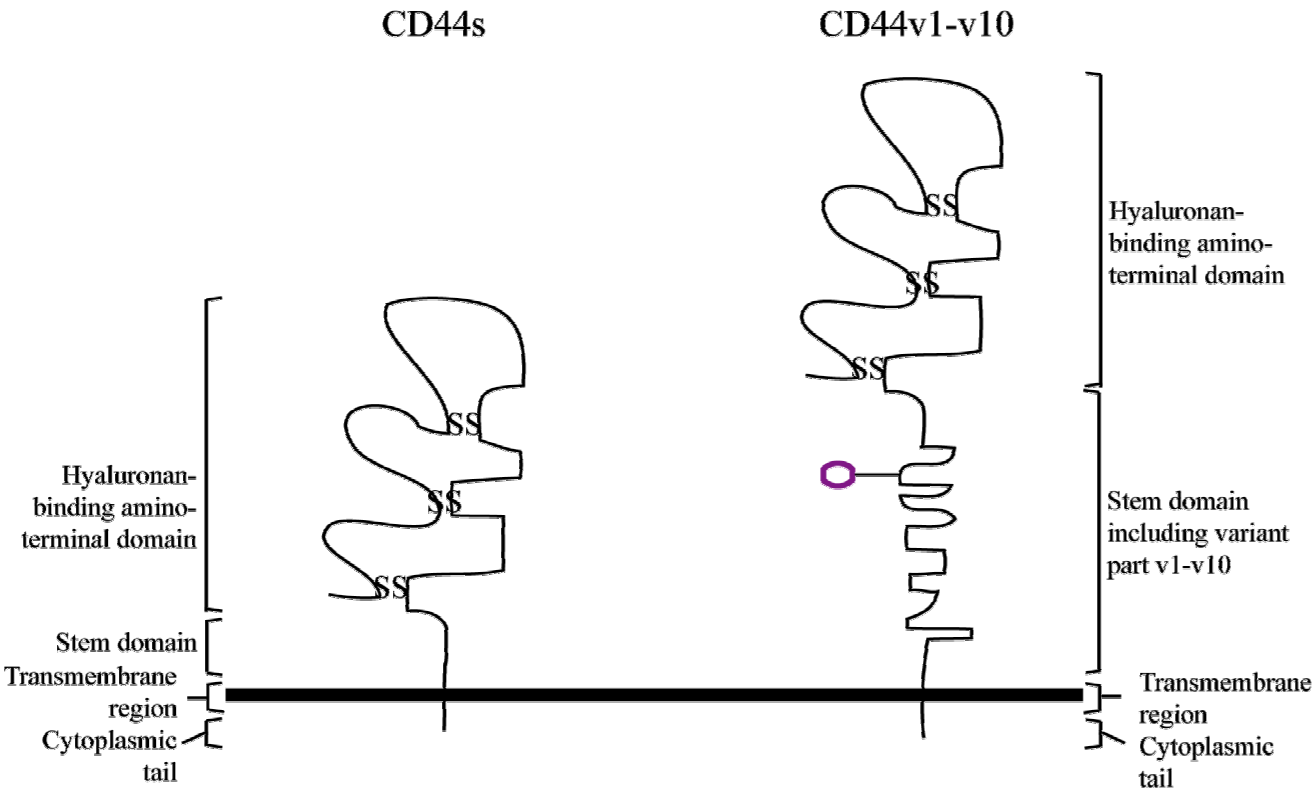

Figure 3: CD44 proteins.
Scheme of CD44 standard and the largest variant isoform CD44v1-v10. The sequences encoded by the variant exons are in the stem region. The stability of the amino-terminal domain is based on disulfide links (SS) between highly conserved cysteine residues. Exon v3 is coding for the unique heparan sulphate addition site (Violet open circle) which is important for binding of heparan-sulphate-dependent growth factors. The glycosylation sites present all over CD44 structure are not represented here.

2.2 Molecular mechanisms of CD44 function

Most evidence for the functional roles of CD44 has been obtained by interfering with these functions with antibodies directed either against all CD44 molecules or against subsets of variant proteins, and by using mice with germline deletions of different portions of the CD44 gene. Any proposed mechanism that tries to explain the function of CD44 must take into account the structural heterogeneity of CD44 proteins, which is the result of extensive alternative splicing (Figure 4) and post-translational modifications.

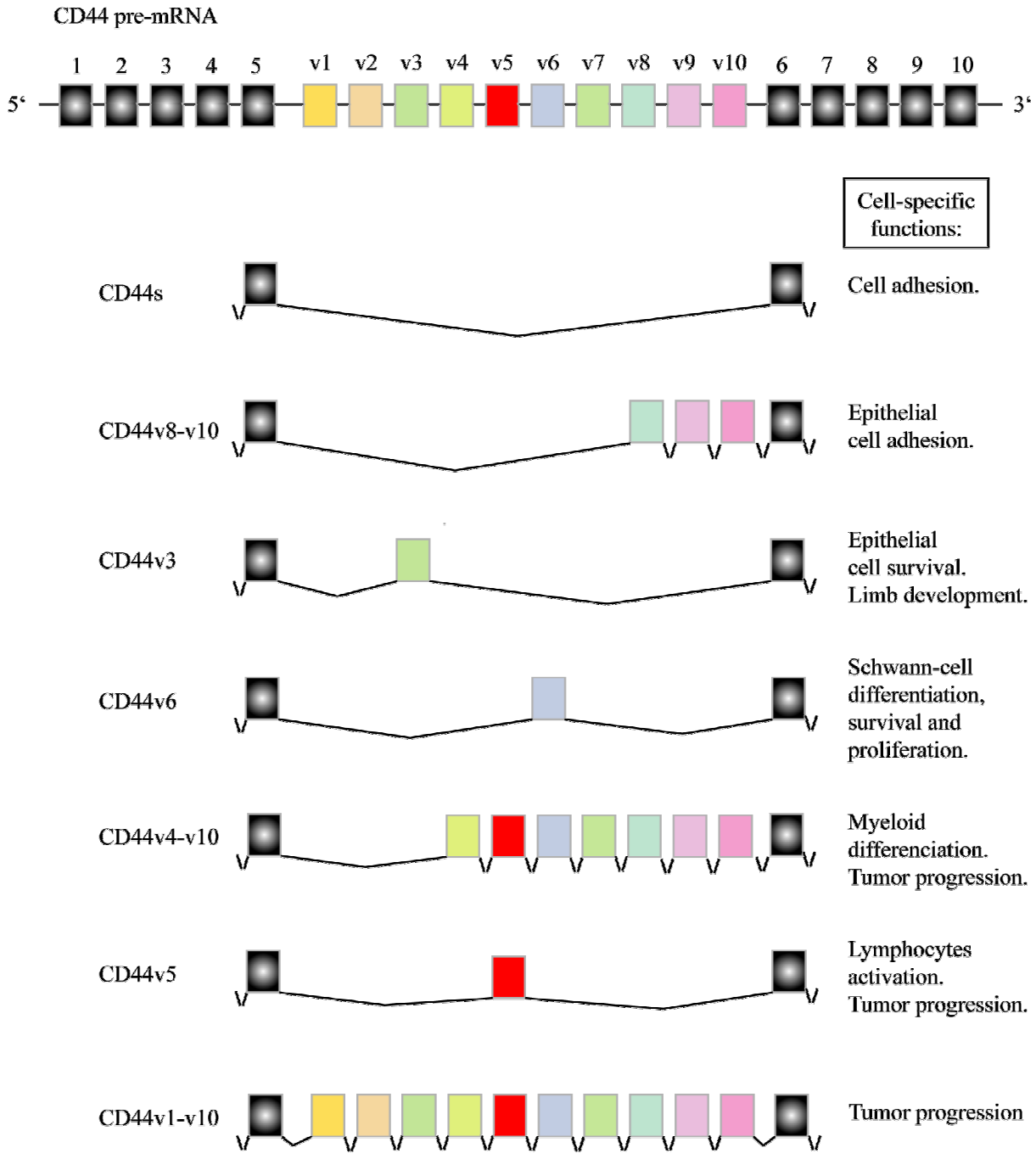

Figure 4: CD44 transcripts.
Only few examples are represented here. CD44 gene is composed of 20 exons and many different isoforms can be produced by alternative splicing, by the inclusion of up to 10 variant ('v') exons in the mRNA. The smallest CD44 isoform, known as CD44 standard (CD44s) is ubiquitously expressed in vertebrates in developing and adult organisms, whereas the larger variant isoforms are expressed mainly in epithelial tissues, in proliferating cells, and in several cancers (Naor et al., 1997).

2.2.1 CD44 in cellular adhesion and migration

CD44 can act as a ligand-binding surface protein. CD44 interacts with various components of the extracellular matrix (ECM), like hyaluronan. The binding affinity for Hyaluronan seems to be modulated from inside the cells by mitogenic stimuli (Naor et al., 1997) which directly influence the inclusion of variant exons, and by the glycosylation (Sleeman et al., 1997; Skelton et al., 1998) of the extracellular domain (Bennet et al., 1995; Naor et al., 1997) which is cell-type- and growth-condition-specific. Indeed binding studies with melanoma transfectants expressing CD44s or CD44 including v8 to v10 exons showed that CD44s expressing cells had a better affinity for Hyaluronan than CD44v8-v10 expressing cells. This alternative splicing resulted in changes in global protein glycosylation (as the 2 segments encoded by the variant exons were heavily glycolysed) likely leading to a change in CD44 conformation which could alter the affinity of CD44 for hyaluronan (Yu et al., 2002). The modulation of the binding affinity of CD44 is probably important for cellular migration in hyaluronan-matrices and for CD44- and hyaluronan-dependent leucocytes rolling, which is the first of the two step mechanism by which white blood cells adhere to the endothelium (Naor et al., 1997; Gonda et al., 2005; Bonder et al., 2006).

2.2.2 CD44 in cell survival

CD44 proteins can function as specialized platforms for growth factor and metaloproteinases (MMPs), the interactions of which are necessary for various crucial cell-signalling events. In one study, MMP7 is recruited to the surface of cells (tumor cell lines, postpartum uterine, lactating mammary gland epithelium cells, and uterine smooth muscle cells), probably by CD44. MMP7 triggers the proteolytic cleavage of the heparin-binding epidermal growth factor (HBEGF), which is dependent on the binding of the pro-form to the heparan-sulphate side chain that is encoded by exon v3 of CD44 (Yu et al., 2002)(Figure 3). Isoforms of CD44 that contain v3 sequences are typically modified by heparan-sulfate side chains, which convert CD44 to a heparan-sulfate proteoglycane (HSPG) (Bennett et al., 1995). The binding of heparin-binding growth factors to an HSPG is a prerequisite for the activation of their high-affinity receptors. Activating HBEGF is engaged in the remodelling of mice female reproductive tissue by activating the ERBB receptor tyrosine kinase ERBB4 that stimulates cell survival (Opanashuk et al., 1999). So, the recruitment of MMP7 by CD44v3 could account for the suppression of apoptosis, as observed in tumour cells (Yu et al., 1997).

2.2.3 CD44 in development

In a study concerning limb development, CD44 isoforms containing sequences encoded by v3 exon bind fibroblast growth factor (FGF) in order to induce proliferation of the mesenchymal cells of the limb buds (Wainwright, 1998).

2.2.4 CD44 in differentiation

Human myeloid progenitor cell lines produce variant CD44 proteins, predominantly a new variant CD44v4-v10, when stimulated towards myeloid differentiation. This can be explained by an increased capacity of CD44v4-v10 to bind hyaluronan, which might also be enhanced by glycosylation of the CD44 extracellular domain (Moll et al., 1998).

In another study, CD44 isoforms that contain exon v6 sequences can act as essential co-receptors for the activation of Met, which is a tyrosine kinase receptor that binds scatter factor/hepatocyte growth factor (SF/HGF), implicated in differentiation, invasive growth and morphogenesis (Orian-Rousseau et al, 2002).

2.2.5 CD44 in cancer

Many studies have implicated a role of CD44 proteins, as the CD44 v4-v7 isoform (Stamenkovic et al., 1991, Gunthert et al., 1991), in the dissemination and metastatic spread of tumor cells. In one study, lymphoma cells transfected with CD44 v4-v10, but not LB cells transfected with CD44s or their parental LB cells, displayed accelerated local tumor formation and enhanced accumulation in the peripheral lymph nodes after subcutaneous inoculation, in mice (Wallach-Dayan et al., 2001). The expression of CD44 epitopes has been examined through carcinogenesis and metastatic progression of several cancers and some studies have identified CD44 as a useful prognostic marker for disease progression (Stauder et al., 1995; Ponti et al., 2006).

HTra2-beta1, a member of the extended family of serine/arginine-rich (SR) splicing factors, enhances the in vivo inclusion of CD44 exons v4 and v5. In a matched pair analysis of human breast cancers and their corresponding non pathologic tissue controls, Tra2-beta1 was shown to be significantly induced in invasive breast cancer, both on the RNA and protein levels. Induction of this splicing factor might be responsible for splicing of CD44 isoforms associated with tumor progression and metastasis (Watermann et al., 2006).

In some cancers, the misregulated expression of CD44 seems not to be the result of CD44 mutations (Ponta et al., 2003). Genes that are implicated in promoting carcinogenesis seem to control the patterns of CD44 expression in cancer cells, through alternative splicing

possibly under the control of mitogenic signals including the Ras-MAP kinase cascade (König et al., 1998; Weg-Remers et al., 2001; Matter et al., 2002).

2.2.6a CD44 and lymphocytes activation

A physiological process in which the Ras kinase cascade is implicated, is antigenic activation of lymphocytes. Treatment of Lymphoma cells with phorbol ester can partially mimic reactions following antigen contact and target activation of T-cell receptors (TCR) which involves the downstream activation of $p21^{ras}$ (Castagna et al., 1982; Cantrell, 1996) (see above). Activation of T lymphocytes by injection of allogeneic lymphocytes into adult rats (Arch et al., 1992), by TCR stimulation with an anti-CD3 antibody or by phorbol ester treatment (Koopman et al., 1993) results in the generation of alternatively spliced variant CD44 isoforms (Koopman et al., 1993; Weg-Remers et al, 2001).

2.2.6.b CD44 v5 as a model to study signal-dependent splicing in T cells

One CD44 isoforms highly expressed upon T cell activation, included the single exon v5 sequence (König et al., 1998; Weg-Remers et al, 2001). The exon v5 was shown to be included also during tumor progression (Stamenkovic et al., 1991; Gunthert et al., 1991; Lee et al., 2005; Watermann et al., 2006). The CD44 v5-exon may thus provide a very interesting model to study alternative splicing.

In T-cell activation, the inclusion of v5 exon in the CD44 mRNA was shown to be induced upon Ras cascade activation, illustrating the coupling of signal transduction to alternative splicing (König et al., 1998). This positive regulation does not require expression of new factors as inhibitors of translation could not abolish the induction of exon v5 inclusion in the mRNA. A composite exonic splice regulator which is responsive to cell signalling was identified within the v5 exon. Retention or excision from pre-mRNA of CD44 exon v5 is regulated by distinct types of cis-acting elements: an exon recognition element within the subdomain R (Right) and a silencer element composed of two subdomains, L (Left) and M (Middle) (Figure 5). Whereas the exon recognition element is essential for the v5 exon inclusion (deletion abolishes completely exon inclusion in phorbol ester-treated-lymphoma cells), the two silencer elements are necessary for the cell type-specific and inducible usage of the v5 exon. Regulation could be established by the cooperative binding of silencer proteins on the L and M subdomains which might impair the binding or function of positively acting factors at the exon recognition element. Activation of signal transduction pathway as the Ras signalling cascade could modify either, the silencer factors, the enhancer factors or both, thus

affecting their RNA-binding capacity or their ability to interact with each other and with components of the splicing machinery.

The targets of Ras which are responsible for the downstream signalling, were identified in experiments using pathway specific inhibitors. The components of the MAP pathway: Raf, MEK, and ERK were shown to actively contribute to exon v5 inclusion (Weg-Remers et al., 2001). Activation of the JNK pathway may also contribute to the v5 exon splicing regulation in T lymphoma cells. However, since the JNK pathway is not activated in stimulated primary T-cells, its implication should be limited. Further experiments using mutants for the v5 exonic silencer sequences showed that inclusion of the v5 exon in response to activation of the MAP kinase pathway depends on these signal-responsive elements, which implies an inactivation of silencing factors upon the signalling pathway activation (Weg-Remers et al., 2001).

The heterogeneous nuclear ribonucleoprotein A1 was identified as a silencing factor for v5 exon inclusion. It was shown to interact with exon v5 sequences, and in co-transfection experiments in the erythroleukemia cell line CB3 (this cell line shows no detectable expression of hnRNP A1), increasing amounts of an hnRNP A1 expression vector led to exon skipping in a dose-dependent manner (Matter et al., 2000). The same result was obtained upon hnRNP A1 over-expression in cells expressing hnRNP A1 like NIH-3T3 murine fibroblasts, and in KLN205 mouse carcinoma cells. The hnRNP A1 mediated splice silencing is exon-specific since hnRNP A1 overexpression did not repress inclusion of exons v4 or v7. Furthermore, experiments in which a vector expressing a constitutively active Ras was cotransfected with the hnRNP A1 expressing vector showed that Ras expression prevented the silencing effect of hnRNP A1 on v5 exon inclusion. This result indicated that the Ras signalling pathway antagonizes the activity of an exonic splice-silencing complex in which hnRNP A1 plays a decisive role (Matter et al., 2000).

More recently, the RNA-binding protein Sam68 was shown to be directly involved in v5 exon splicing regulation (Matter et al., 2002).

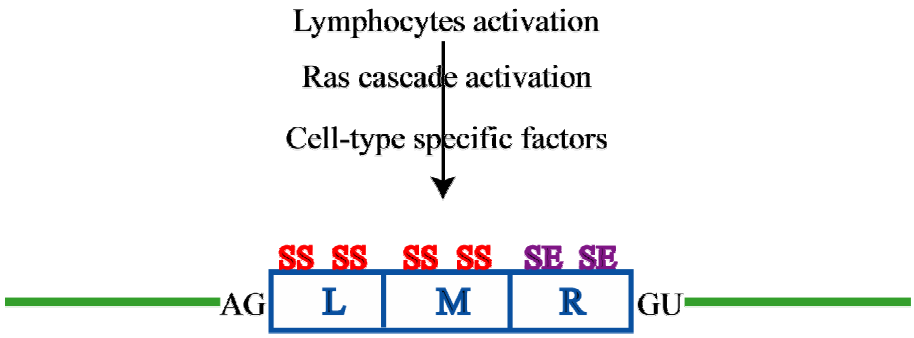

Figure 5: Schematic representation of the splicing regulatory domains within CD44 exon v5.
They are responsive to the cell signalling mediated by Ras cascade activation. Open blue boxes are L (left), M (middle), R (right) subdomains. Splicing silencers are found within L and M, and splicing enhancers (SE) are found withing R. (König et al., 1998).

3. Sam68

The Src-associated substrate during mitosis (Sam68) is a 68 kDa, 443-amino-acid protein belonging to the Signal Transduction and Activation of RNA (STAR) family. It was first described as p62, a protein associated with the p120-RasGTPase-activating protein (Ras-GAP) and identified in cells transformed by tyrosine kinase oncogenes including v-src (Ellis et al., 1990; Moran et al., 1990; Wong et al., 1992; Lock et al., 1996). Its implication in biological processes including signal transduction, cell cycle regulation, tumorogenesis and RNA biogenesis could be better understood by the description of its highly conserved putative functional domains.

3.1 Domain structure of Sam68 (Figure 6)

3.1.1 Sam68 KH domain

Sam68 is an RNA binding protein. It contains the second most prevalent RNA binding motif in proteins (Burd and Dreyfuss, 1994), called KH domain according to its homology with a domain found in the heterogeneous ribonucleoprotein (hnRNP) K. The most conserved sequence GXXXGXXG is located in the middle of the KH domain (Musco et al, 1996).The KH domain is flanked by conserved N- and C-terminal sequences (NK and CK regions) which are required for RNA binding activity (Lin et al., 1997; Chen and Richard, 1998). The entire RNA binding domain contains ~ 200 amino acids and is referred to as the GSG

(*Artemia salina* GRP33, mammalian Sam68, *Caenorhabditis elegans* GLD-1) domain or the STAR domain. The term GSG domain was coined to describe the first three proteins identified that contain this conserved region (Jones and Schedl, 1995; Di Fruscio et al., 1998).

Sam68 can self-associate via its GSG domain, which is impaired by tyrosine phosphorylation (Chen et al., 1997; Zorn and Krieg, 1997; Chen and Richard, 1998). Furthermore, Sam68 can bind, through its KH domain, to ribonucleotide homopolymers with higher affinity for poly (U) (Taylor and Shalloway, 1994) and poly (A) (Chen et al., 1997). A SELEX (systematic evolution of ligands by exponential enrichment) approach was used involving bacterial recombinant Sam68 and A/U-rich sequences. Particularly UAAA or UUUA containing sequences were identified as high affinity RNA targets (Lin et al., 1997). Itoh et al. (2002) could identify 29 potential RNA-binding sites for Sam68. Among them, the mRNA species for hnRNP A2/B1 and beta-actin were found to bind prominently in vivo as well as in vitro, suggesting the possible involvement of Sam68 in the post- transcriptional regulation of these genes.

3.1.2 Sam68 proline-rich domains

Sam68 contains numerous proline-rich sequences that are the binding sites of SH3 and WW domain-containing proteins.

SH3 domain ligands consist of short contiguous proline-rich amino acid sequences with core consensus sequence PXXP. Sam68 was identified as an SH3 domain binding protein for Src kinases: the Shalloway and Courtneidge groups identified a p68 kDa protein that was tyrosine-phosphorylated by Src in mitosis. The interaction was mapped to the SH2 and SH3 domains of Src (Fumagalli et al., 1994; Taylor and Shalloway, 1994).

The WW domain is a short conserved sequence of about 40 amino acid residues in single or tandem repeats with two signature tryptophan residues spaced 22 or 23 residues apart and has an affinity for proline-rich sequences (Bedford et al., 1998; Macias et al., 2002).

WW and SH3 domains share similar or overlapping proline-rich target sequences, and it is conceivable that they may compete for the same ligands in vivo (Bedford et al., 1997; Espejo et al., 2002). STAR proteins, including Sam68, contain proline motifs that have been shown to interact with WW domain-containing proteins (Bedford et al., 2000; Espejo et al., 2002). The Sam68 proline motifs P3 and P4, which are known sites of interactions with SH3 domains, have been shown to interact with the WW domains of the formin binding proteins FBP21 and FBP30 (Bedford et al., 2000). FBP21 is known to be present in spliceosomal

complexes and to interact directly with snRNP U1 and with the branch point binding protein SF1/mBBP.

3.1.3 Sam68 tyrosine-rich domain.

Sam68 has in its C-terminal part a tyrosine-rich domain which represents a potential site for phosphorylation (Wong et al., 1992; Di Fruscio et al., 1999). Indeed, Sam68 has been shown to be tyrosine-phosphorylated by numerous soluble tyrosine kinases including $p60^{src}$ (Wong et al., 1992; Fumagalli et al., 1994; Taylor and Shalloway, 1994; Weng et al., 1994). There are reports of cell surface receptors that induce the tyrosine phosphorylation of Sam68. Insulin, leptin and ligation of the T cell receptor have been observed to increase the tyrosine phosphorylation of Sam68 (Fusaki et al., 1997; Jabado et al., 1998; Martin-Romero and Sanchez-Margalet, 2001; Sanchez-Margalet and Najib, 2001). Tyrosine-phosphorylation of Sam68 leads to the association of Sam68 with numerous SH2 domain-containing proteins including Src family kinases (Fumagalli et al., 1994; Taylor and Shalloway, 1994; Richard et al., 1995), Sik/BRK (Derry et al., 2000), Grb2 (Richard et al., 1995, Trub et al., 1997) (through T cell receptor ligation), PLCγ-1 (Richard et al., 1995), RasGAP (Richard et al., 1995; Guitard et al., 1998), PI3K p85α (Taylor et al., 1995) (through leptin/insulin stimulation). These observations are consistent with the hypothesis that Sam68 may function as an adapter protein in signalling pathway (Richard et al., 1995; Taylor et al., 1995).

3.1.4 Sam68 RGG domains

Another prominent feature of STAR proteins as well as many other proteins involved in RNA metabolism is the presence of RG-rich regions and RGG boxes, which are potential sites for protein arginine methylation (Burd and Dreyfuss, 1994). The arginine–glycine sequences of Sam68 often flank proline-rich sequences. Arginine methylation is a prevalent posttranslational covalent modification in eukaryotes that has been shown to modulate several cellular processes including protein–protein interactions, transcription and intracellular localization (Gary and Clarke, 1998; McBride and Silver, 2001).

Sam68 was shown to be methylated in vivo, and to interact with endogenous Protein-arginine N-methyltransferase 1 (PRMT1; Cote et al., 2003). What functions or roles of Sam68 are affected by arginine methylation? Arginine methylation is not a quick and rapid mode of regulation such as tyrosine phosphorylation and does not affect protein/RNA interactions. Hypomethylated Sam68 was shown to localize to the cytoplasm (Cote et al., 2003). This suggests that arginine methylation of RNA binding proteins may be a maturation process

required for the proper localization and function of a protein. This maturation step may be either co-translational or coupled to the nuclear import machinery. Since arginine methylation is most likely irreversible (Gary and Clarke, 1998), it may be a constitutive pathway for the maturation of proteins.

3.1.5 Sam68 nuclear localisation signal (NLS).

The predominantly nuclear localization of mammalian Sam68 is dictated by a non conventional nuclear localization signal (NLS) embedded in the last 24 amino acids in the C-terminal of the polypeptide (Ishidate et al., 1997).

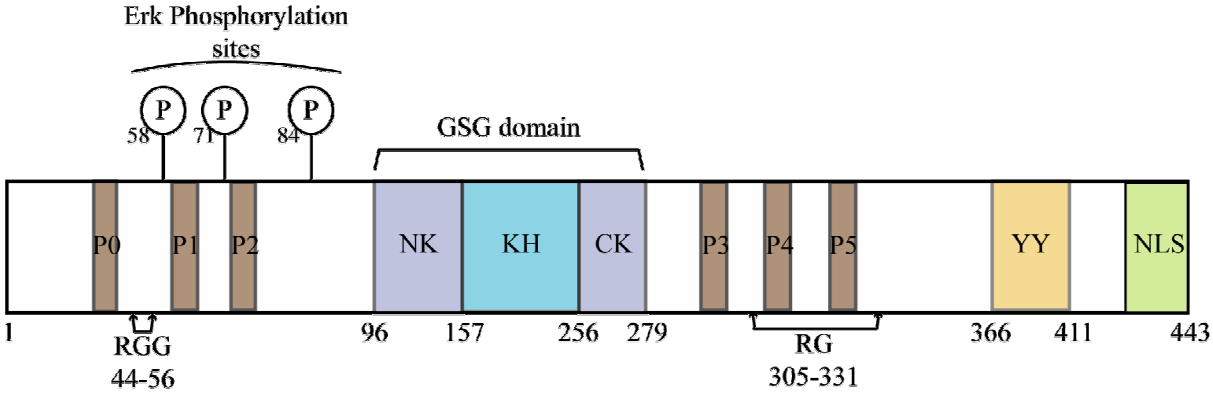

Figure 6: Schematic diagram representing the structural/functional domains of Sam68 (Reviewed in Lukong and Richard, 2003). The molecule is composed of the GSG domain, a tripartite of a single RNA-binding KH domain of a KH segment flanked by NK (N-terminal of KH) and CK (C-terminal of KH) segments; six consensus proline-rich motifs (P0-P5); RGG boxes; C-terminal tyrosine-rich domain (YY), and a nuclear localisation signal(NLS). The three Erk phosphorylation sites are serine 58, threonine 71 and 84. Relative amino acid positions are also indicated.

3.2 Biological roles of Sam68

3.2.1 Mitosis and cell cycle regulation

A role of Sam68 in cell cycle progression is supported by the growth-arresting potential of a natural spliced isoform of Sam68 with a deletion in the KH domain (Sam68ΔKH) (Barlat et al., 1997). Ectopic expression of Sam68ΔKH in NIH3T3 cells down-regulates cyclin D1 expression, thus inhibiting G1 to S phase entry, an effect overcome by Sam68 (Barlat et al., 1997). These data suggested that Sam68, through its KH domain and

hence its RNA-binding properties and/or its oligomerization properties, can regulate cell proliferation by promoting S phase entry. Moreover, targeted disruption of Sam68 in chicken DT40 cells causes growth retardation mainly due to elongation of the G2–M phase (Li et al., 2002). The growth defect is overcome by expression of exogenous wild-type Sam68 in the knock-out cells, indicating again that Sam68 is involved in cell cycle progression.

3.2.2 Tumor suppression

By using random homozygous knock-out (RHKO) in NIH 3T3 cells, a retroviral-based RNA strategy employed to identify chromosomal genes whose inactivation produces a specific phenotype (Li and Cohen, 1995), Sam68 was implicated in cell proliferation and tumorigenesis (Liu et al., 2000). RHKO NIH3T3 cells were shown to express less than 25% of Sam68 compared to wild-type levels, and in a Src-independent manner, these cells exhibited anchorage-independent growth, defective contact inhibition and formed metastic tumors in nude mice (Liu et al., 2000). This study suggests that Sam68 can modulate neoplastic transformation, and therefore has tumor suppression or growth inhibition properties. No other STAR protein has been associated to tumorigenesis by the RHKO strategy and the mechanism by which Sam68 modulates tumorigenesis is still unclear.

3.2.3 Retroviral transport (RREs and CTEs)

Sam68 has been shown to facilitate the export of retroviral unspliced RNAs containing a HIV Rev responsive element (RRE; Reddy et al., 1999) and RNAs containing a constitutive transport element (CTE; Coyle et al., 2003). The mechanism by which Sam68 performs these tasks still remains unknown. Tyrosine phosphorylation of Sam68 has been observed to impair its ability to facilitate the export of unspliced RNAs (Derry et al., 2000; Coyle et al., 2003).

3.2.4 Signal transduction

Sam68 is tyrosine phosphorylated upon leptin stimulation of peripheral blood mononuclear cells. This phosphorylation enhances its association with the SH2 domain of the PI3K p85 subunit (Martin-Romero and Sanchez-Margalet, 2001). Insulin binding to its receptor induces the tyrosine phosphorylation of the insulin receptor substrate 1 (IRS), as well as the cytoplasmic relocalization and tyrosine phosphorylation of Sam68 (Sanchez-Margalet and Najib, 2001). Both phosphorylated proteins are capable of interacting with the PI3K p85 regulatory subunit, thus activating the PI3K catalytic subunit (p110). Activation of the IRS-

PI3K intracellular signaling cascade is crucial for most of insulin's effects, including regulation of glucose levels (Li et al., 2002).

Stimulation of the T cell receptor (TCR) triggers the sequential activation of the Src-family kinases p56^{lck} and p59^{fyn}, which initiated TCR signaling. Sam68 also associates with and is tyrosine-phosphorylated by both p59^{fyn} and p56^{lck} (Fusaki et al., 1997) in activated T cells, implicating Sam68 in the signal transduction downstream of the TCR-coupled Src family kinases. In all these examples, Sam68 may be part of a multifunctional module required for the activation of overlapping pathways. Because tyrosine phosphorylation of Sam68 has been shown to negatively regulate the RNA-binding properties of Sam68 in vitro (Wang et al., 1995; Barlat et al., 1997), the association of tyrosine-phosphorylated Sam68 to signaling molecules may represent an unresolved but important link between RNA metabolism and signal transduction.

3.2.5 Regulation of CD44 exon v5 alternative splicing (Matter et al., 2002)

A binding site for Sam68, corresponding to a high-affinity Sam68-binding sites previously defined by SELEX was identified in the CD44 exon v5 subdomain L. Sam68 can also bind the subdomains M and R but no consensus binding site for Sam68 was found within them. Forced expression of Sam68 in mouse EL4 T lymphoma cells affected only weakly the inclusion of v5 exon. However, when the cells were activated with phorbol ester, it markedly enhanced the exon inclusion in a dose-dependent manner. A mutation replacing two nucleotides in L binding site sequence by cytidine (L/cc) abolishes Sam68 binding to the subdomain. Some experiments, with EL4 lymphoma cells, using a transfected splice-reporter-minigene carrying the v5 exon and surrounding sequences showed that the introduction of this mutation was affecting the v5 exon inclusion in the minigene mRNA, suggesting that binding of Sam68 to the high-affinity site in subdomain L is critical for the general level of v5 exon inclusion. However, induction by phorbol ester treatment of the EL4 cells was only mildly affected in the mutant, which might be attributed to additional Sam68-binding sites, or additional v5 regulatory elements. The response to phorbol ester raised the question of whether Sam68 was subjected to activation through signal transduction by Ras cascade activation. Indeed Sam68 was found to be phosphorylated by ERK *in vitro* and *in vivo*, on the Serine 58, Threonine 71, and Threonine 84 (Figure 6). Co-transfections using Sam68 mutated for these sites and *in vitro* splicing experiments could then link the ERK-phosphorylated Sam68 to the induction of v5 exon inclusion, suggesting direct splice regulation by Sam68 phosphorylation. Moreover, Sam68 is crucial to the regulation of v5 exon alternative splicing

since the knock-down of Sam68 expression abolished completely Ras-dependent inclusion of the exon. Sam68 appears to be a first splicing regulatory factor to be linked to signal transduction and modulated directly by ERK MAP kinase.

Aim of the project

The aim of my project was to understand how Sam68, upon Ras signalling and ERK phosphorylation, could provoke the inclusion of exon v5 in CD44 mRNA.

A hypothesis was that Sam68-binding to v5 RNA elements, could stabilize or attract spliceosomal components to the pre-mRNA and/or modulates their activity upon Ras pathway activation. Therefore, in the first place, I wished to identify the RNA regulatory elements bound by Sam68 which could be implicated in the regulation. Furthermore, I aimed at identifiiyng the Sam68 functional domains which link the factor to splicing regulation, and at finding Sam68 partners which may participate in the signal-dependent inclusion in CD44 mRNA.

Materials and Methods

Materials

All general chemicals were supplied from Carl Roth GmbH & Co (Karlsruhe), Merck (Darmstadt), Sigma Chemie GmbH (Deisenhofen), PeqLab (Erlangen), with highest purity grade.

1. Primers

Sam68G178E-f: 5'-gtg ggg aag att ctt gaa cca caa gga aat aca-3'

Sam68G178E-r: 5'-tgt att tcc ttg tgg ttc aag aat ctt ccc cac-3'

a/cbpv5-for: 5'-gaa gag gat tat tac aga cta ttt gat tag-3'

a/cbpv5-rev: 5'-cta atc aaa tag tct gta ata atc ctc ttc-3'

mSamΔN57-for: 5'-cgg gat ccg ccc gcc acg cag ccg ccg c-3'

mSamΔN100-for: 5'- cgg gat ccg aat aag tac ctg cct gaa ctc atg-3'

myc-mSamΔN57-for: 5'-cgg aat tcg ccc gcc acg cag ccg ccg c-3'

myc-mSamΔN100-for: 5'-cgg aat tcg aat aag tac ctg cct gaa ctc atg-3'

A1DS-3': 5'-ttt aaa cgg gcc ctc tag ac-3'

A1DS-5': 5'-act taa gct tgg tac cga gc-3'

myc-mSamEco-for: 5'-cgg aat tcg aga aga gac gat cct gcc tcg-3'

mSamΔC309-Bsi: 5'-gca cgt acg agg tgg tcc aac acc acg tcc-3'

mSamΔC364-Bsi: 5'-gca cgt acg ttc tgg tgc agg tgt ggg agg c-3'

mSamΔC412-Bsi: 5'-gca cgt acg caa gat gac tgg aat ggg acc-3'

v5r: 5'-tac ttg tgc ttg tag cat gtg g-3'

Delv4-for: 5'-tca tta tga cag ttg cca cca g-3'

2. Plasmid constructions

pcDNA3.1 (Invitrogen); pET (=pL53In; Mobitec); pQE-32 (Qiagen)

Name	Description
pcDNA3-Sam68	Expression of wild type mSam68 under the control of a CMV promoter. Described in Matter et al. 2002
pcDNA3-myc-Sam68	Expression of myc-tagged wild type mSam68 under the control of a CMV promoter. Gift from S. Richard
pcDNA3-Sam68 ΔKH	Expression of mSam68 KH domain deletion mutant under the control of a CMV promoter.
pcDNA3-myc-Sam68 ΔKH	Expression of myc-tagged mSam68 KH domain deletion mutant under the control of a CMV promoter.
pcDNA3-Sam68 G178E	Expression of mSam68 G178E mutant under the control of a CMV promoter.
pcDNA3-myc-Sam68 G178E	Expression of myc-tagged mSam68 G178E mutant under the control of a CMV promoter
pcDNA3-Sam68 Δ309-412	Expression of mSam68 mutant with a deletion between the amino acids 309 and 412 under the control of a CMV promoter.
pcDNA3-myc-Sam68 Δ309-412	Expression of myc-tagged mSam68 mutant with a deletion between the amino acids 309 and 412 under the control of a CMV promoter.
pcDNA3-Sam68 Δ364-412	Expression of mSam68 mutant with a deletion between the amino acids 364 and 412 under the control of a CMV promoter.
pcDNA3-myc-Sam68 Δ364-412	Expression of myc-tagged mSam68 mutant with a deletion between the amino acids 364 and 412 under the control of a CMV promoter.
pcDNA3-Sam68 ΔN57	Expression of mSam68 mutant with a deletion of the first 57 amino acids under the control of a CMV promoter.
pcDNA3-myc-Sam68 ΔN57	Expression of myc-tagged mSam68 mutant with a deletion of the first 57 amino acids under the control of a CMV promoter.
pcDNA3-Sam68 ΔN100	Expression of mSam68 mutant with a deletion of the first 100 amino acids under the control of a CMV promoter.
pcDNA3-myc-Sam68 ΔN100	Expression of myc-tagged mSam68 mutant with a deletion of the first 100 amino acids under the control of a CMV promoter.

pETLucv5 (=pETCatEBLucv5)	Expression of Luciferase dependent on CD44 v5-exon inclusion. Described in Weg-Remers et al. 2001.
pETLuc-L/cc	pETLucv5 mutated in the left part for the Sam68 binding site. Described in Matter et al. 2002.
pETLuc-a/c	pETLucv5 mutated in the upstream intronic binding site for Sam68.
pETLuc-dble	pETLucv5 carrying the double mutation: L/cc and a/c.
pETv5	Minigene construct containing exon v4 deleted, exon v5, and surrounding intron sequences. Described in Koenig et al. 1998.
pQE-32-His-Sam68	Expression of His-tagged-Sam68 under the control of a T5 promoter.

2.1 Construction of pcDNA3-Sam68G178E and pcDNA3-myc-Sam68G178E

Codon GGA for Glycine 178 was changed to GAA, encoding Glutamic acid, by QuickChange^{TM}Site-Directed Mutagenesis kit (STRATAGENE). The reaction was set up as indicated below: 5 µl of 10x reaction buffer, 50 ng of DNA template (pcDNA-Sam68 wt prepared from DH5α bacteria), 125 ng of primer Sam68G178E-f and Sam68G178E-r respectively, 1 µl of dNTP mix (provided in the kit), ddH_2O was added to make a final volume of 50 µl and 1µl of pfu DNA polymerase (2.5 µg/µl) was added. The reaction was subjected to the following PCR program: 30 sec at 95°C, 1 min at 55°C, 14 min at 68°C; 18 cycles totally. After PCR amplification, 1µl of *DpnI* restriction enzyme (10 U/µl, provided in the kit) was directly added to the reactions and incubated at 37°C for 1 hr. The DNA was then extracted by phenol/chloroform followed by precipitation, and dissolved in 4µl ddH_2O. These 4 µl were transformed in 50 µl of XLblue supercompetent cells according to the instructions of the manufacturer. Colonies were inoculated for plasmid mini-preparation. Maxi-preparation of the positive clones are then done. The mutation was verified by sequencing.

2.2 Construction of pETLuc-a/c and pETLuc-dble

A mutagenesis was performed on pETLuc-v5, exchanging an Adenine for a Cytosine (See Figure beneath) giving pETLuc-a/c, using the QuickChange^{TM}Site-Directed Mutagenesis kit (STRATAGENE). The primers used were a/cbpv5-for and c/cbpv5-rev.

The exact same mutagenesis was then performed on pETLuc-L/cc to produce the double mutant: pETLuc-dble.

Mutations were verified by sequencing.

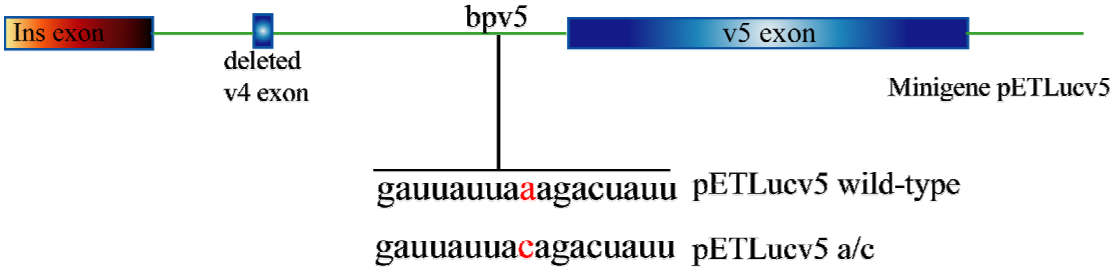

Mutation a/c introduced in pETLucv5
Scheme representing Sam68 putative binding site bpv5. Nature and location of the mutation a/c introduced in pETLucv5 by QuickChangeTMSite-Directed Mutagenesis kit (STRATAGENE). Mutated nucleotide represented in red.

2.3 Construction of pcDNA3-Sam68ΔN57, pcDNA3-Sam68ΔN100

These two N-terminal deletion constructs were generated by PCR-mediated deletions from pcDNA3-Sam68: Forward primers were mSamΔN57-for and mSamΔN100-for. mSamΔN57-for hybridizes on Sam68 sequence after the 170th nucleotide (corresponding to the position of the 57th amino-acid) and exhibits a *BamHI* site at the 5' end. mSamΔN100-for hybridizes on Sam68 sequence after the 310th nucleotide (corresponding to the position of the 100 amino-acid) and exhibits a *BamHI* site at the 5' end.

The reverse primer was A1DS3' and hybridized downstream of the Sam68 sequence on the pcDNA vector sequence.

The PCR DNA fragments obtained and pcDNA3-1 are then submitted to digestion with *BamHI* and *EcoRI*. The two digested fragments were then ligated in the digested pcDNA3-1 vector (see methods for the protocol).

The constructs were verified by sequencing.

2.4 Construction of pcDNA3-myc-Sam68ΔN57, pcDNA3-myc-Sam68ΔN100

These N-terminal Sam68 deletion mutants are cloned in pcDNA3-myc vector, between *EcoRI* sites in 5' and 3'. The strategy is the same than for pcDNA3-Sam68ΔN57 and pcDNA-Sam68ΔN100: Forward primers designed are myc-mSamΔN57-for and myc-mSamΔN100-for. Myc-mSamΔN57-for hybridizes on Sam68 sequence after the 170th nucleotide (corresponding to the position of the 57th amino-acid) and exhibits an *EcoRI* site at the 5' end. Myc-mSamΔN100-for hybridizes on Sam68 sequence after the 310th nucleotide (corresponding to the position of the 100 amino-acid) and exhibits an *EcoRI* site at the 5' end. The PCR DNA fragments obtained and pcDNA3-myc vector are then submitted to digestion with *EcoRI*. The two digested fragments are then ligated in the EcoRI digested pcDNA3 myc vector (see methods for the protocol).

After phenol/chloroform extraction and precipitation, the DNA is transformed in DH5α bacteria and incubated for 1 hr at 37°C. All the bacteria are plated on LB plates (100mg/ml Ampicillin) and incubated overnight at 37°C. Colonies were inoculated for mini-preparation. Mini-prepared plasmids are then digested with *EcoRI* to select the positive clones. The constructs were sequenced before application.

2.5 Construction of pcDNA3-Sam68ΔKH and pcDNA3-myc-Sam68ΔKH

This Sam68 mutant was deleted, by PCR, for the entire KH domain which contains the RNA Binding Domains of Sam68:

A first fragment was amplified from the region upstream the Sam68 KH domain using A1DS5' as the forward primer and ΔKHtot-rev as the reverse primer. A1DS5' is located upstream Sam68 sequence in pcDNA3 sequence. ΔKHtot-rev hybridizes just upstream the Sam68 KH domain and exhibits a *BsiWI* site at the 5' end. This fragment was then digested with BamHI, whose site is located at the 5' end of Sam68 sequence and BsiWI, whose site is located at the 3' end of the fragment.

The second fragment was amplified from the region downstream Sam68 KH domain using ΔKHtot-for as the forward primer and A1DS3' as the reverse primer. ΔKHtot-for hybridizes downstream Sam68 KH domain and exhibits a *BsiWI* site at the 5' end. A1DS3' is located downstream Sam68 sequence in pcDNA3 sequence. This fragment was then digested with *BsiWI*, whose site is located at the 5' end of the fragment, and *EcoRI*, whose site is located at the 3'end of Sam68 sequence.

The two digested fragments were ligated together into pcDNA-Sam68 digested with *BamHI*/*EcoRI*.

To construct the pcDNA3-myc-Sam68ΔKH plasmid an ApaI fragment from pcDNA-myc-Sam68ΔKH was ligated in the ApaI digested pcDNA3-myc-Sam68wt, replacing the wt sequence with the KH domain deleted sequence.

The constructs were sequenced before application.

2.6 Construction of pcDNA3-Sam68Δ309-412, pcDNA3-Sam68Δ364-412 and pcDNA3 myc-Sam68Δ309-412, pcDNA3-myc-Sam68Δ364-412

These C-terminal deletion mutants for Sam68 were generated by PCR-mediated deletions of the coding region for amino-acids 309 to 412 or for amino-acids 364 to 412 from the Sam68 sequence.

The strategy requires two Pwo amplifications on pcDNA3-Sam68wt.

A first fragment was amplified from the region upstream of the 309th or of the 364th amino-acid using mycSamEco-for as the forward primer and mSamΔC309-Bsi or mSamΔC364-Bsi as reverse primers. mycSamEco-for hybridizes in the 5' part of Sam68 sequence and carries an *EcoRI* site at the 5' end. mSamΔC309-Bsi and mSamΔC364-Bsi hybridize just downstream the 922th nucleotide (corresponding to the 309th amino-acid) or downstream the 1147th nucleotide (corresponding to the 364th amino-acid) of Sam68, respectively, and exhibit a *BsiWI* site at the 5' end. This fragment is then digested with *SacII* and *BsiWI*. The *SacII* site is located in the 5' part of Sam68 sequence.

A second fragment was amplified from the region downstream the 412th amino-acid of Sam68 using mSamΔC412-Bsi as the forward primer and A1DS3' as the reverse primer. mSamΔC412-Bsi hybridizes just downstream the 1285th nucleotide (corresponding to the 412th amino-acid) of Sam68 and exhibits a *BsiWI* site at the 5' end. A1DS3' is located downstream Sam68 sequence in pcDNA3 sequence. This fragment was then digested with *BsiWI*, and *XhoI*, whose site is located downstream Sam68 sequence in pcDNA3.

The two digested fragments are ligated together in a pcDNA-Sam68 digested with *SacII*/*EcoRI*.

The constructs were verified by sequencing.

Corresponding pcDNA3-myc constructs were obtained as follows:

pcDNA-Sam68Δ309-412 was digested with SacII and XhoI. SacII is located in the 5' part of Sam68 sequence and XhoI in the 3' part. The fragment obtained was ligated in a SacII/XhoI digested pcDNA-myc-Sam68 wt vector.

pcDNA-Sam68Δ364-412 was digested with ApaI. There are two ApaI sites: one located in the 5' part of Sam68 sequence and one located in the 3' part. The fragment obtained was ligated in a ApaI digested pcDNA-myc-Sam68 wt vector.

3. Radiochemicals

[^{32}P]γ-ATP (Amersham Life Science) 100µl = 1mCi = 37 MBq

4. Antibodies

Anti-Sam68 (C20) rabbit polyclonal; Santa Cruz Biotech., Heidelberg

Anti- GST (Z5) rabbit polyclonal; Santa Cruz Biotech, Heidelberg

Anti-myc (9E10) mouse monoclonal; Roche

Anti-IgG mouse monoclonal; Sigma-Aldrich

Anti-hnRNPA1 mouse monoclonal; gift from Dr. Gideon Dreyfuss

Anti-U2AF65 mouse monoclonal; Sigma-Aldrich

5. Cell lines

LB cells: mouse T-cell lymphoma cell line (Zahalka et al., 1993) cultured in RPMI medium (Invitrogen), supplemented with 10% FBS (Foetal Bovine Serum, PAA), 1x non-essential amino-acids, 10mM Hepes pH 7.4, 1mM sodium pyruvate, 100 units of streptomycin/penicillin, 50µM β-Mercaptoethanol (all from GIBCO BRL), and 0.5 mg/ml bovine insulin (SIGMA).

Jurkat cells: human T cell leukemia cell line, cultured in RPMI medium containing: 10% FCS, and 100 units of streptomycin/penicillin.

METHODS

1. Plasmid minipreparation

Individual colonies (DH5α bacteria) were picked from an LB agar plate (1% tryptone, 0.5% yeast extract, 1% NaCl, 1.5% Agar and corresponding antibiotic) and inoculated into 3 ml of LB medium (1% tryptone, 0.5% yeast extract, 1% NaCl) containing an antibiotic. After overnight incubation at 37°C with shaking speed at 220 rpm, 1.5 ml of bacteria were pelleted by centrifugation at 10000 rpm for 10 sec. The pellet was resuspended in 100μM of solution I . 200 μL of solution II was added and mixed gently by inverting the eppendorf tube for 6 times. After 5 min incubation at room temperature, 150 μL of 3M sodium acetate pH 4.8 was added, mixed gently and incubated on ice for 5 min. The protein-DNA complex was cleared off by centrifugation at 10000 rpm for 15 min. The supernatant was transferred into a new eppendorf tube, and the DNA was extracted with 225 μL of phenol and 225 μL of chloroform/Isoamylic alcohol (24/1). After mixing thoroughly, the samples were centrifuged 5 min at 12000 rpm. The supernatant was again transferred to a new eppendorf tube and DNA was precipited on ice for 15 min, by adding 2.5 volume of 100% ethanol and 1/10 volume of 3M sodium acetate pH 4.8. The plasmid was finally recovered by centrifugation at 12000 rpm (Centrifuge Eppendorf 5415D) for 15 min. The pellet was washed once with 75% Ethanol. After air-drying, the plasmid was resuspended in 50 μL of DDH_2O containing RNase A (20 μg/ml).

buffers	compositions
Solution I	50mM Glucose; 25mM Tris-HCl, pH 8.0; 10mM EDTA pH 8.0.
Solution II	200 mM NaOH, 1% SDS, made freshly

2. Plasmid maxipreparation

According to the protocol from QIAGEN, 200 μL of LB medium containing bacteria, left from the minipreparation, was inoculated into 200 ml of selective LB medium, and

incubated at 37°C for 14hr. the bacteria were harvested by centrifugation at 4500 rpm (centrifuge Hermle ZKH01) at 4°C for 15 min. The pellet was resuspended in 10 ml of buffer 1, and 10 ml of buffer 2 was added and mixed gently. The mixture was incubated at room temperature for 5 min. 10 ml of chilled buffer 3 was added, mixed and the sample were incubated on ice for 15 min. After centrifugation at 9000 rpm (centrifuge Swing-out Beckmann Avanti J-20) for 30 min at 4°C, supernatant was applied to a pre-equilibrated (buffer QBT) QIAGEN-tip 500 and allow to enter the resin by gravity flow. The QIAGEN-tip 500 was then washed 2 times with 30 ml of buffer QC and DNA was eluted with 15 ml of buffer QF. DNA was then precipitated on ice for 15 min, by adding 15 ml of isopropanol to the eluted DNA fraction. The samples were then centrifuged for 15 min, at 4000 rpm (centrifuge eppendorf 5810R) at 4°C. The pellet was washed with 15 ml 75% Ethanol and re-centrifuged for 5 min, at 4000 rpm (centrifuge eppendorf 5810R) at 4°C. After being air-dried, the pellet was dissolved in 300 μL of ddH_2O. DNA concentration was determined by UV spectrophotometry and calculated according to the following formula: 1 OD260=50 μg/ml of double-strand DNA.

Buffers	Composition
Buffer P1 (Resuspension Buffer)	10 mM EDTA;100 μg/ml RNase A
Buffer P2 (Lysis Buffer)	200 mM NaOH; 1% SDS
Buffer P3 (Neutralization Buffer)	3 M potassium acetate, pH 5.5
Buffer QBT (Equilibration Buffer)	700 mM NaCl; 50 mM MOPS, pH 7.0; 15% isopropanol (v/v) ; 0.15% Triton® X-100 (v/v)
Buffer QC (Wash Buffer)	1 M NaCl ; 50 mM MOPS, pH 7.0 ; 15% isopropanol (v/v)
Buffer QF (Elution Buffer)	125 mM NaCl ; 50 mM Tris-Cl, pH 8.5 ; 15% isopropanol (v/v)

3. Preparation of electro-competent bacteria

One colony was inoculated into 5 ml YENB medium (0.75% bacto yeast extract; 0.8% Bacto Nutrient Broth) and incubated overnight at 37°C with shaking (220 rpm). 1 liter of YENB was then inoculated with 5 ml bacterial culture and incubated at 37°C with shaking

(220 rpm) until the OD at 600nm reaches 0.6. To harvest the bacteria, the flask was first chilled on ice for 5 min and then the bacteria were spun at 4000 rpm (centrifuge Hermle ZKH01) at 4°C for 10 min. The pellet of bacteria was washed 2 times with 100 ml of ice cold water. Each of these steps required a centrifugation at 4000 rpm (centrifuge Hermle ZKH01) at 4°C for 10 min. The pellet was resuspended in 20 ml of cold 10% glycerol, then the sample was again centrifuged at 4000 rpm (centrifuge Hermle ZKH01), at 4°C for 10 min. The pellet was finally resuspended in 3 ml cold 10% glycerol and aliquoted and frozen in dry ice cold eppendorfs (40µL/tube) before to be stored at -80°C.

4. Ligation of DNA fragment into a vector

In all cases, the insert and vector were loaded on agarose gel to check the DNA content before ligation, and ligated at the amount ratio of about 4x the amount of insert for 1x the amount of vector.

The vector cut by restriction enzymes was, before the ligation, treated with Shrimp Alkaline phosphatase (1U/µl; Promega): 41µL DNA (5µg) was incubated with 5µL 10x buffer and with 4µL Phosphatase at 37°C for 15 min, then at 65°C for 15 min to inactivate the enzyme. The DNA vector was recovered by phenol/chloroform extraction and ethanol precipitation.

Ligation was performed in a total volume of 20 µL with insert and vector, 1x ligation buffer and 1µL of Ligase (Promega). The sample was incubated either at 16°C if the cut ends were sticky or at 4°C if the cut ends were blunt, overnight.

5. Transformation of electro-competent bacteria

Usually, DNA was introduced in DH5α bacteria.

The aliquot of electro-competent bacteria were thawed on ice.

One electroporation cuvette (0.1 cm gap; PEQLAB) per transformation was also placed on ice. In an eppendorf tube, 10 ng DNA were then mixed with 40 µL of competent bacteria suspension, by pipetting up and down. The mix was transferred into the cuvette which was placed in the E.coli Pulser (BioRad) and pulsed at 1.8 kV. Immediately 1 ml of SOC medium (20 g/L Bacto-tryptone; 5 g/L Bacto-yeast extract; 10 mM NaCl; 2.5 mM KCl freshly supplemented with 10mM $MgCl_2$/$MgSO_4$ and 20mM Glucose) was added into the cuvette and mixed to the bacteria by pipetting up and down. The bacteria suspension was then transferred into a 15 ml blue cap tube and incubated at 37°C with shaking (220 rpm) for 1 hr.

100 µl of the transformed bacteria suspension was plated on an agar plate containing the appropriate antibiotic for selection of plasmid containing cells.

6. SDS-polyacrylamide gel electrophoresis (SDS-PAGE)

Proteins were electrophoretically separated on the basis of size using the method of Laemmli (1970). The resolving gel (10% acrylamide) and the stacking gel (5% acrylamide) were cast according to Sambrook *et al.* (1989). Samples are run into the stacking gel at 120 V, and then run at 160 V during the day or 30 V overnight.

The running buffer contained 30.3 g/L Tris-base, 144g/L Glycine, and 1% SDS.

7. Western Blotting

After proteins were separated by SDS-PAGE, they were electrically transferred onto Immobilon membrane (Millipore, type PVDF, pre-soaked in methanol) at 35 V for at least 6 hrs in Transfer Buffer (25 mM Tris-base, 190 mM Glycine, 20% Methanol). Following the completion of the transfer, in order to reduce unspecific binding of the antibodies to the PVDF membrane, the blot was incubated in PBS-0.2% Tween containing 10% non-fat dried milk (Blocking solution), for 45 min at room temperature with shaking. For detection of proteins of interest, the membrane was further incubated in PBS-0.2% Tween blocking solution containing the appropriate primary antibody (at the manufacturer-recommended dilution) for 1 hr at room temperature with shaking. After 3 washes (5 min each at room temperature with shaking), the membrane was incubated in blocking solution containing a 1:1000 dilution of HPR-conjugated secondary antibody. The membrane was then washed 5 times 5 min in PBS-Tween. The detection of specific proteins was achieved by enhanced chemiluminescence using ECL Western blotting detection reagents (Amersham) ECL hyperfilms (Amersham) according to the manufacturer's instructions

8. Purification of recombinant His-Sam68

Recombinant His-Sam68 was purified from M15 bacteria using NI-NTA agarose (Qiagen).

20 ng pQE-32-His-Sam68 were transformed in 40µL M15 bacteria (same procedure than DH5α). 100µL of the bacterial suspension were used to inoculate 20ml LB medium containing 1mg/ml Ampicillin and 250µg/ml Kanamycin, followed by incubation at 37°C

overnight with shaking (220 rpm). 5 ml of the pre-culture inoculates 200ml LB medium (1mg/ml Ampicillin and 250 µg/ml Kanamycin). The culture was incubated at 37°C with shaking until the OD at 600nm reaches 0.6. His-Sam68 production was induced by adding 1mM IPTG to the culture, followed by 4 hrs incubation at 37°C with shaking (220 rpm).

The cells were harvested on ice and spun at 6000 rpm (centrifuge Hermle ZKH01) at 4°C for 15 min. The pellet was resuspended in ice cold lysis-buffer (2ml of lysis buffer/g pellet) and transferred into 15 ml blue cap tube. The bacteria were then sonified 3 times with 10 sec pulses, with 30 sec of break between the sonication steps. The bacterial lysate was then centrifuged for 15 min at 10 000 rpm (centrifuge Swing-out Beckman Avanti J-20). The supernatant was transferred to a new tube and 250µL of 50% Ni2+-beads slurry/ml supernatant were added (beads were previously equilibrated in lysis buffer and finally resuspended in lysis buffer to obtain a 50% beads slurry). The sample was incubated at 4°C for 1hr with slow rotation, to allow an efficient binding of His-Sam68 on the Ni2+ beads. The beads were then spun at 4°C for 1 min, at 1000 rpm (centrifuge Hermle Z233 MK). The supernatant was removed and the beads were washed 3 times with 5 ml of ice cold washing buffer (each step of washing separated by centrifugation step at 1000 rpm for 1 min at 4°C). To eluate His-Sam68 from the beads, a volume of elution buffer, corresponding to the volume of the beads slurry was added to the beads, and this was incubated at room temperature for 10 min, with rotation. This elution step was repeated 3 times, each time the elutate was removed from the beads after 1 min centrifugation at 1000 rpm (centrifuge Hermle Z233 MK) at 4°C. The 3 eluates were mixed and dialysed 3 times for 50 min in 600 ml of dialysis buffer. The concentration of the recombinant was estimated by running an aliquot on a SDS-page gel in parallel to different amounts of BSA, followed by coomassie staining. A Bradford assay was also performed in parallel in order to estimate better the recombinant protein concentration. The recombinant His-Sam68 was aliquoted and stored at -20°C after the dialysis.

Buffers	Composition
Lysis Buffer	50 mM NaH_2PO_4; 300 mM NaCl; 10 mM Imidazole; adjusted to pH 8.0; contains EDTA-free proteases inhibitors cocktail (1 tablet for 50ml) and 1mg/ml Lysosyme added freshly)
Washing Buffer	50 mM NaH_2P0_4; 300 mM NaCl;

	20 mM Imidazole; adjusted to pH 8.0
Elution Buffer	50 mM NaH_2PO_4; 300 mM NaCl; 250 mM Imidazole; adjusted to pH 8.0
Dialysis Buffer	20 mM Hepes pH 8.0; 50 mM NaCl; 2 mM EDTA; 1 mM DTT; 50% Glycerol

9. Determination of protein concentration

Protein concentration was determined by performing a Bradford assay.

Different amounts of BSA were used as a standard: 2µg, 5µg, 7.5µg and 10µg of BSA were mixed with 100µL 0.15M NaCl and 1ml Bradford solution (0.01% Coomassie blue G250; 5% Ethanol; 8.5% Orthophosphorique acid; filtered and kept at 4°C) and incubated at room temperature for 2 min. The optic density (OD) of the different samples was taken at 595 nm (BioPhotometer; Eppendorf).

The equation: y=ax+b, where y corresponds to the amount of protein in µg and x corresponds to the OD ("a" represents the the slope of the line and "b" the origin on y axis), could be determined in function of the results obtained with BSA.

Different amounts of the recombinant protein were mixed with 100 µL 0.15 M NaCl and 1 ml Bradford solution. After 2 min incubation at room temperature, the OD of the different samples was measured at 595nm. The equation allowed calculation of recombinant protein concentration.

10. In Vitro phosphorylation of His-Sam68 by recombinant ERK

Four steps of phosphorylation are necessary to phosphorylate 60 to 80 % of His-Sam68.

The first reaction is set up in 70µL: 2µg of His-Sam68 are incubated with 1x Kinase buffer, 1mM ATP-γ-S, and 200 units of P42 MAP Kinase (100 000U/ml; New England Biolabs) at 30°C for 30 min.

After this first step, a second is started by adding 10µl of reactive solution containing 1x Kinase buffer, 1mM ATP-γ-S and 200 units of Kinase and after mixing by pipetting up and down, the sample is again incubated at 30°C for 30 min. This step is again repeated 2 times.

The phosphorylation of His-Sam68 is checked by running a SDS-Page gel with an aliquot of the phosphorylated His-Sam68 in parallel with an aliquot of non-phosphorylated

His-Sam68. Proteins are then transferred to Immobilon membrane (Millipore) followed by detection through Western blotting with Sam68 antibody (C20). Phosphorylation efficiency was checked by the phosphorylation dependent shift in the apparent molecular weight of Sam68.

11. Electro-Mobility-Shift-Assays (EMSA) with RNA-oligo-probes

11.1 Oligonucleotide labelling

4 different RNA oligos were radioactively labelled :

Oligo L-wt: 5'-auagacagaaucagcaccagugcucauggagaa**a**a**u**uggacc-3'

Oligo L/cc: 5'-auagacagaaucagcaccagugcucauggagaa**c**a**c**uggacc-3'

Oligo bpv5-wt: 5'-gaagaagaggauuauua**a**agacuauuugauuaga-3'

Oligo bpv5-a/c: 5'-gaagaagaggauuauua**c**agacuauuugauuaga-3'

The reaction was set up in 30µl: 50ng of RNA oligo was mixed with 1x Polynucleotide Kinase buffer (Promega), 3µl [^{32}P] γ-ATP (Amersham) and 2µl (20 units) Polynucleotide kinase (PNK) and was incubated at 37°C for 1 hr. The unincorporated [^{32}P] γ-ATP was removed through a Sephadex-G50 spin column and the RNA probe precipitated with ethanol and sodium acetate in the presence of 20µg tRNA. After washing with 75% Ethanol, the RNA oligo was resuspended in 100µl DDH$_2$O. The efficiency of the labelling was measured on 2µl of RNA oligo using a Liquid Scintillation Counter (Kendro Laboratory Products). The probes were diluted to 4000 cpm/µl in EMSA buffer (10 mM HEPES pH 7.9; 100 mM KCl; 0.025% NP40; 10% glycerol).

11.2 EMSA reaction

Reactions were set up in 25µl in EMSA buffer (freshly supplemented with 1mM DTT; 1 mM PMSF; and specific phosphatase inhibitors: 500 nM Okadaïc acid, 50µM Dephostatin, 1µM Cypermethrin). The EMSA buffer was added first in the eppendorf tube. Each reaction required then 3µg yeast tRNA, 0.3µg RNasin RNase inhibitor, 100 ng of BSA and the recombinant His-Sam86 (25 to 50 ng when Oligo L-wt or L/cc used or 150 to 250 ng when Oligo bpv5-wt or bpv5-a/c used). After pre-incubation was started at 30°C for 10min, 20 000 cpm (5µl) of probe were added and mixed by pipetting up and down. The samples were then incubated at 30°C for 15 min and loaded on 4% native polyacrylamide gels (Acrylamide: Bisacrylamide 19:1; in 0.5x TBE, Tris-Borate-EDTA) without dye. Gels were run for 30min

at 90 V before loading the samples. After running the gels at 90V for 1.5hr in 0.5x TBE, they were then dried on a pre-heated gel dryer for 30 min followed by autoradiography overnight

12. Co-immunoprecipitation (CoIP)

12.1 Preparation of antibody conjugated beads

40µL of Protein A/G agarose beads/ CoIP were equilibrated in CoIP buffer [50 mM Tris-HCl pH 8.0; 100 mM NaCl; 0.5% NP40, freshly supplemented with 0.1 mM DTT; 1 mM PMSF; 2µg/ml Aprotinin and Leupeptin; if the cells were treated with TPA, the CoIP buffer was also supplemented with specific phosphatase inhibitors: 500 nM Okadaïc acid; 50 µM Dephostatin; 1 µM Cypermethrin (Calbiochem)]. The volume was adjusted to have 40µL of agarose beads in 300 µL of CoIP buffer. The beads were then coupled with 3µg of antibody at 4°C for 3 hrs with rotating.

12.2 Cell lysis

Cells were plated to $8x10^5$ cells/ml the day before the experiment.

Cells were left untreated or were treated with 40ng/ml TPA (Sigma)

$3x10^7$ cells (about 20 ml) were spun at 1300 rpm (centrifuge Eppendorf 5810R) and washed once with 20 ml cold PBS (without Calcium and without Magnesium), then lysed in 1ml CoIP buffer (containing specific phosphatase inhibitors if the cells were treated with TPA) and transferred into eppendorf tubes, followed 15 min incubation on ice. The lysates were then centrifuged at 60 000 rpm (Ultracentrifuge Sorvall Discovery M120SE) at 4°C for 15 min.

12.3 Immunoprecipitations

The antibody conjugated beads were spun at 300 rpm (centrifuge Hermle Z233 MK) and the supernatant was removed. The centrifuged lysates were directly transferred on the antibody conjugated beads, and incubated for 1hr at 4°C with rotating. The agarose beads were then spun at 300 rpm (centrifuge Hermle Z233 MK) and washed 300 µL of lysis buffer. This step was repeated 3 times. Then, the beads were resuspended in 40µL sample buffer (120 mM Tris-HCl pH 6.8; 2% SDS; 10% glycerol; 1% Bromophenol blue) and boiled at 95°C for 5min. The beads were span and the supernatant was loaded on a 10% SDS-PAGE gel. Proteins were then electrically transferred onto PVDF membrane and the membrane was treated with appropriate antibodies: When the CoIPs were done with GST, or Sam68

antibodies, the membrane was treated with U2AF65 antibody; when the CoIPs was done with IgG, hnRNPA1 or U2AF65 antibodies, the membrane was treated with Sam68 antibody.

13. Transfection of LB17 cells with SuperFect reagent (Qiagen)

13.1 Cell preparation

Cells were plated to $8x10^5$ cells/ml the day before the transfection.

Prior to transfection, $7x10^6$ cells/transfection were pelleted and resuspended in 5 ml of fresh medium.

13.2 Reagent preparation

5µg of plasmid DNA were mixed with 150 µl RPMI medium without any additives, then 15 µl of SuperFect reagent were added to the DNA, mixed by pipetting up and down, and incubated at room temperature for 5 min. The transfection mix was then added dropwise to the cells and the plate gently swirled to distribute the transfection mix.

The cells were incubated at 37°C for 2hrs in a CO_2 incubator, then washed with 1x PBS (without calcium and magnesium) and resuspended in 5ml of fresh medium. The cells were harvested 24 hrs after the transfection.

14. Luciferase assay

14.1 Cell lysis

LB17 lymphoma cells were transfected (see chapter 13.Transfection of LB17 cells with SuperFect reagent) with 5 µg pETv5Luc vector 24 hrs prior to luciferase assay. In some experiments, Sam68 wt and Sam68 deletion mutants (2µg of pcDNA-Sam68 transfected) were co-expressed with pETv5Luc (3µg transfected).

24 hrs after transfection, cells were left untreated or were treated with 40 ng/ml TPA at 37°C for 5 hrs in the cell incubator.

The transfected cells were transferred in blue cap tubes on ice, spun at 4°C for 3 min at 1300 rpm (centrifuge Eppendorf 5810R), washed once with 5 ml ice-cold PBS (without calcium and magnesium) and resuspended in 1ml ice-cold PBS before being transferred to an eppendorf tube.

The cells were pelleted at 4°C for 10 sec at 10 000 rpm (centrifuge Hermle Z233 MK) and lysed in 300µl of ice-cold Luciferase assay lysis buffer on ice for 10 min. After clearing

the lysates by a 5 min centrifugation step at 10 000 rpm (centrifuge Hermle Z233 MK), at 4°C, the supernatant was used immediately for the luciferase assay.

14.2 Luciferase assay (Weg-Remers et al., 2001)

The assay buffer and luciferin assay solution were prepared freshly. The luciferin assay solution was prepared in a glass tube and protected against light.

200 µL of lysate was mixed with 350µl assay buffer and 100 µl luciferin assay solution to perform the luciferase assay in a Berthold luminometer (Lumat 9501). 200 µL of the luciferase assay lysis buffer were used to measure the background activity. Values were normalized for the protein concentration in the lysates as measured by the Bradford assay.

Buffers	compositions
Luciferase Assay Lysis Buffer	0.1 M Tris-acetate pH 7.5; 2 mM EDTA; 1% Triton X-100.
Glycylglycine Buffer	25 mM Glycylglycine ; 15 mM MgSO4 ; 4 mM EDTA ; adjusted to pH 7.8 with NaOH.
Assay Buffer	Glycylglycine Buffer containing 1 mM DTT; 2 mM ATP; freshly prepared.
Luciferine assay buffer	10 mM D-Luciferin Firefly (Biosynth AG) diluted 1:50 in Glycylglycine Buffer; freshly prepared.

15. Electroporation of Jurkat cells

Jurkat cells were seeded at $8x10^5$/ml the day before the transfection.

2.10^7 cells per transfection were pelleted at 1300 rpm (centrifuge Eppendorf 5810R) and resuspended in 350µl RPMI without supplements. The cells were mixed with 20 to 30 µg plasmid DNA, incubated at room temperature for 5 min and transferred into electroporation cuvettes (4mm-gap cuvettes; Biorad). Electroporation was performed at 250 mV and 960 µF using a Gene Pulser™ (Biorad). Immediately after electroporation, 1 ml of complete medium

was added into the cuvette to resuspend the cells, which were then transferred in 10ml fresh medium. The cells were harvested 16 to 24 hrs after transfection.

16. Preparation of nuclear extracts by NP40 lysis

Jurkat cells were harvested on ice and washed once with ice-cold PBS. Cells were then lysed in NP40 lysis buffer with 1ml/2x10^7 cells by pipetting up and down 2 to 3 times and by 5 min incubation on ice. The nuclei were then spun at 2000 rpm (centrifuge Hermle Z233 MK) for 2 min at 2°C, resuspended in ice-cold Dignam buffer C (150µl/2.10^7 cells) and incubated on ice for 30 min with occasional agitating. The lysed nuclei were then centrifuged at 60 000 rpm (Ultracentrifuge Sorvall Discovery M120SE), at 2°C, for 15 min, and the supernatant was taken as nuclear extract. Protein concentration was measured by the Bradford Assay.

Buffers	Compositions
NP40 lysis buffer	10 mM Tris-HCl pH 7.4; 10 mM NaCl; 3 mM MgCl2; 0.5% NP40. And 1 mM DTT; 2µg/ml Aprotinin and Leupeptin freshly added.
Dignam buffer C (Dignam, 1990)(18)	20 mM HEPES pH 7.9; 420 mM NaCl; 1 mM EDTA; 1.5 mM MgCl2; 10% glycerol And 1 mM DTT; 2µg/ml Aprotinin and Leupeptin freshly added.

17. RNA affinity precipitation

17.1 Pre-clearing of the nuclear extracts

50µg of Jurkat nuclear extracts were mixed with 20µl of Ultralink-NeutrAvidin slurry [Pierce; pre-equilibrated in EMSA buffer (10 mM HEPES pH 7.9; 100 mM KCl; 0.025% NP40; 10% glycerol and 1 mM DTT; 1 mM PMSF freshly added)], in a total volume of 250µl of EMSA buffer. After 30 min incubation, with rotating, the beads were centrifuged and the supernatant was taken as the pre-cleared extract.

17.2 Binding reaction

Biotinylated RNA oligonucleotides (Eurogentec Bel S.A.) are used to characterize the affinity of Sam68 wild type and deletion mutants for RNA (Matter et al. 2000):

Biot-oligo L-wt: 5'-auagacagaaucagcaccagugcucauggagaaaauuggacc-3'

Biot-oligo Blue: 5'-gguaucgauaagcuugauaucgaauuccugcagcccgcgucg-3'

"Blue" refers to an unrelated 42-mer RNA oligonucleotide derived from the polylinker sequence of pBluescript. It was used as a negative control for the binding of Sam68 to RNA.

Binding reactions were set up in 250µl EMSA buffer. Pre-cleared extracts were incubated with 36µg tRNA and 5µl RNasin at 30°C for 10 min. 250 ng of biotinylated RNA oligonucleotide was added and mixed by pipetting up and down. The mix was then incubated for 15 min at 30°C. 15µl of Ultralink-NeutrAvidin slurry was added and the binding reaction was then incubated, with rotating, at room temperature for 30 min. The Ultralink beads were spun at 3000 rpm (centrifuge Hermle Z233 MK) for 10 sec, and the supernatant was discarded. The beads were washed 4 times with 300 µl EMSA buffer without glycerol. The beads were then resuspended in SDS-sample buffer and boiled at 95°C for 5 min. The supernatant was loaded on a 10% SDS-Page gel and then, the proteins were transferred onto a PDVF membrane by western blotting. The blots were treated with specific antibodies in order to detect if Sam68 or its deletion mutants interact with the RNA element.

18. Ribonucleoprotein immunoprecipitation (RNP-IP) (Niranjanakumari. et al, 2002)

$7x10^6$ LB17 cells were transfected 24 hrs before the RNP-IP with 5µg pETv5, using the SuperFect reagent (Qiagen). Where indicated, Sam68 wt was also coexpressed: 2µg pcDNA-Sam68 wt was then co-transfected with 3µg pETv5.

18.1 In vivo formaldehyde fixation of cells

24 hrs after transfection, cells were treated or not with 40ng/ml TPA (Roche) at 37°C, for 10 min, in the cell incubator. Then, the cells were pelleted at 1300 rpm (centrifuge Eppendorf 5810R) at 4°C, for 3 min, and washed once with 5 ml ice-cold PBS (without Calcium and Magnesium). Cells were resuspended in 5 ml (room temperature) PBS containing 0.1 % formaldehyde (v/v, 0.36M) and incubated for 10 min at room temperature with slow mixing. The crosslinking reactions were then quenched by the addition of glycine

(pH 7.0) to the final concentration of 0.25 M followed by incubation at room temperature for 5 min. The cells were harvested by centrifugation at 1300 rpm (centrifuge Eppendorf 5810R) at 4°C for 3 min, followed by 2 washes with 5ml ice-cold PBS. Fixed cells are lysed in 500µL RIPA buffer.

18.2 Solubilization of crosslinked complexes by sonication

The cells were lysed by 3 rounds of 20 sec sonication with a Bioruptor (Diagenode) adjusted to "middle power". There were 2 min breaks between each cycle. The samples were kept in an ice-water bath during the procedure.

18.3 Fragmentation of RNA

To generate fragments of 400 to 800 base pairs, the samples were subjected to a further sonication: Pulses of 30 sec at the "low power" with 20 sec of breaks in between the sonication, for 3 min. As the samples must be kept in ice-water during the procedure, the water from the bath was then changed again to ice cold water and the samples were sonified for 3 further min.

Determination of RNA Fragments size

The size of the RNA fragments were checked on a 1% Formaldehyde/Agarose gel. The gel is composed of 1g Agarose melted in 76 ml ddH_2O. When the mix is cooled down to 65°C, 5ml 20x MOPS (83.7g MOPS; 13.6g sodium acetate, 3.7g EDTA, equilibrated at pH 7.0 with 5M NaOH) and 18 ml Formaldehyde (37%) were added and mixed. The gel was then poured. RNA extracted from samples were resuspended in 20µL loading buffer mix (freshly prepared: 500µl Formamide; 175µl Formaldehyde (37%); 50µl 20% MOPS; 275µl ddH_2O). After denaturation of the RNA at 56°C for 15 min, it was loaded on the gel. The gel was running at 70 Volts in 1x MOPS.

Insoluble material was removed by centrifugation at 13 000 rpm for 15 min at 4°C. All identical samples are mixed together in order to normalize each RNP IP, and 100µL was saved as a control for RNA extraction, in order to check the amount of input RNA in the different samples.

18.4 Pre-clearing lysates

450µL of lysate was used per RNP-IP and was pre-cleared by mix with 20µl Protein A/G agarose beads (equilibrated in RIPA buffer), and non-specific competitor tRNA (final concentration of 100µg/ml). The mixture was rotated for 1hr at 4°C. The pre-cleared supernatant was removed and used for immunoprecipitation.

18.5 Immunoprecipitation of crosslinked RNP complexes

20µl Protein A/G agarose beads, equilibrated and resuspended in 300µL RIPA buffer were coated with either 2µg anti-GST antibody, anti-Sam68 antibody, or 3µg IgG, anti-hnRNPA1 antibody, anti-U2AF65 antibody, at 4°C, for 3hrs, with rotating. Before the immunoprecipitation, the beads were incubated with 0.5µl of RNasin (40U/µL, promega) for 10 min at 4°C, with rotating. The RNP-IPs were performed for 1.5 hrs at room temperature, with rotating, after the precleared lysate was added on the antibody coated beads. The beads were then washed 4 times with 300µl high-stringency RIPA buffer. Each washing step was followed by 30 sec centrifugation at 4°C at 3000 rpm. The beads were then collected and resuspended in 100µL De-crosslinking buffer.

18.6 Reversal of the crosslinked RNA complexes and RNA purification

The beads resuspended in 100µL Decrosslinking buffer, and the 100µl samples taken as control for RNA extraction, were incubated for 45 min at 70°C, in order to reverse the crosslinks. The RNA was extracted from these samples using 300µl PeqGold reagent (Peqlab) and 80µl Chloroform. The content was mixed thoroughly and incubated at room temperature for 10 min and centrifuged at 12000 rpm, at room temperature, for 10min. The aqueous phase was collected and subjected to isopropanol precipitation (750µl) in the presence of 5g Glycogen (Boehringer) as a carrier. RNA precipitates were collected by centrifugation at 12000 rpm, at room temperature for 15 min, washed with 500µl 75% EtOH, air-dried, and resuspended in 240 µl ddH_2O. The samples are digested by adding 30µl DNase I and 30µl 10x DNase buffer (Promega) (in a final volume of 300µl), for 30 min at 37°C. The RNA are then extracted with phenol/chloroform/isoamylic alcohol (25/24/1) and precipitated with 2.5 vol of 100% EtOH, 0.3 M sodium acetate, and 5µg Glycogen. The RNA pellets were collected by 15 min centrifugation at 12000 rpm, at room temperature, air-dried and resuspended in 20µl ddH_2O.

Buffers	Compositions
RNP-IP RIPA Buffer	50 mM Tris-HCl pH 7.5; 1% NP40; 0.5% sodium deoxycholate; 0.05% SDS; 1 mM EDTA; 150 mM NaCl. Contains complete EDTA-free protease inhibitors cocktail tablet, one tablet for 50 ml; Roche.
RNP-IP high stringency RIPA Buffer	50 mM Tris-HCl pH 7.5; 1% NP40; 1% sodium deoxycholate; 0.1% SDS; 1 mM EDTA; 1 M NaCl; 1 M Urea. 0.2 mM PMSF freshly added.
RNP-IP Decrosslinking Buffer	50 mM Tris-HCl pH 7.0; 1% SDS; 5 mM EDTA; 10 mM DTT added freshly.

18.7 RT-PCR

10µl of RNA was transferred into a new eppendorf for cDNA synthesis.

A 2x reaction mix was then prepared in 10µl: 4µl of 5x RT-buffer is mixed with 1µlDDH20, 2µl 2.5 mM dNTP (Promega), 1µl RNasin (40U/µl, promega), 1µl Random hexamer primers (200ng/µl) and 1µl AMV-reverse transcriptase (200U/µL; promega). The RNA samples were denaturated at 70°C for 3min and rapidly chilled in ice-water. 10µL of the RT-mix was then added to the RNA samples. After incubation at 25°C, for 10 min, the samples were transferred to 41°C for 45 min, following by an incubation at 70°C for 15 min. The RT reaction was then diluted to 100µl with ddH_2O. A RT reaction was also set up without reverse transcriptase in order to check, after the PCR, for contaminating genomic DNA.

5µl of the RT-reaction was used for the PCR; they are added to 20µl ddH_2O in a 200µl PCR tube. Then a mix containing 3.25µl ddH_2O, 10µl 5x Green PCR buffer, 1.25µl of 10mM dNTP, 5µl of 2 pM forward primer, 5µl of 2 pM reverse primer and 0.5µl GoTaq polymerase (4U/µL; Promega), was prepared (25µl final volume), and added to the cDNA.

The PCR reaction was performed in Crocodile III Thermocycler (Appligene, Heidelberg).

To amplify the RNA sequences, coming from the transfected minigene pET-v5, the delv4-for and v5-r primers are used. The delv4 primer is spanning the deletion junction of exon v4 (the

primer is then unable to recognize the endogenous sequence). In this case, 35, 38 or 40 cycles are performed with 3 steps per cycle: 1 min at 95°C; 1 min at 55.4°C; 1.5 min at 72°C.

As a control to check for the amount of beads present in each sample, GAPDH sequence is also amplified using GAPDH-for and GAPDH-rev primers. GAPDH RNA appears to be unspecifically bound to the beads, but as its binding should be the same in all samples, it would indicate any loss of material during the procedure. In this case, 30 cycles are performed with 3 steps per cycle: 1 min at 95°C; 1 min at 55°C; 1.5 min at 72°C.

The amplification products were analysed on 2% agarose gels containing Ethidium Bromide (agarose melted in 1x TAE. 50x TAE: 242g/L of Tris-Base, 57.1 ml/L Acetic Acid, 18.6g/L EDTA). Running buffer was 1x TAE. DNA bands were visualized by UV transillumination.

Results

1. Two RNA binding sites for Sam68

A Sam68 RNA binding site was previously identified in the 5'part of the CD44 v5 exon (also called L part for Left; Matter et al. 2002). It comprises the sequence AAAAUU (Figure 7A) which resembles high-affinity Sam68-binding sites previously defined by SELEX (Lin et al., 1997). The interaction of recombinant Sam68 with this L subdomain was detectable in the Electrophoretic Mobility Shift Assay (EMSA), and replacement of two nucleotides with cytidines (L/cc mutation; see Figure 7A) abolished complex formation with Sam68 (Matter et al., 2002). This mutation reduced the general level of v5 exon inclusion, whereas induction mediated through Ras-pathway activation seemed not to be affected. This result implicated that the signal-dependent induction of splicing might depend on other Sam68 binding sites. Therefore, I inspected the vicinity of the CD44 v5 exon for further potential Sam68 binding sites. An RNA sequence located in the intron upstream of the v5 exon, close to the putative branch point of the intron, resembled the concensus binding site for Sam68 (bpv5; see Figure 7A). In order to determine if this element could in fact act as a second Sam68 binding site, I performed EMSA experiments using recombinant His-tagged-Sam68 and radioactively labelled RNA oligonucleotides carrying the sequence of interest (Figure 7B). As a positive control, I used the sequence derived from the v5 exon L RNA element. Increasing amounts of His-Sam68 led to an increase in the shifted radioactive probes for both the L (Figure 7B, lanes 1 to 4) and the intronic sequence (bpv5) (Figure 7B lanes 5 to 8). Two shifted complexes appeared in the case of the L element. As Sam68 can homodimerize (Chen et al., 1997; Zorn et al., 1997; Chen et al., 1998), the higher molecular weight complex might correspond to a Sam68 dimer bound to the L element, whereas the lower one might be caused by the monomer. Sam68 showed a stronger affinity for the L element compared to the intronic element (bpv5), as a higher amount of His-Sam68 was required to detect the interaction with the bpv5 element. The introduction of an a/c mutation (bpv5 a/c), which was previously shown to impair Sam68 binding to the consensus sequence, actually impairs its binding to the intronic element (Figure 7B, lanes 9 to 12). This result suggests that the bpv5 element is a RNA binding site for Sam68.

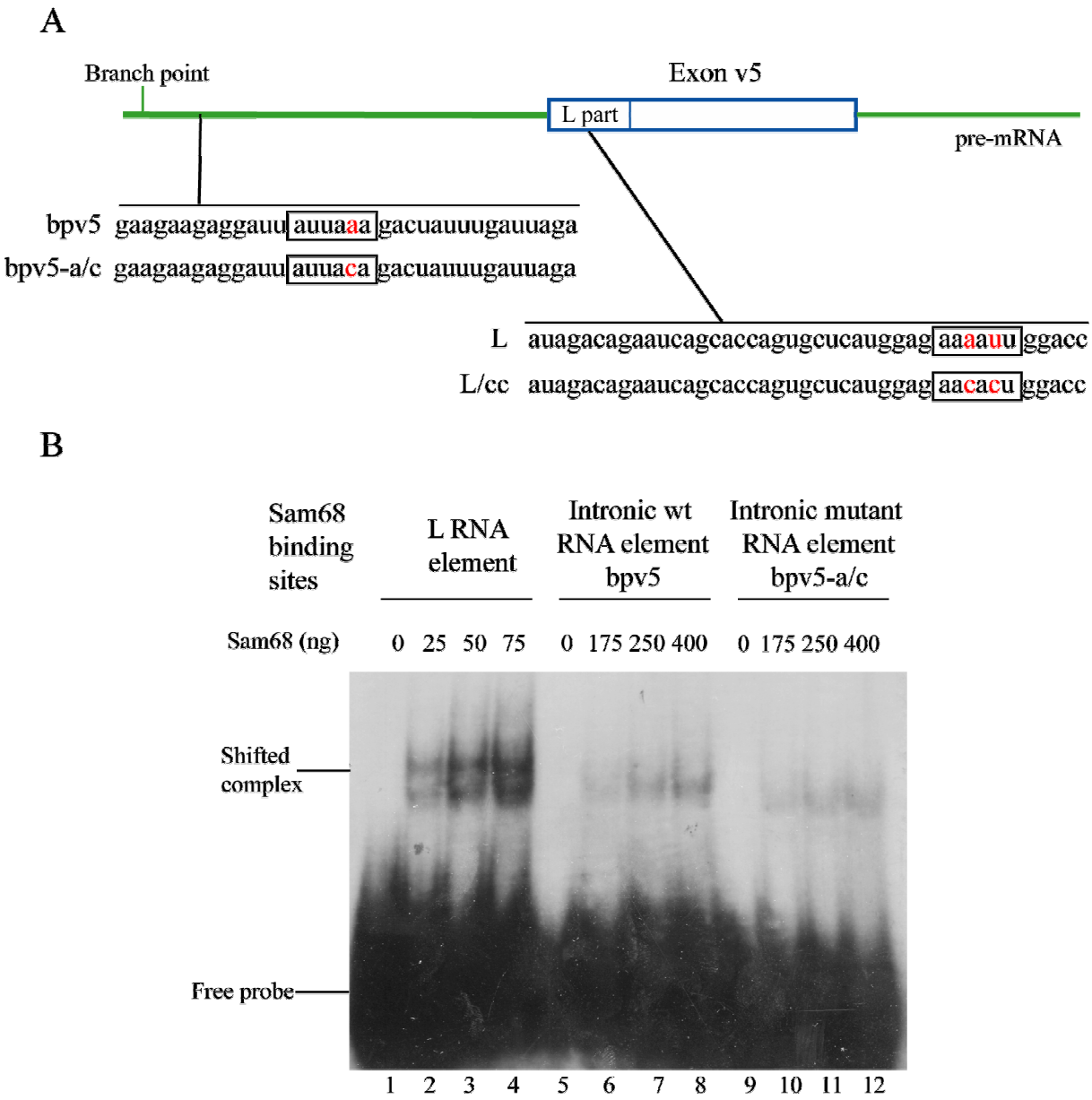

Figure 7: Splice regulatory sequences bound by Sam68.
A: Sequences and location of putative Sam68 binding sites in the CD44 v5 exon (blue square) and surrounding intron sequences (green lines). Elements similar to Sam68 high-affinity binding sequences defined by SELEX (Lin et al., 1997) are boxed; mutated nucleotides are in red. **B:** EMSA experiments using recombinant His-Sam68 and [32P] labelled RNA probes, corresponding to the two Sam68 binding sites. Increasing amounts of His-Sam68 (0 to 400ng) were incubated with 20 000 cpm of L RNA element as a positive control for interaction (lanes 1 to 4), and with the wild-type (lanes 5 to 8) or mutated a/c intronic (lanes 9 to 12) RNA elements. Binding reactions were resolved on a native 4% Polyacrylamide gel.

2. The Sam68 RNA binding sites are not implicated in Ras-induced splicing regulation

Mutation of the Sam68-binding site in subdomain L showed no marked effect on Ras induced splicing of the v5 exon (Matter et al., 2002). To test whether the intronic Sam68 binding site is implicated in the regulation, I transfected different minigenes (based on pETLucv5) expressing luciferase dependent on v5 exon inclusion (Weg-Remers et al., 2001; see Figure 8A) into mouse LB17 lymphoma cells, in which the Ras-MAP kinase pathway and v5 exon inclusion can be stimulated by treatment with the phorbol ester TPA. These minigenes carry either the wild-type sequences for both Sam68 binding sites or mutated sequences for one (L/cc or a/c) or both (dble) Sam68 binding sites. 24 hrs after the transfection, the cells were lysed and the luciferase activity was measured. When the v5 exon is excised from the mRNA, a stop codon appears upstream of the luciferase sequence, whereas the luciferase sequence is in frame when the v5 exon is included (Figure 8A). The Luciferase activity is thus a read-out for v5 exon inclusion. Similarly to the L/cc mutant (as shown in Matter et al. 2002), the mutation of the bpv5 element affected strongly the level of v5 exon inclusion, both without and with phorbol ester treatment (Figure 8B): a four to five fold decrease in luciferase splice-reporter activity was detectable when compared to the wild-type minigene. Mutation of both Sam68 binding sites did not have a stronger effect compared to the single mutations (Figure 8B). Interestingly, induction of v5 exon inclusion, upon phorbol ester treatment (fold induction), was not impaired but rather enhanced when the Sam68 RNA binding sites were mutated (Figure 8C).

A

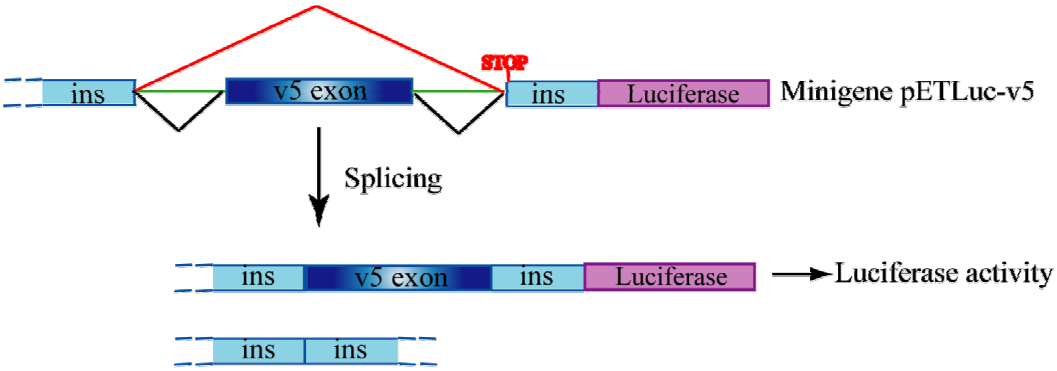
STOP
ins
v5 exon
ins
Luciferase
Minigene pETLuc-v5
Splicing
ins
v5 exon
ins
Luciferase
Luciferase activity
ins
ins

B

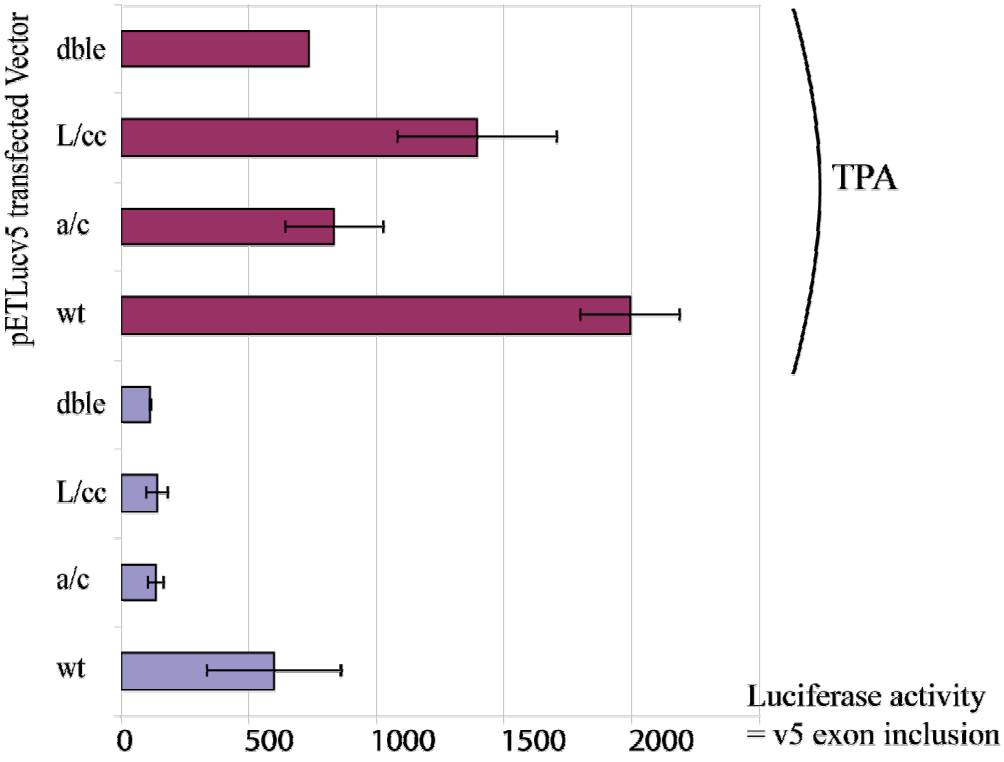
pETLucv5 transfected Vector
dble
L/cc
a/c
wt
dble
L/cc
a/c
wt
TPA
0
500
1000
1500
2000
Luciferase activity
= v5 exon inclusion

C

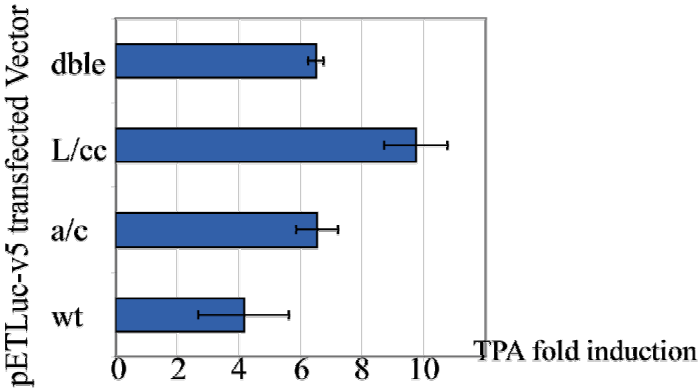
pETLuc-v5 transfected Vector
dble
L/cc
a/c
wt
0
2
4
6
8
10
TPA fold induction

Figure 8: Sam68 RNA-binding sites and Ras-induced regulation.
Mouse LB17 lymphoma cells ($7x10^6$) were transfected with 5µg pETLuc-v5 constructs carrying the wild-type v5 sequence (wt) or v5 sequences mutated in the v5 bp element (a/c), in the L element (L/cc) or in both (dble). 24 hrs after transfection, cells were lysed in luciferase assay lysis buffer and luciferase assays were performed. **A:** Scheme representing pETLuc-v5 splicing. Luciferase activity is a read-out for v5 exon inclusion, as a STOP codon appears upstream of the Luciferase sequence if the v5 exon is excised (ins: insulin exons). **B:** Luciferase assays showing the influence on v5 exon inclusion of mutations in Sam68 binding sites. Cells were left untreated or were treated with TPA to induce the Ras MAP kinase pathway. **C:** Fold induction of v5 exon inclusion after 5 hours TPA treatment (Luc activity with TPA/ Luc activity without TPA).

These results suggest that binding of Sam68 to the high-affinity site in subdomain L and to the upstream intronic site is critical for the general level of v5 exon inclusion. Induction by TPA, however, might depend on other or multiple RNA sequences, not identified yet. Alternatively, the result could indicate that the binding of Sam68 to RNA is not necessary for the signal-dependent induction of v5 splicing, or that the loss or the weakening of Sam68 RNA-binding is part of the induction process.

3. Signal-mediated induction of exon v5 splicing does not require RNA binding of Sam68

To examine whether Sam68 has to bind RNA to induce inclusion of the v5 exon following MAP kinase activation, I tested the activity of two Sam68 mutants: Sam68ΔKH was deleted for the entire KH domain, which contains the RNA binding region (Lin et al., 1997). Large deletions may change the global folding of the protein and can thus cause a change in the protein function. To be sure that the results observed were really provoked by a loss of affinity for RNA, another more subtle mutant was tested. Sam68G178E is a single codon mutant, which was shown to interfere with Sam68 binding to the highest-affinity RNA sequence, similarly to the deletion of the KH domain (Lin et al., 1997). Using RNA affinity precipitation, I tested their affinity for a biotinylated RNA oligonucleotide carrying the sequence of the exon v5 L element. To do so, expression constructs for myc-epitope-tagged Sam68 wt, myc-Sam68ΔKH or myc-Sam68G178E were transfected into human Jurkat leukemia cells. RNA affinity precipitation was then performed with nuclear extracts prepared from the transfected cells. As shown in Figure 9, the myc-Sam68 wt protein was affinity-precipitated with the biotinylated L sequence (lane 3) but not without an RNA oligonucleotide

(lane 1) or with an unrelated sequence (lane 2), indicating specific precipitation. Myc-Sam68ΔKH could not be precipitated (Figure 9, lane 4), showing that the deletion of the KH-RNA-Binding domain abolished completely the affinity of Sam68 for RNA *in vitro*. Myc-Sam68G178E showed a residual affinity for the L RNA element in this assay (Figure 9, lane 5).

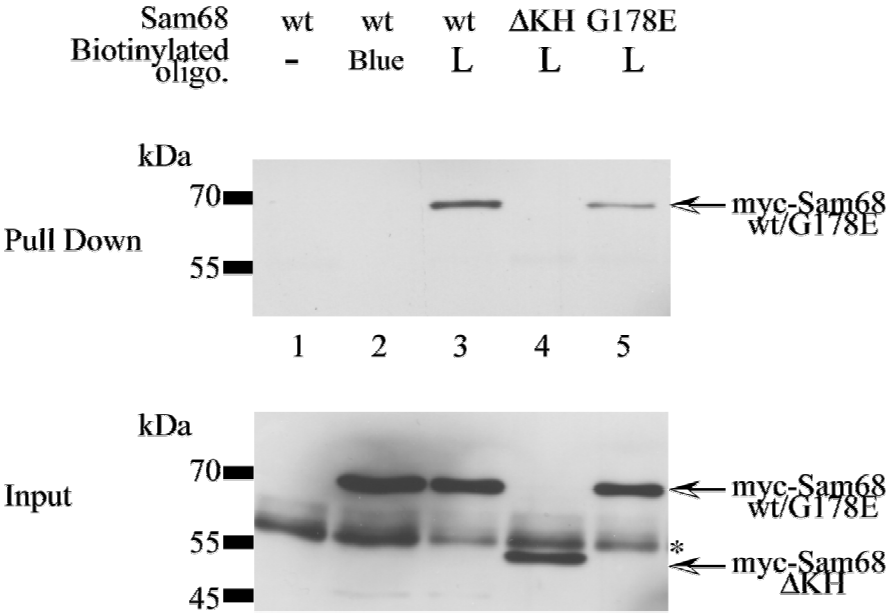

Figure 9: myc-Sam68 ΔKH cannot bind RNA in vitro. The mutation G178E impairs the binding of Sam68 in vitro.
RNA-affinity precipitation of myc-Sam68 wt (lanes 1-3), myc-Sam68 ΔKH (lane 4) and myc-Sam68G178E (lane 5) with biotinylated RNA oligonucleotides. $2x10^7$ human Jurkat leukemia cells were transfected with 30µg pcDNA expression constructs for myc-Sam68 wt or mutants. After 24hrs, nuclear extracts were prepared from the transfected cells and incubated with 15µl Ultralink-NeutrAvidin slurry and 250ng of biotinylated 42-mer RNA oligonucleotides: L corresponds to the L RNA element and "Blue" refers to an unrelated RNA sequence derived from the polylinker sequence of pBluescript (lane2). After washing, the Ultralink NeutrAvidin beads were boiled in SDS-sample buffer and the supernatant was loaded on a SDS-PAGE **(upper panel)**. As a control for myc-Sam68 content in the input material, 20µg of nuclear extract was subjected to SDS-PAGE **(lower panel)**. After transfer to a PVDF membrane, myc-Sam68 was detected with anti-myc antibody. * Corresponds to an unspecific band.

To determine the activity of the Sam68 RNA-binding mutants on CD44 v5 exon splicing, I co-transfected the splice-reporter minigene pETLucv5 with expression constructs for murine Sam68 (wild-type or mutants ΔKH, G178E) or with the empty expression vector into murine LB17 lymphoma cells. Forced expression of Sam68 led only to a slight increase in luciferase splice-reporter activity in the absence of TPA (as also shown by Matter et al., 2002), but it enhanced v5 exon inclusion 2-3 fold, once the cells were activated with TPA (Figure 10A and 10B). Both mutants, Sam68ΔKH and Sam68G178E, behaved very similarly to the Sam68 wt protein (Figure 10A and 10B). This result suggests that Sam68 binding to RNA is not necessary for the signal-dependent induction of CD44-v5 exon inclusion. The result further shows that the KH domain of Sam68 is not an essential domain for this process.

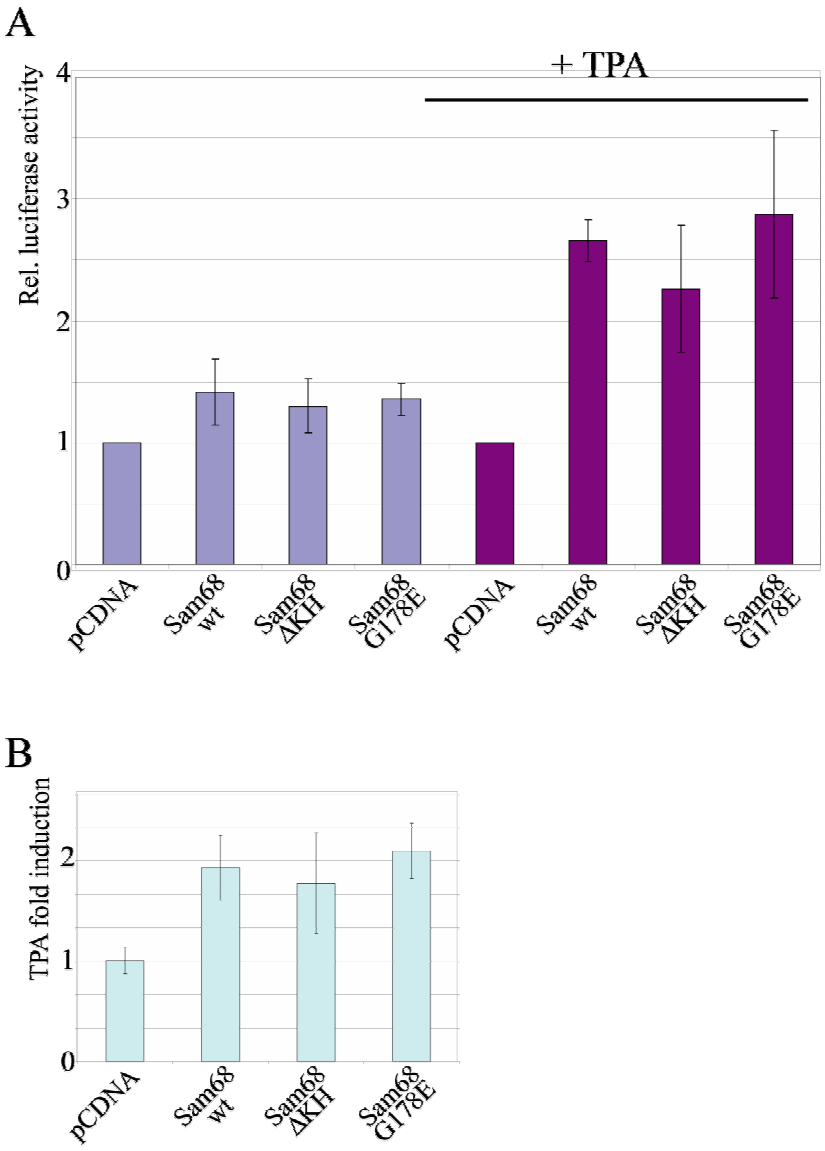

Figure 10: Sam68 is able to mediate signalling-induced splicing without binding to RNA. Mouse LB17 lymphoma cells ($7x10^6$) were transfected with 3µg pETLuc-v5 wt, and either 2µg of pcDNA empty vector as a control, or 2µg of pcDNA expression constructs for Sam68 wt, Sam68-ΔKH or Sam68-G178E. 24hrs after transfection, cells were lysed in Luciferase assay lysis buffer and luciferase assays were performed. **A:** Luciferase assay showing pETLuc-v5 splicing influenced by forced expression of Sam68 wt, Sam68ΔKH or Sam68G178E. Luciferase activity is a read-out for v5 exon inclusion. The activity of each assay is divided by the activity measured with the cotransfected pcDNA empty vector (set as 1). Cells were either left untreated or treated with TPA to induce the MAP-kinase pathway. **B:** Fold induction of v5-exon inclusion in mRNA after 5 hours TPA treatment (Luc activity with TPA / Luc activity without TPA).

4. ERK phosphorylation of Sam68 impairs its binding to RNA *in vitro* and *in vivo*

RNA-binding of Sam68 appears not to be required for Ras-pathway-induced exon v5 splicing. Moreover, induction of v5 exon inclusion, upon Ras-pathway activation, was not impaired but rather enhanced when the Sam68 RNA-binding sequences were mutated (see Figure 8C). Considering these facts, loss or weakening of Sam68 binding to RNA could be a necessary step in the induction process. Since phosphorylation of Sam68 by ERK MAP-kinase is involved in Ras-induced v5 splicing (Matter et al., 2002), I tested the possibility that this modification of Sam68 could affect its binding to RNA. To do so, I performed Electrophoretic Mobility Shift Assays (EMSA) using different amounts of recombinant His-Sam68 or His-Sam68 phosphorylated by ERK *in vitro* (resulting in approximately 80% phosphorylated Sam68; see Figure 11B), and radioactively labelled RNA oligonucleotides containing the L subdomain of exon v5 or the upstream intronic RNA element. As shown in Figure 11A with both the L element (lanes 1 to 5) and the intronic element bpv5 (lanes 6 to 10), less shifted radioactive probe could be detected when incubated with different amounts of phosphorylated His-Sam68 compared to non-phosphorylated His-Sam68. Since the amounts of phosphorylated and non-phosphorylated His-Sam68 used in this assay were equal (Figure 11B), the result suggests that ERK phosphorylation of Sam68 impairs its binding to RNA *in vitro*.

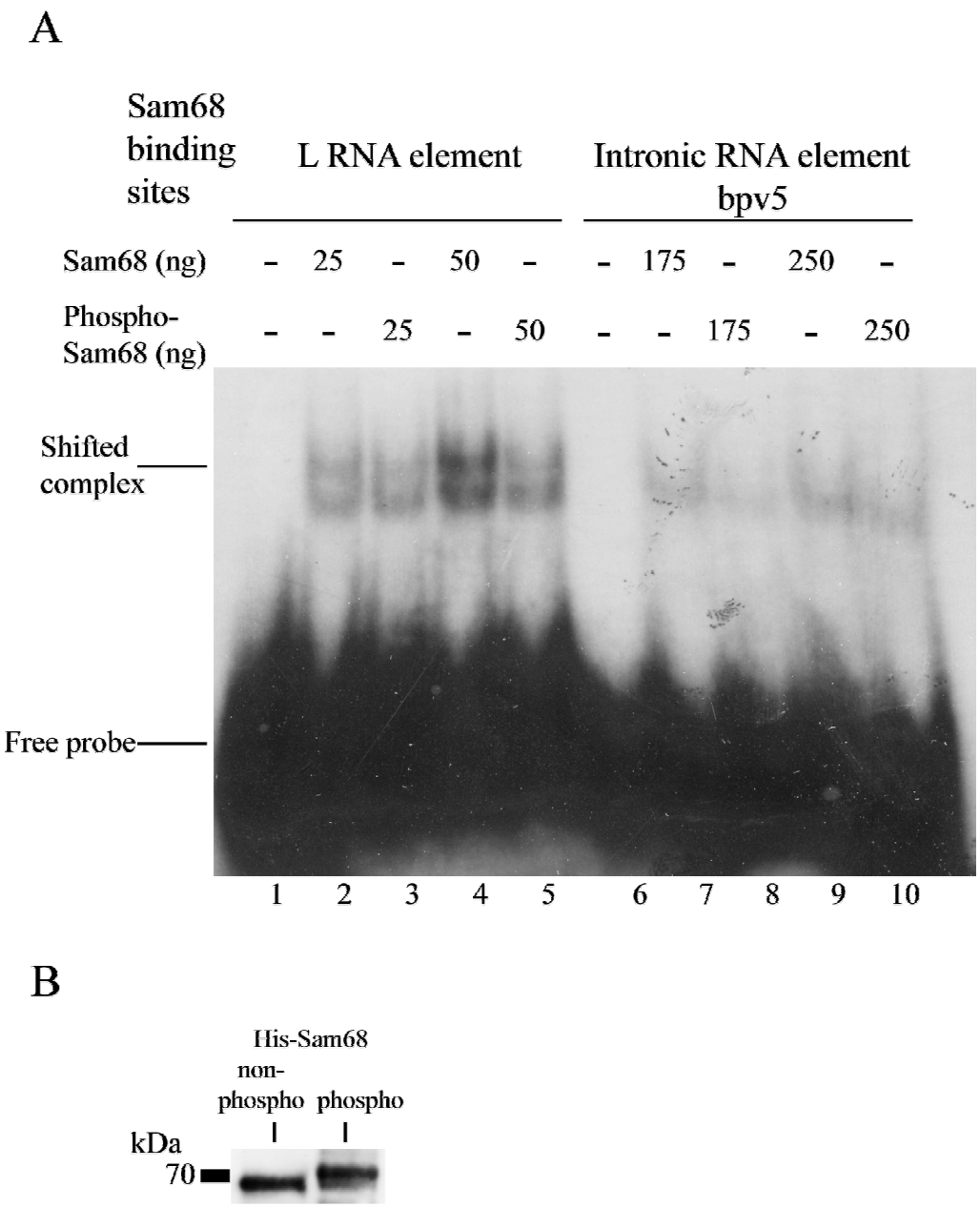

Figure 11: Phosphorylation of Sam68 by Erk impairs its RNA-binding capability in vitro.

A: EMSA experiments using recombinant His-Sam68 and [32P] labelled RNA oligonucleotides. Different amounts of His-Sam68 or of His-Sam68 phosphorylated by Erk in vitro were incubated with 20 000 cpm of RNA oligonucleotides containing the L subdomain of exon v5 (lanes 1 to 5) or the upstream intronic RNA element (bpv5; lanes 6 to 10). Binding reactions were resolved on a native 4% Polyacrylamide gel. **B:** 250ng of recombinant non-phosphorylated His-Sam68 was loaded in parallel with 250ng of recombinant His-Sam68 phosphorylated with ERK in vitro, on a 10% SDS-PAGE, followed by western-blotting with an anti-Sam68 antibody.

To test whether binding of Sam68 to the RNA elements in the v5 exon and the upstream intronic sequence changes upon ERK stimulation in cells, I established Ribonucleoprotein Immunoprecipitations (RNP-IP) with pre-mRNA (see scheme Figure 12). The underlying method (Niranjanakumari et al., 2002) allows characterization of *in vivo* interactions between RNA and proteins. Since only a small proportion of CD44 pre-mRNA molecules include CD44 exon v5 upon TPA stimulation (König et al., 1998), changes in protein binding to this minority of molecules upon Ras pathway activation would be difficult to detect. To overcome this issue, mouse LB17 lymphoma cells were transfected with a minigene carrying the v5 exon and surrounding intron sequences, flanked by insulin exons (pETv5; König et al., 1998). The majority of pre-mRNA-molecules from this construct include the v5 exon upon TPA treatment. Twenty-four hours later, the cells were fixed *in vivo* with formaldehyde in order to crosslink interactions between RNA and proteins (Figure 12; step 1). After cell lysis (Fig. 12; step 2), the RNA is fragmented to an average size of 500 base pairs, to reduce the size of the RNA sequences which will co-precipitate with the crosslinked protein. These crosslinked complexes were then immunoprecipitated with an anti-Sam68 antibody (Fig 12; step 3). An anti-GST antibody was used as a control in order to check the specificity for precipitation. After the immunoprecipitation, the crosslinks were reversed, and RNA was extracted from the samples and analysed by RT-PCR to detect the RNA fragments of interest in the precipitates (Fig 12; steps 4 to 7).

1-Formaldehyde fixation: crosslink RNA-Protein interactions

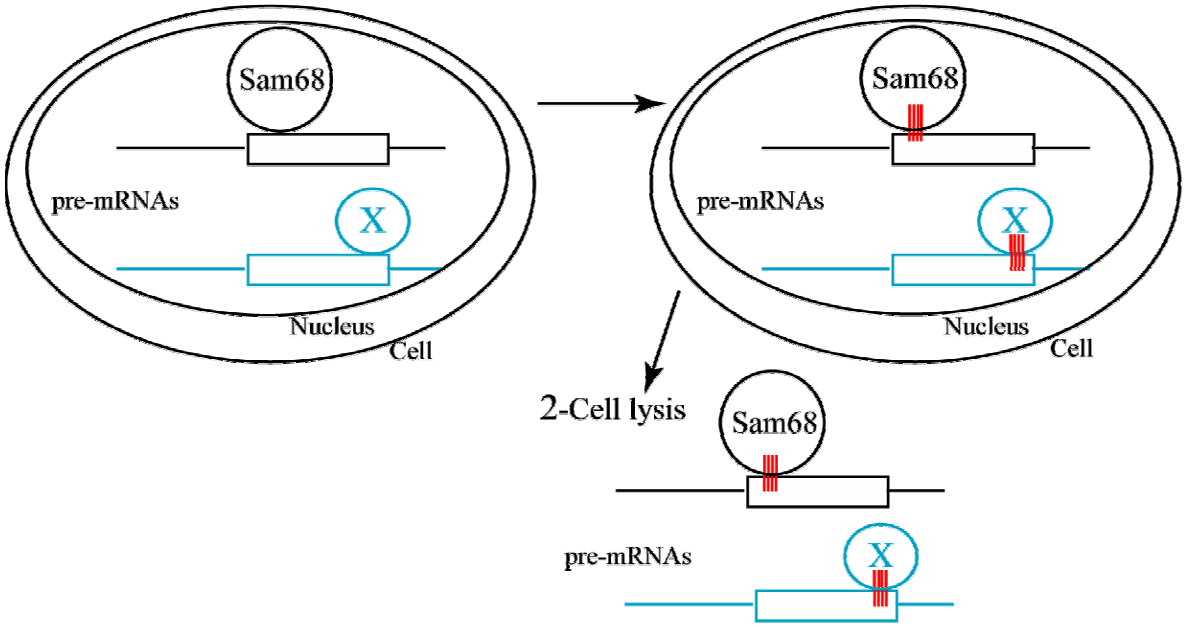

3-Immunoprecipitation of the protein of interest Sam68

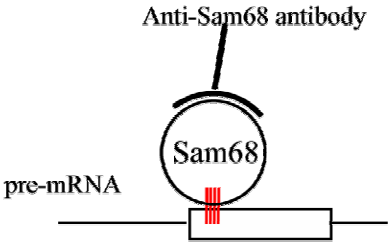

4- Crosslinked complexes are reversed

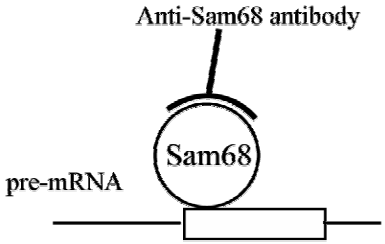

5-Extraction of RNA co-precipitated with Sam68
Reverse transcription using Random primers

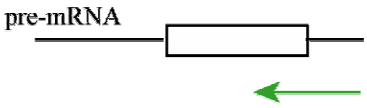

6- PCR using specific primers

7- Analyse on agarose gels

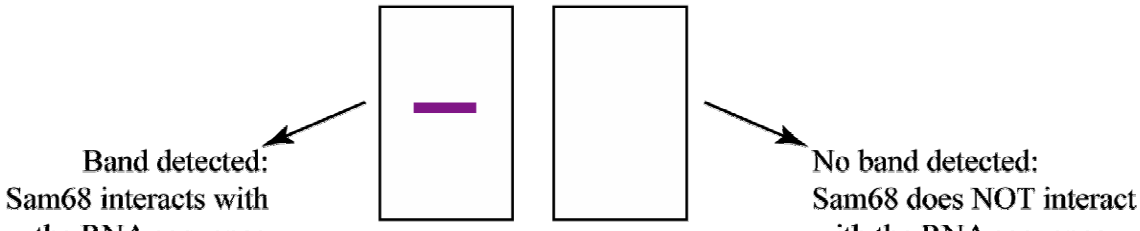

Band detected:
Sam68 interacts with
the RNA sequence

No band detected:
Sam68 does NOT interact
with the RNA sequence

Figure 12: Scheme representing the different steps of the in vivo Ribonucleoprotein Immunoprecipitation (RNP-IP) method (Niranjanakumari et al., 2002).
The RNA-fragmentation step is not represented here.

Specific primers were used to amplify the region of interest from the pre-mRNA fragments of the minigene pETv5 (Figure 13A). As shown in Figure 13B, the RNA-fragments generated were 400 to 700 base pairs in size, allowing the precipitation of the 570 bp minigene fragments. To check that differences seen in the RT-PCR were not due to a loss of material during the procedure, an amplification to detect unspecifically bound transcripts (GAPDH) was performed (Figure 13C, lower panel).

The portion of the minigene pre-mRNA spanning exon v5 and the upstream intron was immunoprecipitated with the anti-Sam68 antibody, and the level of bound RNA was lower when the cells were treated with TPA (Figure 13C, upper panel, lanes 2 and 3). The Sam68 immunoprecipitation was specific since the product amplified from the sample precipitated with the anti-GST antibody was barely detectable (Figure 13C, upper panel, lane 1). As shown in Figure 13D, the western-blot analysis confirmed that TPA treatment of the LB cells was effective, resulting in phosphorylation of part of the Sam68 molecules (Matter et al., 2002).

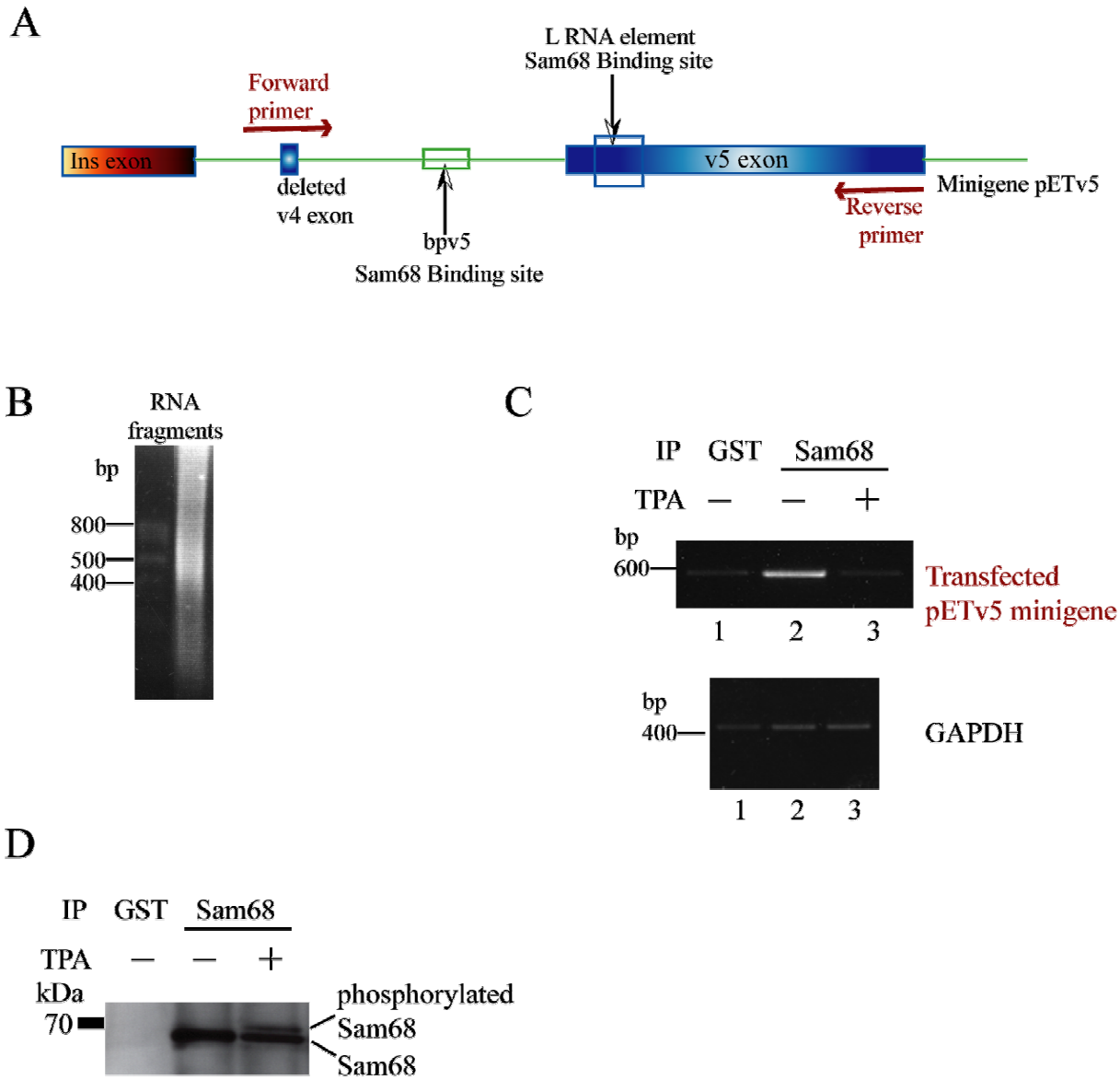

Figure 13: Binding of Sam68 to pre-mRNA in vivo is impaired following Ras-MAP kinase pathway activation.
Ribonucleoprotein immunoprecipitation using mouse LB17 lymphoma cells transfected with 5µg pETv5, either left untreated or stimulated with TPA to induce the Ras-MAP kinase pathway. Cells were fixed with 0.1% formaldehyde and were then lysed in RIPA buffer. RNA was fragmented by 2 rounds of 3 min sonication (30 sec of pulse, and 20 sec of break). Sam68 was then immunoprecipitated with 3µg anti-Sam68 antibody C20 and 20µL of protein A/G agarose beads. An antibody against GST was used as a specificity control. Crosslinks were reversed by incubating the washed beads in decrosslinking buffer at 70°C for 45 min. RNA was extracted and RT-PCR was performed to detect RNA fragments of interest. **A:** Scheme representing the region on the transfected minigene amplified by RT-PCR. **B:** Analysis of RNA fragmentation. The fragment size was checked on 1% Formaldehyde/Agarose gels. An RNA ladder (Low range RNA Ladder, Fermentas) was loaded in parallel as a size marker. **C:** Analysis of RT-PCR products on 2% agarose gels. Expected sizes for the amplification products were 570 bp for the pETv5 minigene-derived fragment and 400 bp for GAPDH fragment. **D:** Immunoprecipitation control. Beads used in the RNP-IP were resuspended in

SDS-sample buffer and boiled at 95°C for 5 min. The supernatant was loaded on a 10% SDS-PAGE gel and after transfer on PDVF membrane, Sam68 was detected with anti-Sam68 antibody.

Taken together, the *in vitro* and *in vivo* RNA-binding data suggest that the Ras-pathway induced phosphorylation of Sam68 through ERK results in impaired binding of Sam68 to RNA elements involved in CD44 v5 splicing. The release of Sam68 from the mRNA is thus an important step in this signalling-induced splicing process.

5. Sam68 N- and C-terminal domains are functional in alternative splicing of v5 exon

The highly conserved KH domain characterizes the STAR family proteins, such as Sam68, and its integrity was shown to be essential for many physiological processes (Jones et al., 1995; Barlat et al., 1997). However, I showed that the KH domain of Sam68 is not an essential domain for the Ras-induced v5 exon splicing. To understand how Sam68 may affect the splicing machinery, I wished to determine the protein domain(s) necessary for the splice regulation. To do so, I co-transfected the splice-reporter minigene pETLucv5 with expression constructs for Sam68 wild-type or for Sam68 carrying deletions of the C-terminal portions (Sam68 Δ309-412; Sam68 Δ364-412), or of the N-terminal parts (Sam68 ΔN100; Sam68 ΔN57), into murine LB17 lymphoma cells. As a control the empty expression vector was co-transfected. The effect of forced expression of these different Sam68 proteins on v5 exon inclusion was then studied by Luciferase assays.

5.1 Deletion of the tyrosine-rich C-terminal domain of Sam68 abolished the induction of v5- exon inclusion

As shown in Figure 14A, the basal and phorbol-ester-induced activity of Sam68 Δ309-412 and Sam68 Δ364-412 C-terminal deletion mutants was 2-3 fold reduced compared with the activity of Sam68 wt. The calculation of the fold induction upon TPA treatment (Figure 14B) confirmed that both Sam68 mutants were unable to induce v5 exon inclusion upon the Ras-MAP kinase pathway activation (Sam68 Δ309-412 and Δ364-412 TPA fold induction is similar to the TPA fold induction by the pcDNA empty vector). In fact, these mutants have a

trans-dominant-negative effect on v5 exon inclusion (Figure 14A; activity of the mutants compared with pcDNA empty-vector activity and with Sam68 wt activity). There was no significant difference in activity between Sam68 Δ309-412 and Sam68 Δ364-412, suggesting that the two proline-rich domains, lacking in mutant Δ309-412 but not in mutant Δ364-412 (See Figure 6 in introduction section), are not required for Sam68 activity. Conversely, the tyrosine-rich domain deleted in both mutants appears to be crucial for Sam68-mediated inclusion of the v5 exon.

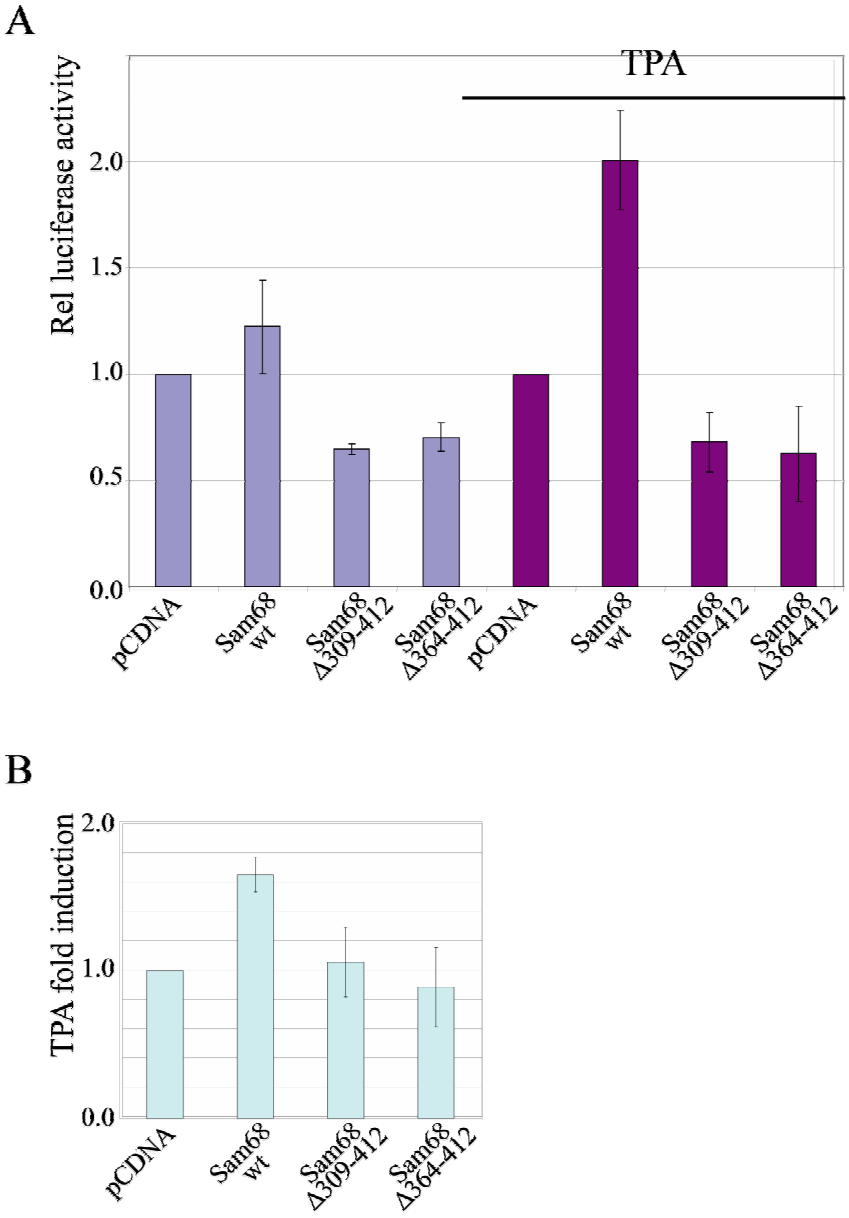

Figure 14: Deletion of the tyrosine-rich domain of Sam68 interferes with v5 exon inclusion.

Mouse LB17 lymphoma cells ($7x10^6$) were transfected with 3µg pETLuc-v5 wt, and either, 2µg of pcDNA empty vector, as a control, or 2µg of pcDNA expression constructs for Sam68 wt, Sam68-Δ309-412 or Sam68-Δ364-412. 24hrs after transfection, cells were lysed in Luciferase assay lysis buffer and luciferase assays were performed. **A:** Luciferase assay showing pETLuc-v5 splicing influenced by forced expression of Sam68 wt, Sam68-Δ309-412 or Sam68-Δ364-412. Luciferase activity is a read-out for v5 exon inclusion. The activity of each assay is divided by the activity measured with the cotransfected pcDNA empty vector (set as 1). Cells were left untreated or were treated with TPA to induce the MAP kinase pathway. **B:** fold induction of v5-exon inclusion after TPA treatment (Luc activity with TPA / Luc activity without TPA).

These large deletions could have modified the global folding of the protein, affecting its function. Any conformational change could affect the natural ability for Sam68, as a STAR protein, to bind RNA. Therefore, I performed RNA affinity precipitations with extracts from Jurkat cells transfected either with the wild-type myc-Sam68 or with the deletion mutants: myc-Sam68 Δ309-412 and myc-Sam68 Δ364-412. Figure 15 (lanes 4 and 5) shows that both deletion mutants can be affinity-precipitated with the v5 subdomain L similarly to the wild-type protein, indicating that RNA affinity *in vitro* was not impaired and suggesting that the global protein folding is not affected by C-terminal deletions.

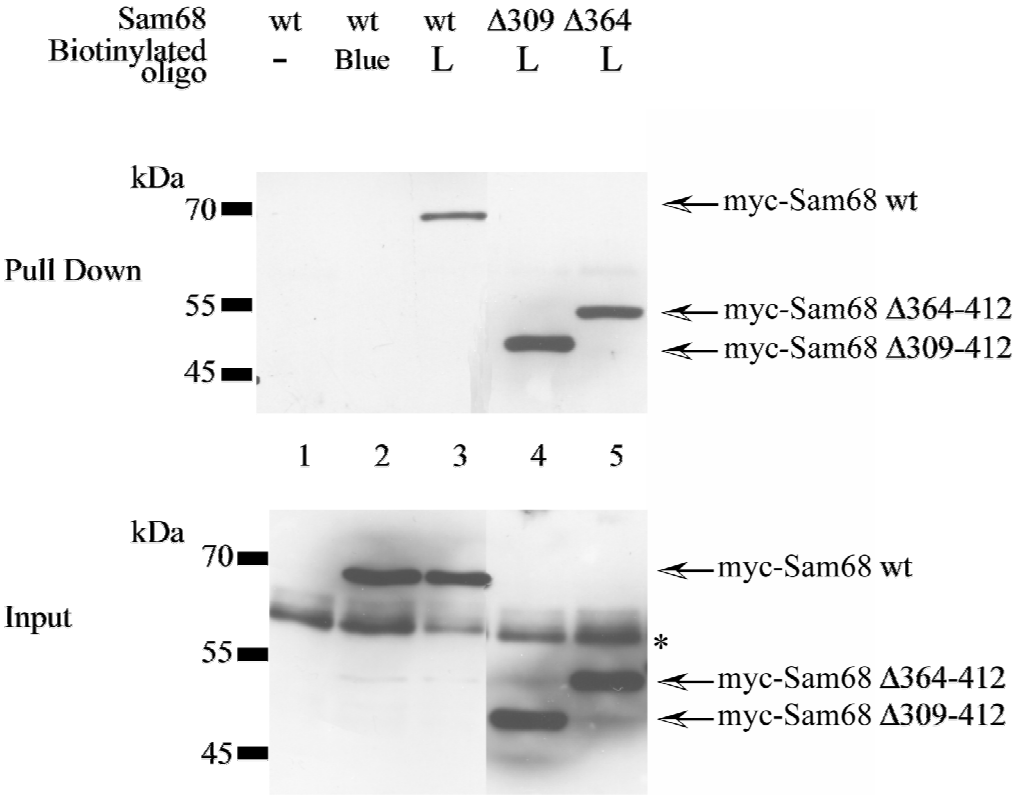

Figure 15: myc-Sam68 ΔC-terminal mutants can bind RNA in vitro.
RNA affinity precipitation of myc-Sam68 wt (lanes 1-3), myc-Sam68 Δ309-412 (lane 4) and myc-Sam68 Δ364-412 (lane 5) with biotinylated RNA oligonucleotides. 2x107 human Jurkat leukemia cells were transfected with 30µg pcDNA expression construct for myc-Sam68 wt or mutants. After 24hrs, nuclear extracts were prepared from the transfected cells and incubated with 15µl Ultralink-NeutrAvidin slurry and 250ng of biotinylated 42-mer RNA oligonucleotides: L corresponds to the L RNA element and "Blue" refers to an unrelated RNA sequence derived from the polylinker sequence of pBluescript (lane2). After washing, the Ultralink NeutrAvidin beads were boiled in SDS-sample buffer and the supernatant was loaded on a SDS-PAGE (**upper panel**). As a control for myc-Sam68 content in the input material, 20µg of nuclear extract was subjected to SDS-PAGE (**lower panel**). After transfer to a PVDF membrane, myc-Sam68 was detected with anti-myc antibody. * Corresponds to an unspecific band.

5.2 Deletion of the Sam68 N-terminal domain increases the activity of Sam68 to induce v5 exon inclusion.

To test the role of the N-terminal domains, I used the mutants Sam68 ΔN57 and ΔN100. They are both deleted for the proline-rich domain P0 and for the RGG motif, whereas Sam68 ΔN100 in addition lacks the portion which contains the proline-rich domains P1 and P2 as well as the phosphorylation sites for ERK (serine 58; threonine 71, threonine 84; See Figure 6 in introduction section). As shown in Figure 16A, the N-terminal Sam68 deletion mutants ΔN100 and ΔN57 showed a similar effect than the wild-type Sam68 on luciferase splice-reporter activity without TPA treatment. Upon Ras pathway activation, however, the forced expression of the N-terminal deletion mutants had a tendency to increase v5 exon inclusion. Considering the TPA fold induction, at least Sam68 ΔN100 enhanced v5-exon inclusion significantly compared with the wild-type Sam68 (Figure 16B). Interestingly, three MAP-kinase phosphorylation sites, lacking in Sam68 ΔN100, were shown to be necessary for at least part of the induction of v5 exon splicing upon phorbol ester treatment. Mutation of these three amino-acids to alanine impaired the ability of Sam68 to mediate phorbol ester-induced exon inclusion (Matter et al., 2002). Their complete deletion together with the proline-rich domains however, showed a positive effect on Sam68 activity upon activation of the Ras-MAP kinase pathway (Figure 16B).

A

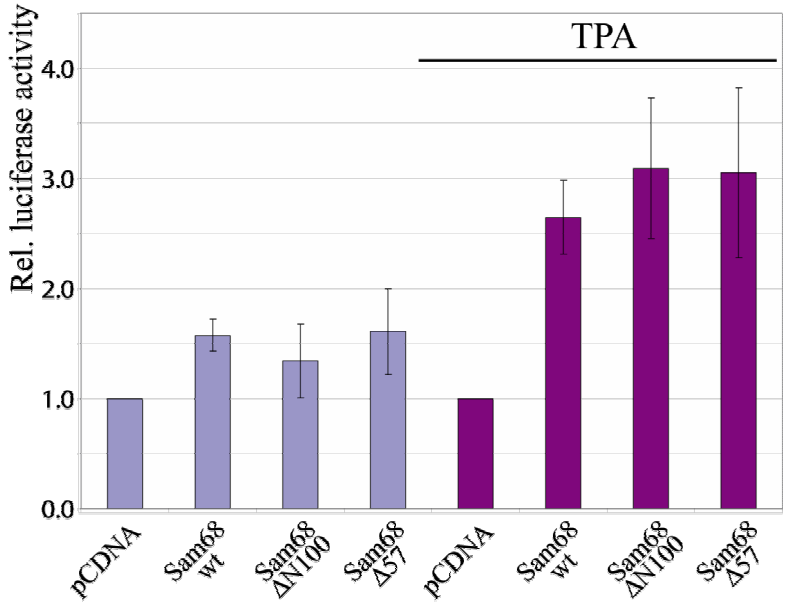

B

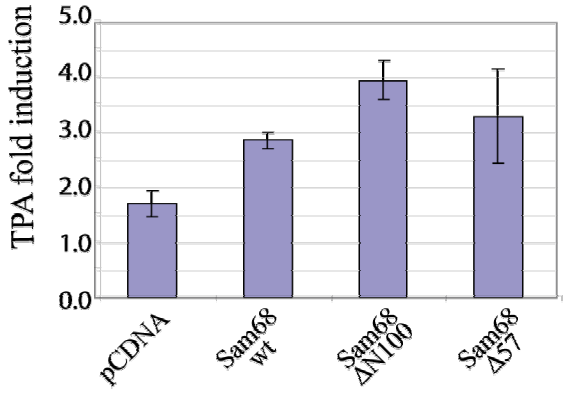

Figure 16: Deletion of Sam68 N-terminal domain led to an increase of Sam68 activity in induction of v5-exon inclusion.
Mouse LB17 lymphoma cells ($7x10^6$) were transfected with 3µg pETLuc-v5 wt, and either, 2µg of pcDNA empty vector, as a control, or 2µg of pcDNA expression constructs for Sam68 wt, Sam68-ΔN100, Sam68-ΔN57. 24hrs after transfection, cells were lysed in Luciferase assay lysis buffer and luciferase assays were performed. **A:** Luciferase assay showing pETLuc-v5 splicing influenced by forced expression of Sam68 wt, Sam68-ΔN100 or Sam68-ΔN57. Luciferase activity is a read-out for v5 exon inclusion. The activity of each assay is divided by the activity measured with the cotransfected pcDNA empty vector (set as 1). Cells were left untreated or were treated with TPA to induce the MAP kinase pathway. **B:** fold induction of v5-exon inclusion in mRNA after 5 hours TPA treatment (Luc activity with TPA / Luc activity without TPA).

Since phosphorylation of these sites impairs Sam68 RNA binding (see Figure 11 and 13), I wished to test the possibility that the N-terminal domains are involved in modulating the RNA-binding capability of the protein. Therefore I performed RNA affinity precipitations with extracts from Jurkat cells transfected either with the wild-type myc-tagged-Sam68 or with the deletion mutants myc-Sam68 ΔN100 and myc-Sam68 ΔN57. Surprisingly, both N-terminal mutants had lost their affinity for RNA *in vitro*. Both of them could not be affinity-precipitated with the exonic v5-splice regulatory element (Figure 17, lanes 4 and 5), although the KH domain (containing RNA Binding domains) remains intact in these mutants. Together with the phosphorylation effect on RNA binding, this result suggests a role for the N-terminal region in modulating RNA binding in a phosphorylation-dependent manner.

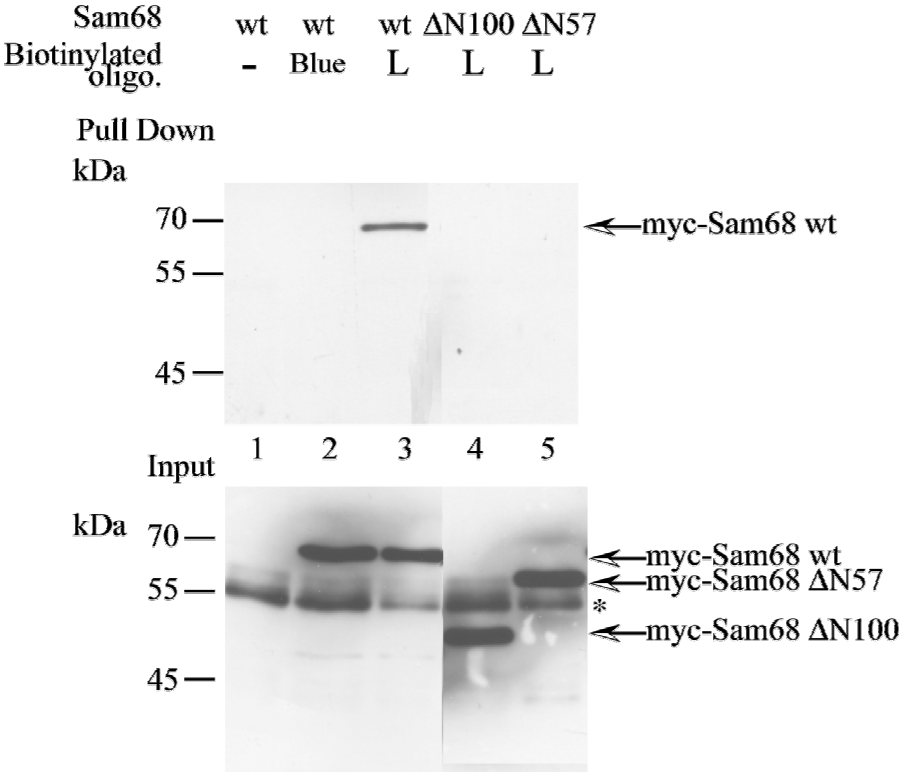

Figure 17: The deletion of the N-terminal 57 or 100 amino-acids of Sam68 abolishes its binding to RNA in vitro.
RNA affinity precipitation of myc-Sam68 wt (lanes 1-3), myc-Sam68 Δ100 (lane 4) and myc-Sam68 ΔN57 (lane 5) with biotinylated RNA oligonucleotides. $2x10^7$ human Jurkat leukemia cells were transfected with 30µg pcDNA expression construct for myc-Sam68 wt or mutants. After 24hrs, nuclear extracts were prepared from the transfected cells and incubated with 15µl Ultralink-NeutrAvidin slurry and 250ng of biotinylated 42-mer RNA oligonucleotides: L corresponds to the L RNA element and "Blue" refers to an unrelated RNA sequence derived from the polylinker sequence of pBluescript (lane2). After washing, the Ultralink NeutrAvidin beads were boiled in SDS-sample buffer and the supernatant was loaded on a SDS-PAGE (**upper panel**). As a control for myc-Sam68 content in the input material, 20µg

of nuclear extract was subjected to SDS-PAGE (**lower panel**). After transfer to a PVDF membrane, myc-Sam68 was detected with anti-myc antibody. * Corresponds to an unspecific band.

To understand how Sam68 can actually affect the splicing machinery, I needed to identify the interacting partners of Sam68 that can be part of the regulating complex on the v5 exon and/or that link Sam68 to the spliceosome.

6. hnRNPA1 and U2AF65 interact with Sam68 in T cells

6.1 The exon-silencing factor hnRNP A1 interacts with Sam68 in vivo

The heterogeneous ribonucleoprotein (hnRNP) A1 was previously identified as part of the exon-silencing complex on the v5 exon, and its overexpression was shown to prevent v5 exon inclusion dependent on exonic RNA-elements (Matter et al., 2000). Moreover, Ras signalling was shown to relieve this hnRNPA1-dependent exon silencing. As Sam68 activity in v5 exon splicing is also dependent on Ras signalling, hnRNPA1 and Sam68 could be functionally connected in the regulation of CD44-v5 exon splicing. To test whether Sam68 could interact with hnRNPA1 *in vivo*, I performed co-immunoprecipitations (CoIPs). Extracts from murine LB17 lymphoma cells were prepared and immunoprecipitations were performed with an anti-hnRNP A1 antibody. Sam68 could be detected in the precipitate of the antibody against hnRNP A1 but not in that of an isotype-matched IgG antibody (Figure 18A lanes 1 and 2), indicating that Sam68 is associated with hnRNPA1 *in vivo*. This association is not caused by RNA bridging (which could be envisaged because both factors are RNA-binding proteins), since treatment of the extracts with RNase A did not impair the co-precipitation of Sam68 with the anti-hnRNPA1 antibody (Figure 18B, compare lanes 2 and 5), although RNAse treatment was effective (Figure 18B, lower panel). As the molecular weight of A1 is in the same molecular weight range as the immunoglobulin light chains, the reverse CoIP, followed by anti-A1 immunoblotting is not possible. To test if Ras signalling had an influence on the association between hnRNP A1 and Sam68, CoIPs were performed with extracts from cells treated with TPA (for 10 min). As shown in Figure 18A, lane 5, TPA treatment induced phosphorylation of Sam68 by ERK, indicated by a characteristic shift in the apparent molecular weight of Sam68 (Matter et al., 2002) upon western-blotting. Whereas I could still detect Sam68 coimmunoprecipitating specifically with A1 antibody, it was not possible to detect the phosphorylated Sam68 (Figure 18A, lane 3). As only 40% of Sam68 in the lysate

was phosphorylated, the amount coprecipitated with A1 antibody might not be enough to be detected by Western-Blotting. Thus, the experiment does not allow one to prove or disprove a change in the interaction between hnRNPA1 and Sam68 upon Ras pathway activation. However, independent of a change in interaction, modification of Sam68 could be involved (e.g. by allosteric effects) in the relief of the hnRNPA1-dependent exon silencing.

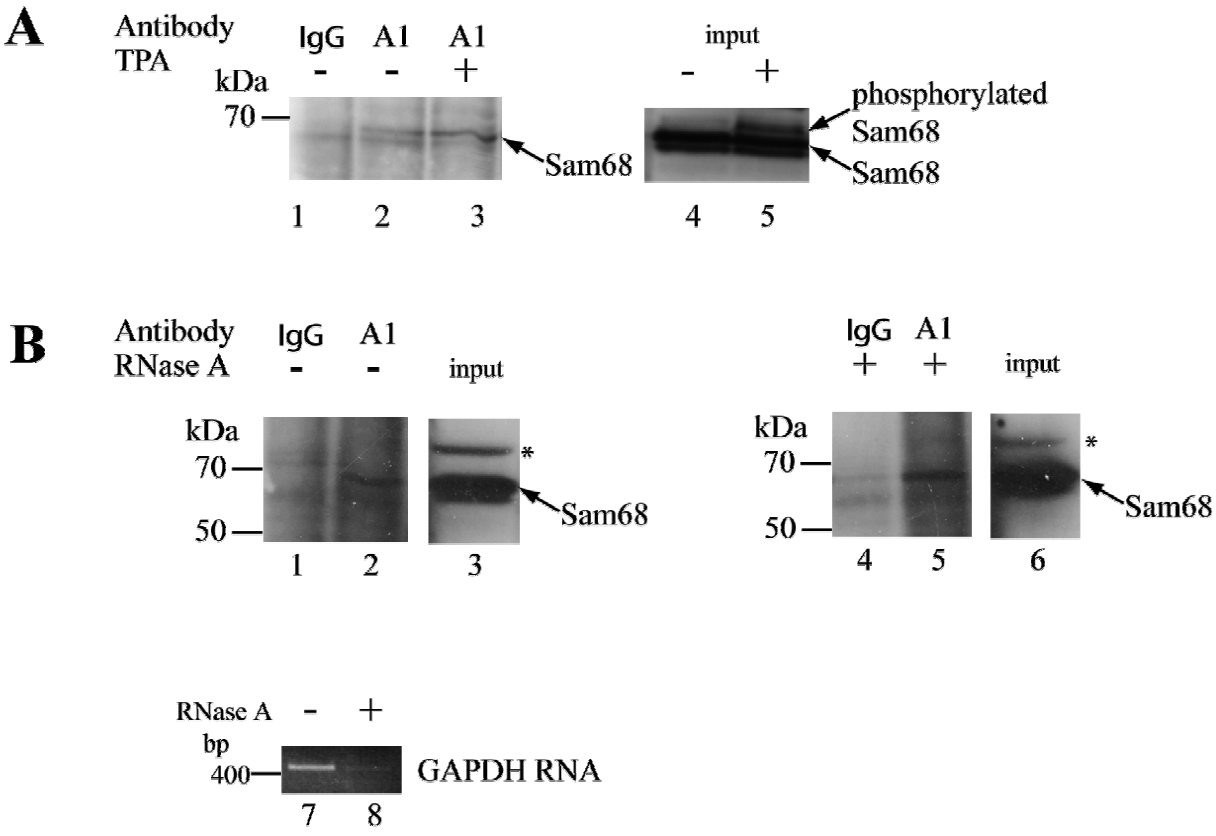

Figure 18: In vivo association between Sam68 and hnRNP A1.
Mouse LB17 lymphoma cells ($2x10^7$ cells), either left untreated (lanes 1, 2 and 4) or treated for 10 min with 40 ng/mL TPA (lanes 3 and 5) to induce the Ras-pathway, were lysed in modified RIPA buffer. **A:** 1/3 of the lysate was incubated with IgG, or anti-A1 antiboby and with 40 µl of equilibrated protein A/G agarose beads. After washing, the beads were boiled and resolved on a SDS-PAGE, followed by western blotting, with an anti-Sam68 antibody. **B:** Samples were treated like in A, but 0.2µg/µl RNase A was added to the lysates 1 hr before precipitation (lanes 4 to 6). RNA was extracted from 100µl of untreated or RNase-treated lysates, and checked by RT-PCR, with specific primers for GAPDH, for RNase effectivity (lanes 7 and 8). Expected sizes for the amplification products were 400 bp. * corresponds to an unspecific band.

6.2 The spliceosome factor U2AF65 interacts with Sam68 in vivo

Alternatively, or in addition, to modulate the activity of the splice-regulatory complex on the v5 exon, Sam68 may regulate the recruitment of spliceosome components and/or spliceosome assembly at the v5 splice sites. Exon v5, as many alternatively spliced exons, is preceeded by a weak 3' splice site with a polypyrimidine tract interrupted by purines. A key factor for 3' splice site recognition appears to be U2 snRNP auxiliary factor (U2AF) (Reed, 1989; Zamore et al., 1992; Coolidge et al., 1997): U2AF35 binds the 3' "AG" dinucleotide whereas U2AF65 recognizes the pyrimidine tract. As the pyrimidine tract does not correspond to a concensus, U2AF65 may need to be attracted and stabilized on the pre-mRNA. Sam68, through protein-protein interaction, could help to stabilise this factor on the pre-mRNA as a prerequisite for spliceosome assembly and v5 exon inclusion.

GST-pull down experiments performed in our group involving recombinant His-Sam68 and GST-U2AF65 indeed showed that U2AF65 and Sam68 can interact *in vitro* (H. König, unpublished). To test whether Sam68 could interact with U2AF *in vivo*, I performed co-immunoprecipitations in LB17 lymphoma-cell lysates, using an anti-U2AF65 antibody. There has been no antibody available against U2AF35 which could be used in CoIPs experiments. Figure 19A shows that Sam68 could be specifically detected in the anti-U2AF65 precipitates, by immunoblotting (lanes 1 and 2). In the reverse experiment using an anti-Sam68 antibody for precipitation, U2AF65 could be detected specifically in the precipitates with anti-Sam68 antibody (Figure 19B, lanes 1 and 2), indicating that Sam68 was interacting with U2AF65 *in vivo.* The *in vitro* experiments done previously, suggested that the proteins can interact directly. This conclusion is further supported by the treatment of the extracts with RNase A prior to precipitation, which did not impair the coprecipitation of Sam68 with anti-U2AF65 antibody (Figure 19C, compare lanes 2 and 5). To test if Ras signalling had an influence on this interaction, CoIPs were performed with extracts from cells treated with TPA. Again Sam68 co-immunoprecipitated specifically with the U2AF65 antibody, but it was not possible to detect the phosphorylated Sam68 (Figure 19A). In addition, it seems that the coprecipitation of U2AF65 with the anti-Sam68 antibody did not change upon TPA treatment (Figure 19B, compare lanes 2 and 5). Thus, I cannot conclude on a change in interaction between U2AF65 and Sam68 upon Ras pathway activation.

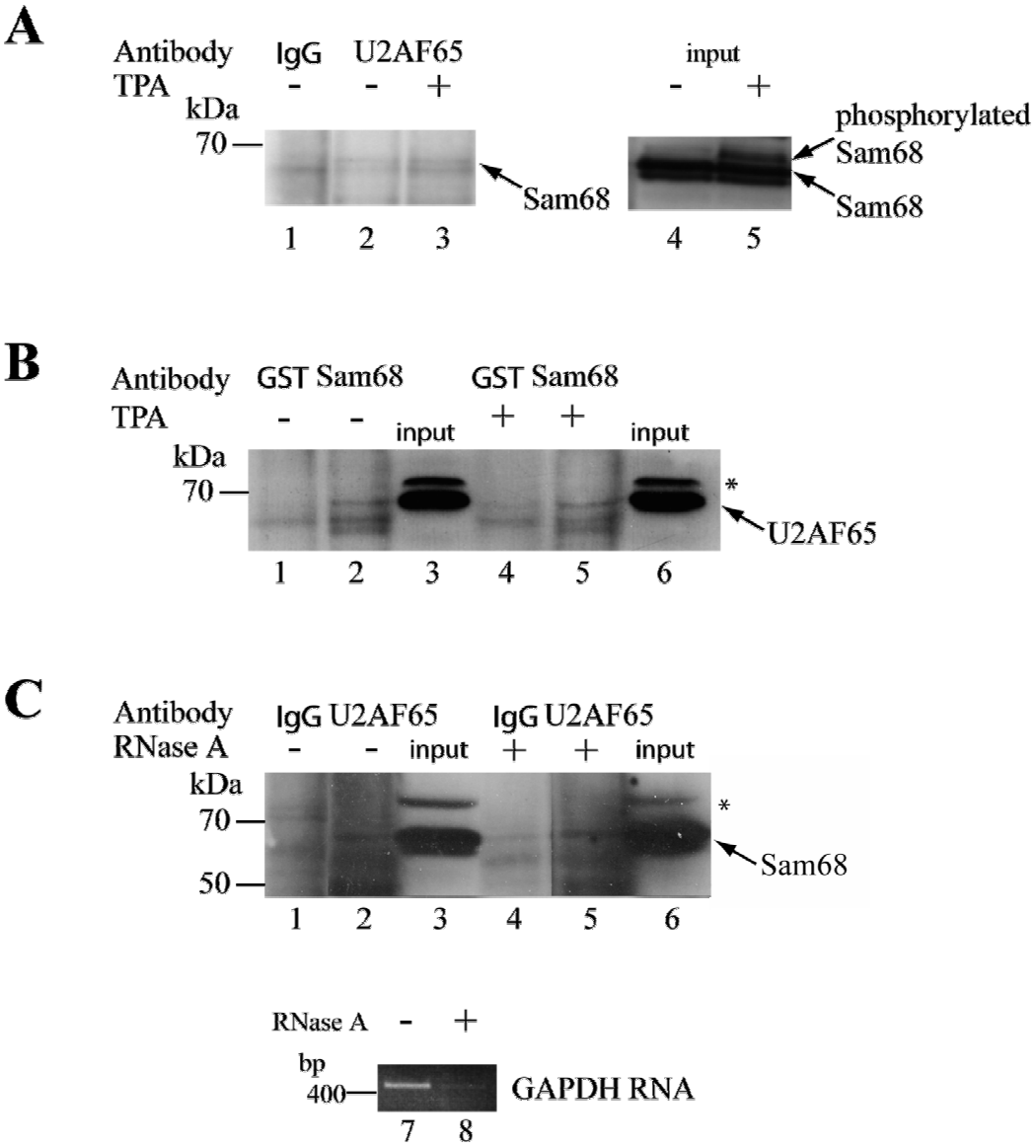

Figure 19: Sam68 interacts with U2AF65 in vivo.
Mouse LB17 lymphoma cells ($2x10^7$ cells), either left untreated (A:lanes 1, 2 and 4; B: lanes 1 to 3) or treated for 10 min with 40 ng/mL TPA (A: lanes 3 and 5; B: lanes 4 to 6), to induce the Ras-pathway, were lysed in modified RIPA buffer. **A:** 1/3 of the lysate was incubated with IgG, or anti-U2AF65 antiboby and with 40 µl of equilibrated protein A/G agarose beads. After washing, the beads were boiled and resolved on a SDS-PAGE, followed by western blotting, with an anti-Sam68 antibody. **B:** 1/3 of the lysate was incubated with anti-GST (as control) or anti-Sam68 antibody and with 40 µl equilibrated protein A/G agarose beads. After washing, the beads were boiled in sample buffer and resolved on a SDS-PAGE, followed by western blotting with an anti-U2AF65 antibody. **C:** Upper panel, samples were treated like in A, but 0.2µg/µl RNase A was added to the lysates 1 hr before precipitation (lanes 4 to 6). Lower panel, RNA was extracted from 100µl of untreated or RNase-treated lysates and checked by RT-PCR for the RNase digestion efficiency, with specific primers for GAPDH (lanes 7 and 8). Expected size for the amplification products is 400 bp. * corresponds to an unspecific band.

6.3 Sam68 can recruit U2AF65 to pre-mRNA in vivo

To test whether Sam68 could not only interact with U2AF65 but also recruit U2AF65 to the v5 exon region on pre-mRNA, I performed Ribonucleoprotein Immunoprecipitations (RNP-IP) with an anti-U2AF65 antibody, after I co-transfected the splice-reporter minigene pETv5 with an expression construct for Sam68 wild-type into LB17 cells. As a control, the empty expression plasmid was co-transfected. After RNA fragmentation, *in vivo* crosslinked proteins-RNA complexes were immunoprecipitated with anti-U2AF65 antibody or with an isotype-matched IgG control. As depicted in Figure 20, the v5 exon and the upstream intron region from the transfected pETv5 minigene pre-mRNA could be immunoprecipitated with the anti-U2AF65 antibody (lane 2) but not with the control antibody (lane 1). Moreover, forced expression of Sam68 resulted in an increase of the corresponding RNA-region precipitating with U2AF65 (lane 3). The experiment was also performed with TPA treated cells. When the Ras pathway was activated, the amount of RNA precipitated with U2AF65 was comparable to that from untreated cells (Figure 20, compare lanes 2 and 5), indicating that U2AF65 does not occupy more splice sites. Similarly upon forced Sam68 expression, the association of U2AF65 with the RNA fragment was similar without and with TPA treatment (Figure 20, compare lanes 3 and 6). These results suggest that Sam68 can recruit U2AF65 to the pre-mRNA around the v5 exon region. However, the recruitment seems not to be enhanced upon Ras-pathway activation.

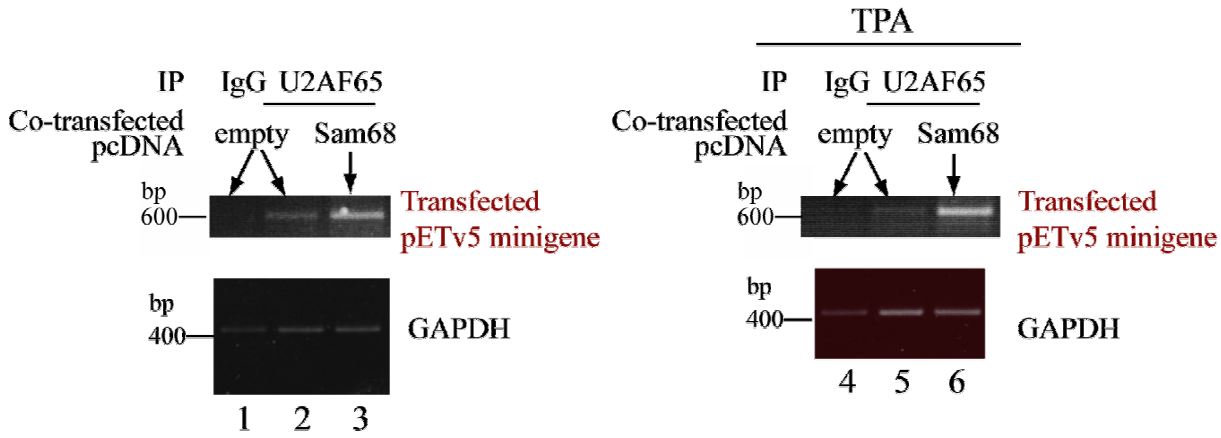

Figure 20: Forced expression of Sam68 increased U2AF65 binding to RNA in vivo. Ribonucleoprotein immunoprecipitations using mouse LB17 lymphoma cells co-transfected with 3µg pETv5 and 2µg pcDNA empty vector, or pcDNA carrying Sam68 wt cDNA, either left untreated (lanes 1 to 3) or stimulated with TPA (lanes 4 to 6) to induce the Ras-MAP kinase pathway. Cells were fixed with 0.1% formaldehyde and lysed in RIPA buffer. U2AF65 was immunoprecipitated from the extract with 3µg anti-U2AF65 antibody and 20µL of protein A/G agarose beads. An IgG antibody was used as a specificity control. Crosslinks were reversed by incubating the washed beads in decrosslinking buffer at 70°C for 45 min. RNA was extracted and RT-PCR were performed to detect RNA of interest. PCR products were analysed on a 2% agarose gel. Expected sizes for the amplification products were 570 bp for the pETv5 minigene derived fragment and 400 bp for GAPDH fragment.

Discussion

Sam68 has previously been described as a first splice regulator protein linked to signal transduction and modulated directly by ERK MAP kinase and is therefore under the control of Ras and growth-factor signalling (Matter et al., 2002). Sam68 can bind RNA regulatory elements in CD44 exon v5 (within the subdomain L; Matter et al., 2002) and close to the putative branch point site in the intron upstream v5 (bpv5; this work). I could show here that the binding of Sam68 to the intronic RNA element bpv5, as shown for exonic RNA element L (Matter et al., 2002), is important for the general level of v5 exon inclusion. Sam68 is part of a regulating complex, occupying regulatory sequences on the pre-mRNA, which influences exon inclusion by the spliceosome machinery. However, Sam68 binding to these sites appears not to be required for the induction step in v5 splicing, since the TPA induction (fold induction) of v5 exon inclusion was not impaired but rather enhanced by the mutation of both RNA elements.

In addition, the deletion of the RNA binding region of Sam68, the KH domain (which impairs Sam68 binding to RNA *in vitro*) did not alter the activity of Sam68 in v5 exon splicing. This result indicates that Sam68 RNA-binding properties are not required for its activity in the Ras-induced activation of v5 exon splicing, although its localization within the regulatory complex is necessary. At the same time, the result also shows that the KH domain of Sam68 is not an essential domain in this process.

Given that Sam68 interacts with RNA regulatory elements but does not need to be bound to these elements to enhance v5 exon inclusion in the mRNA upon Ras-pathway activation, it was interesting to check if ERK phosphorylation affects Sam68 binding to RNA. Together, the *in vitro* and *in vivo* RNA binding data suggest that the Ras-pathway induced phosphorylation of Sam68, through ERK, results in impaired binding of Sam68 to RNA elements involved in CD44 v5 splicing. Thus the loss or the weakening of Sam68 association to RNA seems to be an important step to induce v5 exon inclusion upon Ras-pathway activation.

Compatible with a role for altered RNA binding of Sam68 in the activation process, the Sam68 mutants deleted for the N-terminal 57 or 100 amino acids had the tendency to stimulate the inclusion of the v5 exon more strongly than the wild-type Sam68, following TPA treatment. Interestingly, Sam68 ΔN57 and ΔN100 have no affinity for the v5 RNA element, as shown in the RNA-IP assays, *in vitro*. Both deletion mutants lack the RGG

sequence. RGG boxes were proposed to be RNA-binding motifs and predictors of RNA binding activity (Kiledjian, and Dreyfuss, 1992). However, in Chen et al. (1997) Sam68 proteins containing N-terminal deletions of 67 and 102 residues were shown to bind high affinity sequences comparably to the full-lengh Sam68. The RGG motif might thus be required in a cooperative way with the KH domain, to bind more specifically to the sequences in and upstream of the CD44 v5 exon. ERK phosphorylation of Sam68 occurs in the vicinity of the RGG box and could affect its capacity to bind the bpv5 and subdomain L sequences. As the RGG motif seems to be not generally required for binding high affinity sequences (Chen et al., 1997), Ras-pathway induction would affect specifically the RNA binding of Sam68 to sequences like the ones involved in CD44 exon v5 splicing.

Furthermore, the fact that the Sam68 ΔN100 mutant (which lacks the ERK phosphorylation sites) can still mediate Ras-induced splicing suggests two things. First, the deletion of the RGG sequence, impairing Sam68 RNA binding, would have substituted the effect of ERK phosphorylation. Secondly, as the N-terminal deletion mutants do not exhibit a constitutive activity, it suggests that loss of RNA-binding is not sufficient and that Ras signalling-induced changes in (an) other protein(s) likely contribute to the induction process. This was also suggested by the only partial inhibition of splicing activation upon mutation of the ERK phosphorylation sites (Matter et al., 2002).

In contrast to the deletion of the KH domain of Sam68, the deletion of the tyrosine-rich domain located at the C-terminal part of Sam68 abolished the activity of the resulting protein in the signal-dependent induction of v5 exon splicing. In fact, the co-transfected Sam68 C-terminal mutants have a trans-dominant negative effect on v5 exon inclusion. This might be caused by interaction of the tyrosine-rich domain with (a) positive regulatory factor(s). As shown in the RNA-affinity precipitation assays *in vitro*, the C-terminal deletions did not impair Sam68 binding to the RNA element L. The Sam68 proteins lacking the tyrosine-rich domain could thus still occupy the regulatory RNA elements, but would not be able to attract and stabilize the positive regulatory factor(s). As a consequence, the general level of v5 exon inclusion would be repressed by the forced expression of Sam68 C-terminal deletion mutants. Recently, overexpression of SRm160, a splicing coactivator, was shown to stimulate inclusion of CD44 v5 when Ras is activated (Chen and Sharp, 2006). SRm160 was shown to interact with Sam68, upon overexpression of both proteins and may be a candidate for the positive factor (Chen and Sharp, 2006; See model in Figure 21). A functional link between SRm160 and Sam68 however remains to be established.

In this study, I could show that Sam68 is associated to the spliceosomal factor U2AF65, which is responsible for recognition of the polypyrimidine-tract close to the 3' end of introns (Coolidge et al., 1997; Reed, 1989). In addition to interacting with U2AF65, the data of the *in vivo* RNP-IP strongly suggest that Sam68 recruits U2AF65 to the v5 exon region. Forced expression of Sam68 in T lymphoma cells resulted in an increased precipitation with U2AF65 of the transfected pETv5 minigene-pre-mRNA fragments spanning the v5 exon and its upstream intron. The activation of the Ras-pathway seems not to increase U2AF65 binding to RNA fragments. Thus, in a first step Sam68 appears to stabilize U2AF65 binding to the polypyrimidine tract. This step is essential for the exon definition and, in constitutively spliced exons, involves the binding of Splicing factor 1 (SF1) to the branch point. SF1 facilitates binding of U2AF65 and the interactions between SF1 and U2AF65 with their respective sites were found to be cooperative (Kramer, 1992; Berglund et al., 1998; Manceau et al., 2006). In the context of v5 exon splicing, Sam68 could substitute SF1 in the stabilization of U2AF65 binding (Figure 21A). This step may require the C-terminal tyrosine-rich domain of Sam68. Upon Ras-pathway activation, the preformed U2AF65-containing complexes could then be activated, leading to signal-induced exon v5 splicing. A first step in this activation process, which may involve a remodelling of the complex formed on/around the v5 exon, seems to be a weakening of Sam68 binding to RNA via ERK phosphorylation (As discussed above). The release of Sam68 from the pre-mRNA could allow the access to the branch point for SF1 and promote the further association of the spliceosome on the v5 exon (Figure 21B).

In addition to altering RNA binding of Sam68, its phosphorylation could lead to a conformational change of Sam68, which might modulate its interaction with the splice activator and/or splice silencer proteins in the complex found over and around the v5 exon. The heterogeneous ribonucleoprotein (hnRNP) A1 was previously identified as part of the exon-silencing complex on the v5 exon (Matter et al., 2000). I could show in this study that Sam68 interacts with hnRNP A1 *in vivo*. Although no consensus binding site for hnRNP A1 was identified within exon v5, hnRNP A1 was shown to interact with different v5 exon domains (Matter et al., 2000). HnRNP A1 can reduce the binding of U1 snRNP to the 5' splice site, as shown in Eperon et al., 2000. A role for Sam68 could be to stabilize this silencing factor on the v5 exon (Figure 21A) and upon Ras-pathway activation, and ERK-phosphorylation, to release hnRNP A1 from CD44 pre-mRNA and/or to modulate its function (Figure 21B). In a recent study, hnRNP A1 itself was shown to be phosphorylated upon Ras signalling. Upon T cell activation, the ERK substrates MAP kinase signal-integrating kinases

(Mnks) are activated and then phosphorylate hnRNP A1, which decreases its ability to bind a specific mRNA *in vivo* (Buxade et al., 2005). The combinatorial signal-mediated phosphorylation of Sam68 and of hnRNP A1 could thus lead to the accessibility of the splice sites and allow the spliceosome machinery to assemble on the v5 exon, which would lead to its inclusion in mRNA (Figure 21B).

To fully understand the regulation of CD44 exon v5 splicing and the role of Sam68, it is important to map the interactions between U2AF65, hnRNP A1 and SRm160 with Sam68. According to the model proposed, hnRNP A1 would lose its affinity for exon v5 upon Ras-pathway activation. This remains to be tested by performing RNP-IPs assays *in vivo*. Futhermore, specific inhibitors of Mnks could allow for the testing of a role of hnRNP A1 phosphorylation in v5 exon splicing. Finally, EMSA experiments coupled to RNP-IP assays *in vivo* may allow characterization of the role of SRm160 in the Sam68-mediated splice activation of the CD44 v5 exon.

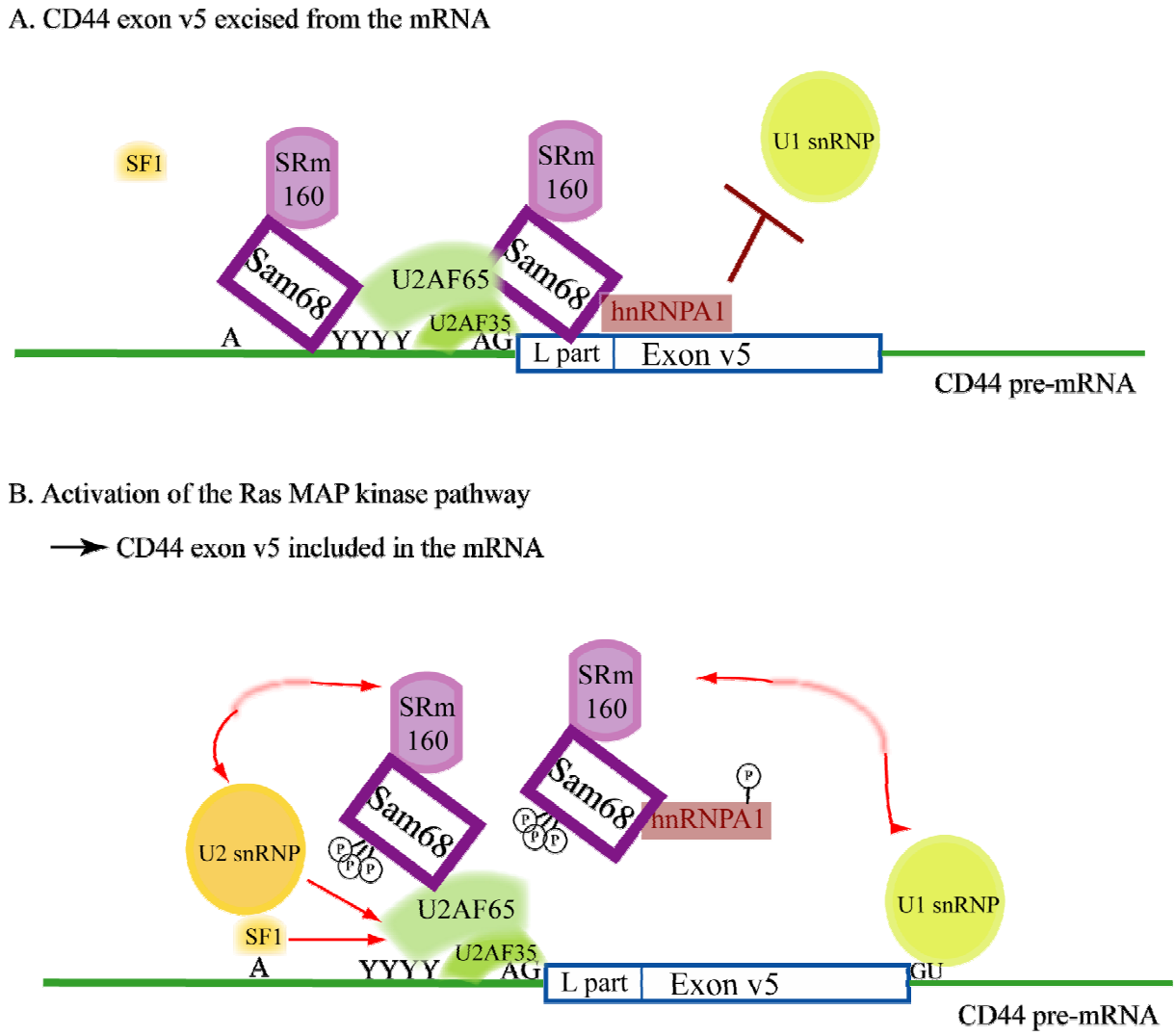

Figure 21: Model for the role of Sam68 in the signal-induced splicing of the CD44 exon v5.

A: Sam68, by binding to RNA regulatory elements, could stabilize U2AF65 on the pyrimidine tract (YYYY). In addition, Sam68 could stabilize the silencing factor hnRNP A1 on the v5 exon, which would reduce the binding of U1 snRNP to the 5' splice site (Eperon et al., 2000). CD44 exon v5 would then be excised from the pre-mRNA. **B:** Upon Ras pathway activation, ERK phosphorylation of Sam68 impairs its binding to RNA. The release of Sam68 from the pre-mRNA could allow the access to the branch point for SF1 and promote the further association of the spliceosome on the v5 exon. HnRNP A1 itself was shown to be phosphorylated upon Ras signalling (Buxade et al., 2005). The combinatorial signal-mediated phosphorylation of Sam68 and of hnRNP A1 could thus lead to the accessibility of the splice sites and allow the spliceosome machinery to assemble on the v5 exon, which would lead to its inclusion in mRNA. SRm160 is represented here since it could be a positive factor in v5 exon splicing (Chen and Sharp, 2006), however the functional link between SRm160 and Sam68 remains to be shown.

References

Arch, R., Wirth, K., Hofmann, M., Ponta, H., Matzku, S., Herrlich, P. and Zöller, M. (1992) Participation in normal immune responses of a splice variant of CD44 that encodes a metastasis-inducing domain. *Science*, **257**, 682–685.

Baker, B.S. (1989) Sex in flies: the splice of life. *Nature.* Aug 17; **340** (6234):521-4.

Barlat, I., Maurier, F., Duchesne, M., Guitard, E., Tocque, B., Schweighoffer, F. (1997) A role for Sam68 in cell cycle progression antagonized by a spliced variant within the KH domain. *J Biol Chem*. Feb 7; **272**(6):3129-32.

Bedford, M.T., Chan, D.C., Leder, P.. (1997) FBP WW domains and the Abl SH3 domain bind to a specific class of proline-rich ligands. *EMBO J.* May 1; **16**(9):2376-83.

Bedford, M.T.; Reed, R.; Leder, P. (1998) WW domain-mediated interactions reveal a spliceosome-associated protein that binds a third class of proline-rich motif: the proline glycine and methionine-rich motif. *PNAS* Sep 1; **95** (18):10602-10607.

Bedford, M.T., Frankel, A., Yaffe, M.B., Clarke, S., Leder, P., Richard, S. (2000) Arginine methylation inhibits the binding of proline-rich ligands to Src homology 3, but not WW, domains. *J Biol Chem.* May 26; **275**(21):16030-6.

Bennett, K.L., Modrell, B., Greenfield, B., Bartolazzi, A., Stamenkovic, I., Peach, R., Jackson, D.G., Spring, F., Aruffo, A. (1995) Regulation of CD44 binding to hyaluronan by glycosylation of variably spliced exons. *J Cell Biol.* Dec; **131**(6 Pt 1):1623-33.

Berget, S.M. (1995) Exon recognition in vertebrate splicing. *J Biol Chem.* Feb 10; **270**(6):2411-4.

Berglund, J.A., Chua, K., Abovich, N., Reed, R., Rosbash, M. (1997) The splicing factor BBP interacts specifically with the pre-mRNA branchpoint sequence UACUAAC. *Cell.* May 30; **89**(5):781-7.

Berglund, J.A., Abovich, N., Rosbash, M. (1998) A cooperative interaction between U2AF65 and mBBP/SF1 facilitates branchpoint region recognition. *Genes Dev.* Mar 15; **12**(6):858-67.

Black, D.L. (2000) Protein diversity from alternative splicing: a challenge for bioinformatics and post-genome biology. *Cell.* Oct 27; **103**(3):367-70.

Blanco, S., Klimcakova, L., Vega, F.M., Lazo, P.A. (2006) The subcellular localization of vaccinia-related kinase-2 (VRK2) isoforms determines their different effect on p53 stability in tumour cell lines. *FEBS J.* Jun; **273**(11):2487-504.

Bonder, C.S., Clark, S.R., Norman, M.U., Johnson, P., Kubes, P. (2006) Use of CD44 by CD4+ Th1 and Th2 lymphocytes to roll and adhere. *Blood.* Feb 23; [Epub ahead of print]

Borland, G., Ross, J.A., Guy, K. (1998) Forms and functions of CD44. *Immunology*. Feb; **93**(2):139-48.

Burd, C.G., Dreyfuss, G. (1994) Conserved structures and diversity of functions of RNA-binding proteins. *Science*. Jul 29; **265**(5172):615-21.

Buxade, M., Parra, J.L., Rousseau, S., Shpiro, N., Marquez, R., Morrice, N., Bain, J., Espel, E., Proud, C.G. (2005) The Mnks are novel components in the control of TNF alpha biosynthesis and phosphorylate and regulate hnRNP A1. *Immunity*. Aug; **23**(2):177-89.

Cantrell, D. (1996) T cell antigen receptor signal transduction pathways. *Annu Rev Immunol.* **14**:259-74.

Cartegni, L., Chew., S.L., Krainer, A.R. (2002) Listening to silence and understanding nonsense: exonic mutations that affect splicing. *Nat Rev Genet.* Apr; **3**(4):285-98.

Castagna, M., Takai, Y., Kaibuchi, K., Sano, K., Kikkawa, U., Nishizuka, Y. (1982) Direct activation of calcium-activated, phospholipid-dependent protein kinase by tumor-promoting phorbol esters. *J Biol Chem.* Jul 10; **257**(13):7847-51.

Cheng, C., Sharp, P.A. (2006) Regulation of CD44 alternative splicing by SRm160 and its potential role in tumor cell invasion. *Mol Cell Biol.* Jan; **26**(1):362-70.

Chen, T., Damaj, B.B., Herrera, C., Lasko, P., Richard, S. (1997) Self-association of the single-KH-domain family members Sam68, GRP33, GLD-1, and Qk1: role of the KH domain. *Mol Cell Biol.* Oct; **17**(10):5707-18.

Chen, T., Richard, S. (1998) Structure-function analysis of Qk1: a lethal point mutation in mouse quaking prevents homodimerization. Chen T, Richard S. *Mol Cell Biol.* Aug; **18**(8):4863-71.

Coolidge, C.J., Seely, R.J. Patton, J.G. (1997) Functional analysis of the polypyrimidine tract in pre-mRNA splicing. *Nucleic Acids Res.* Feb 15; **25**(4):888-96.

Cote, J., Boisvert, F.M., Boulanger, M.C., Bedford, M.T., Richard, S. (2003) Sam68 RNA binding protein is an in vivo substrate for protein arginine N-methyltransferase 1. *Mol Biol Cell.* Jan; **14**(1):274-87.

Coyle, J.H., Guzik, B.W., Bor, Y.C., Jin, L., Eisner-Smerage, L., Taylor, S.J., Rekosh, D., Hammarskjold, M.L. (2003) Sam68 enhances the cytoplasmic utilization of intron-containing RNA and is functionally regulated by the nuclear kinase Sik/BRK. *Mol Cell Biol.* Jan; **23**(1):92-103.

Crews, C.M., Erikson, R.L. (1993) Extracellular signals and reversible protein phosphorylation: what to Mek of it all. *Cell.* Jul 30; **74**(2):215-7.

Dalchau, R., Kirkley, J., Fabre, J.W. (1980) Monoclonal antibody to a human leukocyte-specific membrane glycoprotein probably homologous to the leukocyte-common (L-C) antigen of the rat. *Eur J Immunol.* Oct; **10**(10):737-44.

Del Gatto-Konczak, F., Olive, M., Gesnel, M.C., Breathnach, R. (1999) hnRNP A1 recruited to an exon in vivo can function as an exon splicing silencer. *Mol Cell Biol*. Jan; **19**(1):251-60.

Derry, J.J., Richard, S., Valderrama Carvajal, H., Ye, X., Vasioukhin, V., Cochrane, A.W., Chen, T., Tyner, A.L.(2000) Sik (BRK) phosphorylates Sam68 in the nucleus and negatively regulates its RNA binding ability. *Mol Cell Biol.* Aug; **20**(16):6114-26.

Di Fruscio, M., Chen, T., Bonyadi, S., Lasko, P., Richard, S. (1998) The identification of two Drosophila K homology domain proteins. Kep1 and SAM are members of the Sam68 family of GSG domain proteins. *J Biol Chem.* Nov 13; **273**(46): 30122-30.

Di Fruscio, M., Chen, T., Richard, S. (1999) Characterization of Sam68-like mammalian proteins SLM-1 and SLM-2: SLM-1 is a Src substrate during mitosis *PNAS* Mar 16; **96**(6): 2710-2715.

Dong, C., Yang, D.D., Tournier, C., Whitmarsh, A.J., Xu, J., Davis, R.J., Flavell, R.A. (2000) JNK is required for effector T-cell function but not for T-cell activation. *Nature.* May 4; **405**(6782):91-4.

Downward, J., Graves, J.D., Warne, P.H., Rayter, S., Cantrell, D.A. (1990) Stimulation of p21ras upon T-cell activation. *Nature.* Aug 23; **346**(6286):719-23.

Downward, J., Graves, J., Cantrell, D. (1992) The regulation and function of p21ras in T cells. *Immunol Today*. Mar; **13**(3):89-92.

Dreyfuss, G., Matunis, M.J., Pinol-Roma, S., Burd, C.G. (1993) hnRNP proteins and the biogenesis of mRNA. *Annu Rev Biochem.* **62**:289-321.

Ebinu, J.O., Bottorff, D.A., Chan, E.Y., Stang, S.L., Dunn, R.J., Stone, J.C. (1998) RasGRP, a Ras guanyl nucleotide- releasing protein with calcium- and diacylglycerol-binding motifs. *Science*. May 15; **280**(5366):1082-6.

Ellis, C., Moran, M., McCormick, F., Pawson, T. (1990) Phosphorylation of GAP and GAP-associated proteins by transforming and mitogenic tyrosine kinases. *Nature.* Jan 25; **343**(6256):377-81.

Eperon, I.C., Makarova, O.V., Mayeda, A., Munroe, S.H., Caceres, J.F., Hayward, D.G., Krainer, A.R. (2000) Selection of alternative 5' splice sites: role of U1 snRNP and models for the antagonistic effects of SF2/ASF and hnRNP A1. *Mol Cell Biol.* Nov; **20**(22):8303-18.

Espejo, A., Cote, J., Bednarek, A., Richard, S., Bedford, M.T. (2002) A protein-domain microarray identifies novel protein-protein interactions. *Biochem J.* Nov 1; **367**(Pt 3):697-702.

Faustino, N.A., Cooper, T.A. (2003) Pre-mRNA splicing and human disease. *Genes Dev.* Feb 15; **17**(4):419-37.

Fichter, M., Hinrichs, R., Eissner, G., Scheffer, B., Classen, S., Ueffing, M. (1997) Expression of CD44 isoforms in neuroblastoma cells is regulated by PI 3-kinase and protein kinase C. *Oncogene.* Jun 12; **14**(23):2817-24.

Finco, T.S., Kadlecek, T., Zhang, W., Samelson, L.E., Weiss, A. (1998) LAT is required for TCR-mediated activation of PLCgamma1 and the Ras pathway. *Immunity*. Nov; **9**(5):617-26.

Fumagalli, S., Totty, N.F., Hsuan, J.J., Courtneidge, S.A. (1994) A target for Src in mitosis. *Nature* Apr 28; **368** (6474): 871-874.

Fusaki, N., Iwamatsu, A., Iwashima, M., Fujisawa, J. (1997) Interaction between Sam68 and Src family tyrosine kinases, Fyn and Lck, in T cell receptor signaling. *J Biol Chem*. Mar 7; **272**(10):6214-9.

Gary, J.D., Clarke, S. (1998) RNA and protein interactions modulated by protein arginine methylation. *Prog Nucleic Acid Res Mol Biol.* **61**:65-131.

Genot, E., Cleverley, S., Henning, S., Cantrell, D. (1996) Multiple p21ras effector pathways regulate nuclear factor of activated T cells. *EMBO J.* Aug 1; **15**(15):3923-33.

Genot, E., Reif, K., Beach, S., Kramer, I., Cantrell, D. (1998) p21ras initiates Rac-1 but not phosphatidyl inositol 3 kinase/PKB, mediated signaling pathways in T lymphocytes. *Oncogene.* Oct 1; **17**(13):1731-8.

Genot, E., Cantrell, D.A. (2000) Ras regulation and function in lymphocytes. *Curr Opin Immunol.* Jun; **12**(3):289-94.

Gonda, A., Gal, I., Szanto, S., Sarraj, B., Glant, T.T., Hunyadi, J., Mikecz, K. (2005) CD44, but not l-selectin, is critically involved in leucocyte migration into the skin in a murine model of allergic dermatitis. *Exp Dermatol.* Sep; **14**(9):700-8.

Graveley, B.R. (2001) Alternative splicing: increasing diversity in the proteomic world. *Trends Genet.* Feb; **17**(2):100-7.

Guitard, E., Barlat, I., Maurier, F., Schweighoffer, F., Tocque, B. (1998) Sam68 is a Ras-GAP-associated protein in mitosis. *Biochem Biophys Res Commun.* Apr 17; **245**(2):562-6.

Gunthert, U., Hofmann, M., Rudy, W., Reber, S., Zoller, M., Haussmann, I. Matzku, S., Wenzel, A., Ponta, H., Herrlich, P. (1991) A new variant of glycoprotein CD44 confers metastatic potential to rat carcinoma cells. *Cell.* Apr 5; **65**(1):13-24.

Ishidate, T., Yoshihara, S., Kawasaki, Y., Roy, B.C., Toyoshima, K., Akiyama, T. (1997) Identification of a novel nuclear localization signal in Sam68. *FEBS Lett.* Jun 9; **409**(2):237-41.

Itoh, M., Haga, I., Li, Q.H., Fujisawa, J. (2002) Identification of cellular mRNA targets for RNA-binding protein Sam68. *Nucleic Acids Res.* Dec 15; **30**(24):5452-64.

Izquierdo, M., Leevers, S.J., Marshall, C.J., Cantrell, D. (1993) p21ras couples the T cell antigen receptor to extracellular signal-regulated kinase 2 in T lymphocytes. *J Exp Med.* Oct 1; **178**(4):1199-208.

Jabado, N., Jauliac, S., Pallier, A., Bernard, F., Fischer, A., Hivroz, C. (1998) Sam68 association with p120GAP in CD4+ T cells is dependent on CD4 molecule expression. *J Immunol.* 1998 Sep 15; **161**(6):2798-803.

Johnson, J.M., Castle, J., Garrett-Engele, P., Kan, Z., Loerch, P.M., Armour, C.D., Santos, R., Schadt, E.E., Stoughton, R., Shoemaker, D.D. (2003) Genome-wide survey of human alternative pre-mRNA splicing with exon junction microarrays. *Science.* Dec 19; **302**(5653):2141-4.

Jones, A.R., Schedl, T. (1995) Mutations in gld-1, a female germ cell-specific tumor suppressor gene in Caenorhabditis elegans, affect a conserved domain also found in Src-associated protein Sam68. *Genes Dev.* Jun 15; **9**(12):1491-504.

Kar, A., Kuo, D., He, R., Zhou, J., Wu, J.Y. (2005) Tau alternative splicing and frontotemporal dementia. *Alzheimer Dis Assoc Disord.* Oct-Dec; **19** Suppl 1:S29-36.

Kiledjian, M., Dreyfuss, G. (1992) Primary structure and binding activity of the hnRNP U protein: binding RNA through RGG box. *EMBO J.* Jul; **11**(7):2655-64.

König, H., Ponta, H. and Herrlich, P. (1998) Coupling of signal transduction to alternative pre-mRNA splicing by a composite splice regulator. *EMBO J.* May 15; **17**(10):2904-13.

Koopman, G., Heider, K.H., Horst, E., Adolf, G.R., Van den Berg, F., Ponta, H., Herrlich, P., Pals, S.T. (1993) Activated human lymphocytes and aggressive non-Hodgkin's lymphomas express a homologue of the rat metastasis-associated variant of CD44. *J Exp Med.* Apr 1; **177**(4):897-904.

Kramer, A. (1992) Purification of splicing factor SF1, a heat-stable protein that functions in the assembly of a presplicing complex. *Mol Cell Biol.* Oct; **12**(10):4545-52.

Krawczak, M., Reiss, J., Cooper, D.N. (1992) The mutational spectrum of single base-pair substitutions in mRNA splice junctions of human genes: causes and consequences. *Hum Genet.* Sep-Oct; **90**(1-2):41-54.

Lee, L.N., Kuo, S.H., Lee, Y.C., Chang, Y.L., Chang, H.C., Jan, I.S., Yang, P.C. (2005) CD44 splicing pattern is associated with disease progression in pulmonary adenocarcinoma. *J Formos Med Assoc.* Aug; **104**(8):541-8.

Legg, J.W., Lewis, C.A., Parsons, M., Ng, T., Isacke, C.M. (2002) A novel PKC-regulated mechanism controls CD44 ezrin association and directional cell motility. *Nat Cell Biol.* Jun; **4**(6):399-407.

Li, L., Cohen, S.N. (1995) Tsg101: a novel tumor susceptibility gene isolated by controlled homozygous functional knockout of allelic loci in mammalian cells. *Cell.* May 3; **85**(3):319-29.

Li, Q.H., Haga, I., Shimizu, T., Itoh, M., Kurosaki, T., Fujisawa, J. (2002) Retardation of the G2-M phase progression on gene disruption of RNA binding protein Sam68 in the DT40 cell line. *FEBS Lett.* Aug 14; **525**(1-3):145-50.

Lin, Q., Taylor, S.J., Shalloway, D. (1997) Specificity and determinants of Sam68 RNA binding. Implications for the biological function of K homology domains. *J Biol Chem.* Oct 24; **272**(43):27274-80.

Liu, K., Li, L., Nisson, P.E., Gruber, C., Jessee, J., Cohen, S.N. (2000) Neoplastic transformation and tumorigenesis associated with sam68 protein deficiency in cultured murine fibroblasts. *J Biol Chem.* Dec 22; **275**(51):40195-201.

Lock, P., Fumagalli, S., Polakis, P., McCormick, F., Courtneidge, S.A. (1996) The human p62 cDNA encodes Sam68 and not the RasGAP-associated p62 protein. *Cell.* Jan 12; **84**(1):23-4.

Lukong, K.E., Richard, S. (2003) Sam68, the KH domain-containing superstar. *Biochim Biophys Acta.* Dec 5; **1653**(2):73-86.

Lynch, K.W., Weiss, A. (2000) A model system for activation-induced alternative splicing of CD45 pre-mRNA in T cells implicates protein kinase C and Ras. *Mol Cell Biol.* Jan; **20**(1):70-80.

Macias, M.J., Wiesner, S., Sudol, M. (2002) WW and SH3 domains, two different scaffolds to recognize proline-rich ligands. *FEBS Lett.* Feb 20; **513**(1):30-7.

Manceau, V., Swenson, M., Le Caer, J.P., Sobel, A., Kielkopf, C.L., Maucuer, A. (2006) Major phosphorylation of SF1 on adjacent Ser-Pro motifs enhances interaction with U2AF65. *FEBS J.* Feb; **273**(3):577-87.

Maniatis, T., Tasic, B. (2002) Alternative pre-mRNA splicing and proteome expansion in metazoans. *Nature.* Jul 11; **418**(6894):236-43.

Martin-Romero, C., Sanchez-Margalet, V. (2001) Human leptin activates PI3K and MAPK pathways in human peripheral blood mononuclear cells: possible role of Sam68. *Cell Immunol*. Sep 15; **212**(2):83-91.

Matter, N., Marx, M., Weg-Remers, S., Ponta, H., Herrlich, P., König, H. (2000) Heterogeneous ribonucleoprotein A1 is part of an exon-specific splice-silencing complex controlled by oncogenic signaling pathways. *J Biol Chem.* Nov 10; **275**(45):35353-60.

Matter, N., Herrlich, P., König, H. (2002) Signal-dependent regulation of splicing via phosphorylation of Sam68. *Nature.* Dec 12; **420**(6916):691-5.

Mayeda, A., Krainer, A.R. (1992) Regulation of alternative pre-mRNA splicing by hnRNP A1 and splicing factor SF2. *Cell.* Jan 24; **68**(2):365-75.

McBride, A.E., Silver, P.A. (2001) State of the arg: protein methylation at arginine comes of age. *Cell.* Jul 13; **106**(1):5-8.

McCormick, F. (1993) Signal transduction. How receptors turn Ras on. *Nature.* May 6; **363**(6424):15-6.

Merendino, L., Guth, S., Bilbao, D., Martinez, C., Valcarcel, J. (1999) Inhibition of msl-2 splicing by Sex-lethal reveals interaction between U2AF35 and the 3' splice site AG. . *Nature.* Dec 16; **402**(6763):838-41.

Modrek, B., Lee, C. (2002) A genomic view of alternative splicing. *Nat Genet.* Jan; **30**(1):13-9.

Modrek, B., Resch, A., Grasso, C., Lee, C. (2001) Genome-wide detection of alternative splicing in expressed sequences of human genes. *Nucleic Acids Res.* Jul 1; **29**(13):2850-9.

Moll, J., Khaldoyanidi, S., Sleeman, J.P., Achtnich, M., Preuss, I., Ponta, H., Herrlich, P. (1998) Two different functions for CD44 proteins in human myelopoiesis. *J Clin Invest.* Sep 1; **102**(5):1024-34.

Moran, M.F., Koch, C.A., Anderson, D., Ellis, C., England, L., Martin, G.S., Pawson, T. (1990) Src homology region 2 domains direct protein-protein interactions in signal transduction. *Proc Natl Acad Sci U S A.* Nov; **87**(21):8622-6.

Musco, G., Stier, G., Joseph, C., Castiglione-Morelli, M.A., Nilges, M., Gibson, T.J., Pastore, A. (1996) Three-dimensional structure and stability of the KH domain: molecular insights into the fragile X syndrome. *Cell.* Apr 19;**85**(2):237-45.

Naor, D., Sionov, R.V. and Ish-Shalom, D. (1997) Advances in cancer research *Vol 70* (eds Vande Woude, G.F. and Klein, G.) 243-318 (Academic, San Diego)

Niranjanakumari, S., Lasda, E., Brazas, R., Garcia-Blanco, M.A. (2002) Reversible cross-linking combined with immunoprecipitation to study RNA-protein interactions in vivo. *Methods.* Feb; **26**(2):182-90.

Opanashuk, L.A., Mark, R.J., Porter, J., Damm, D., Mattson, M.P., Seroogy, K.B. (1999) Heparin-binding epidermal growth factor-like growth factor in hippocampus: modulation of expression by seizures and anti-excitotoxic action. *J Neurosci.* Jan 1; **19**(1):133-46.

Orian-Rousseau, V., Chen., L., Sleeman, J.P., Herrlich, P., Ponta, H. (2002) CD44 is required for two consecutive steps in HGF/c-Met signaling. *Genes De,.* Dec 1;**16**(23):3074-86.

Ponta, H., Sherman, L., Herrlich, P.A. (2003) CD44: from adhesion molecules to signalling regulators. *Nat Rev Mol Cell Biol.* Jan; **4**(1):33-45.

Ponti, D., Zaffaroni, N., Capelli, C., Daidone, M.G. (2006) Breast cancer stem cells: An overview. *Eur J Cancer*.Apr 17; [Epub ahead of print].

Reddy, T.R., Xu, W., Mau, J.K., Goodwin, C.D., Suhasini, M., Tang, H., Frimpong, K., Rose, D.W., Wong-Staal, F. (1999) Inhibition of HIV replication by dominant negative mutants of Sam68, a functional homolog of HIV-1 *Rev*. *Nat Med.* Jun; **5**(6):635-42

Reed, R. (1989) The organization of 3' splice-site sequences in mammalian introns. *Genes Dev*. Dec; **3**(12B):2113-23.

Reed, R. (1996) Initial splice-site recognition and pairing during pre-mRNA splicing. *Curr Opin Genet Dev*. Apr; **6**(2):215-20.

Reed, R. (2000) Mechanisms of fidelity in pre-mRNA splicing. *Curr Opin Cell Biol.* Jun; **12**(3):340-5.

Richard, S., Yu, D., Blumer, K.J., Hausladen, D., Olszowy, M.W., Connelly, P.A., Shaw, A.S. (1995) Association of p62, a multifunctional SH2- and SH3-domain-binding protein, with src family tyrosine kinases, Grb2, and phospholipase C gamma-1. *Mol Cell Biol.* Jan; **15**(1):186-97.

Rio, D.C. (1993) Splicing of pre-mRNA: mechanism, regulation and role in development. *Curr Opin Genet Dev*. Aug; **3**(4):574-84

Sambrook, J., Fritsch, E.F., Maniatis, T. (1989) Molecular cloning. A *Laboratory Manual* (Second edition). Cold Spring Harbor Laboratory Press.

Sanchez-Margalet, V. and Najib, S. (2001) Sam68 is a docking protein linking GAP and PI3K in insulin receptor signaling. *Mol. Cell. Endocrinol.* **183**:113–121.

Scotet, E., Houssaint, E. (1998) Exon III splicing switch of fibroblast growth factor (FGF) receptor-2 and -3 can be induced by FGF-1 or FGF-2. *Oncogene.* Jul 9; **17**(1):67-76.

Screaton, G.R., Bell, M.V., Jackson, D.G., Cornelis, F.B., Gerth, U., Bell, J.I. (1992) Genomic structure of DNA encoding the lymphocyte homing receptor CD44 reveals at least 12 alternatively spliced exons. *Proc Natl Acad Sci U S A*. Dec 15; **89**(24):12160-4.

Screaton, G.R., Xu, X.N., Olsen, A.L., Cowper, A.E., Tan, R., McMichael, A.J., Bell, J.I. (1997) LARD: a new lymphoid-specific death domain containing receptor regulated by alternative pre-mRNA splicing. *Proc Natl Acad Sci U S A*. Apr 29; **94**(9):4615-9.

Sharp, P.A. (1994) Split genes and RNA splicing. *Cell.* Jun 17; **77**(6):805-15.

Skelton, T.P., Zeng, C., Nocks, A., Stamenkovic, I.(1998) Glycosylation provides both stimulatory and inhibitory effects on cell surface and soluble CD44 binding to hyaluronan. *J Cell Biol.* Jan 26; **140**(2):431-46.

Sleeman, J.P., Kondo, K., Moll, J., Ponta, H., Herrlich, P. (1997) Variant exons v6 and v7 together expand the repertoire of glycosaminoglycans bound by CD44. *J Biol Chem*. Dec 12; **272**(50):31837-44.

Smith, M.A., Fanger, G.R., O'Connor, L.T., Bridle, P., Maue, R.A. (1997) Selective regulation of agrin mRNA induction and alternative splicing in PC12 cells by Ras-dependent actions of nerve growth factor. *J Biol Chem.* Jun 20; **272**(25):15675-81.

Staknis, D., Reed, R. (1994) SR proteins promote the first specific recognition of Pre-mRNA and are present together with the U1 small nuclear ribonucleoprotein particle in a general splicing enhancer complex. *Mol Cell Biol.* Nov; **14**(11):7670-82.

Stamenkovic, I., Aruffo, A., Amiot, M., Seed, B. (1991) The hematopoietic and epithelial forms of CD44 are distinct polypeptides with different adhesion potentials for hyaluronate-bearing cells. *EMBO J.* Feb; **10**(2):343-8.

Stamm, S. (2002) Signals and their transduction pathways regulating alternative splicing: a new dimension of the human genome. *Hum Mol Genet.* Oct 1;**11**(20):2409-16.

Stauder, R., Eisterer, W., Thaler, J., Gunthert, U. (1995) CD44 variant isoforms in non-Hodgkin's lymphoma: a new independent prognostic factor. *Blood.* May 15; **85**(10):2885-99.

Stevens, S.W., Ryan, D.E., Ge, H.Y., Moore, R.E., Young, M.K., Lee, T.D., Abelson, J. (2002) Composition and functional characterization of the yeast spliceosomal penta-snRNP. *Mol Cell.* Jan; **9**(1):31-44.

Swanson, M.S. (1995) Functions of nuclear pre-mRNA/mRNA binding proteins. Pre-mRNA processing. *Edited by Lamond Al.* Berlin: Springer Verlag; 17-33.

Tange, T.O., Damgaard, C.K., Guth, S., Valcarcel, J., Kjems, J. (2001) hnRNP A1 protein regulates HIV-1 tat splicing via a novel intron silencer element. *EMBO J.* Oct 15; **20**(20):5748-58.

Taylor, S.J., Shalloway, D. (1994) An RNA-binding protein associated with Src through its SH2 and SH3 domains in mitosis. *Nature.* Apr 28; **368**(6474):867-71.

Taylor, S.J., Anafi, M., Pawson, T., Shalloway, D. (1995) Functional interaction between c-Src and its mitotic target, Sam 68. *J Biol Chem*. Apr 28; **270**(17):10120-4.

Tolg, C., Hofmann, M., Herrlich, P., Ponta, H. (1993) Splicing choice from ten variant exons establishes CD44 variability. *Nucleic Acids Res.* Mar 11; **21**(5):1225-9.

Trub, T., Frantz, J.D., Miyazaki, M., Band, H., Shoelson, S.E. (1997) The role of a lymphoid-restricted, Grb2-like SH3-SH2-SH3 protein in T cell receptor signaling. *J Biol Chem.* Jan 10; **272**(2):894-902.

Tsukita, S., Oishi, K., Sato, N., Sagara, J., Kawai, A., Tsukita, S. (1994) ERM family members as molecular linkers between the cell surface glycoprotein CD44 and actin-based cytoskeletons. *J Cell Biol.* Jul; **126**(2):391-401.

Wainwright, D.M. (1998) Growth factor presentation by CD44 variant proteins. *Thesis,* Imperial College of Scienc, Technology and Medecine, London.

Wallach-Dayan, S.B., Grabovsky, V., Moll, J., Sleeman, J., Herrlich, P. Alon, R., Naor, D. (2001) CD44-dependent lymphoma cell dissemination: a cell surface CD44 variant, rather than standard CD44, supports in vitro lymphoma cell rolling on hyaluronic acid substrate and its in vivo accumulation in the peripheral lymph nodes. *J Cell Sci.* Oct; **114**(Pt 19):3463-77.

Wang, L.L., Richard, S., Shaw, A.S. (1995) P62 association with RNA is regulated by tyrosine phosphorylation. *J Biol Chem.* Feb 3; **270**(5):2010-3.

Watermann, D.O., Tang, Y., Zur Hausen, A., Jager, M., Stamm, S., Stickeler, E. (2006) Splicing Factor Tra2-{beta}1 Is Specifically Induced in Breast Cancer and Regulates Alternative Splicing of the CD44 Gene. *Cancer Res.* May 1; **66**(9):4774-80.

Weg-Remers, S. Ponta, H., Herrlich, P., König, H. (2001) Regulation of alternative pre-mRNA splicing by the ERK MAP-kinase pathway. *EMBO J*. **20**, 4194-4203

Weiss, A., Littman, D.R. (1994) Signal transduction by lymphocyte antigen receptors. *Cell.* Jan 28; **76**(2):263-74.

Weiss, L., Whitmarsh, A.J., Yang, D.D., Rincon, M., Davis, R.J., Flavell, R.A. (2000) Regulation of c-Jun NH(2)-terminal kinase (Jnk) gene expression during T cell activation. *J Exp Med.* Jan 3; **191**(1):139-46.

Weng, Z., Thomas, S.M., Rickles, R.J., Taylor, J.A., Brauer, A.W., Seidel-Dugan, C., Michael, W.M., Dreyfuss, G., Brugge, J.S. (1994) Identification of Src, Fyn, and Lyn SH3-binding proteins: implications for a function of SH3 domains. *Mol Cell Biol*. Jul; **14**(7):4509-21.

Wong, G., Muller, O., Clark, R., Conroy, L., Moran, M.F., Polakis, P., McCormick, F. (1992) Molecular cloning and nucleic acid binding properties of the GAP-associated tyrosine phosphoprotein p62. *Cell.* May 1; **69**(3):551-8.

Wu, S., Romfo, C.M., Nilsen, T.W., Green, M.R. (1999) Functional recognition of the 3' splice site AG by the splicing factor U2AF35. *Nature.* Dec 16; **402**(6763):832-5.

Xu, Q., Lee, C. (2003) Discovery of novel splice forms and functional analysis of cancer-specific alternative splicing in human expressed sequences. *Nucleic Acids Res.* Oct 1; **31**(19):5635-43.

Yamanashi, Y., Baltimore, D. (1997) Identification of the Abl- and rasGAP-associated 62 kDa protein as a docking protein, Dok. *Cell.* Jan 24; **88**(2):205-11.

Yao, X.M., Wang, C.H., Song, B.L., Yang, X.Y., Wang, Z.Z., Qi, W., Lin, Z.X., Chang, C.C., Chang, T.Y., Li, B.L. (2005) Two human ACAT2 mRNA variants produced by alternative splicing and coding for novel isoenzymes. *Acta Biochim Biophys* Dec; **37**(12):797-806.

Yu, Q., Toole, B.P., Stamenkovic, I. (1997) Induction of apoptosis of metastatic mammary carcinoma cells in vivo by disruption of tumor cell surface CD44 function. *J Exp Med.* Dec 15; **186**(12):1985-96.

Yu, W.H., Woessner, J.F. Jr., McNeish, J.D., Stamenkovic, I. (2002) CD44 anchors the assembly of matrilysin/MMP-7 with heparin-binding epidermal growth factor precursor and ErbB4 and regulates female reproductive organ remodeling. *Genes Dev.* 2002 Feb 1; **16**(3):307-23.

Zamore, P.D., Patton, J.G., Green, M.R. (1992) Cloning and domain structure of the mammalian splicing factor U2AF. *Nature.* Feb 13; **355**(6361):609-14.

Zhang, W., Sloan-Lancaster, J., Kitchen, J., Trible, R.P., Samelson, L.E. (1998) LAT: the ZAP-70 tyrosine kinase substrate that links T cell receptor to cellular activation. *Cell*. Jan 9; **92**(1):83-92.

Zhang, J., Salojin, K.V., Gao, J.X., Cameron, M.J., Bergerot, I., Delovitch, T.L. (1999) p38 mitogen-activated protein kinase mediates signal integration of TCR/CD28 costimulation in primary murine T cells. *J Immunol.* Apr 1; **162**(7):3819-29.

Zhou, Z., Licklider, L.J., Gygi, S.P., Reed, R.(2002) Comprehensive proteomic analysis of the human spliceosome. *Nature.* Sep 12; **419**(6903):182-5.

Zorio, D.A., Blumenthal, T. (1999) Both subunits of U2AF recognize the 3' splice site in Caenorhabditis elegans. *Nature.* Dec 16; **402**(6763):835-8.

Zorn, A.M., Krieg, P.A. (1997) The KH domain protein encoded by quaking functions as a dimer and is essential for notochord development in Xenopus embryos. *Genes Dev.* Sep 1; **11**(17):2176-90.

Abbreviations

BCR	B Cell Receptor
bp	base pair
bpv5	Branch point for exon v5
CD44	Cluster of Differentiation 44
CD44s	CD44 standard form
CD44v	CD44 variant form
CD44v1-v10	CD44 isoform expressing all variant exon sequences
CD44v3	CD44 isoform expressing v3 exon sequences
CD44v4-v10	CD44 isoform expressing v4 to v10 exon sequences
CD44v5	CD44 isoform expressing v5 exon sequences
CD44v6	CD44 isoform expressing v6 exon sequences
CD44v8-v10	CD44 isoform expressing v8 to v10 exon sequences
CoIP	Co-immunoprecipitation
ECM	Extracellular matrix
EMSA	Electrophoretic Mobility Shift Assay
ERKs	Extracellular signal-regulated kinases
GAPDH	Glyseraldehyde-3-phosphate dehydrogenase
GAPs	GTPase Activating Proteins
GEFs	Guanine nucleotide Exchange Factors
GST	Glutathione-s-transferase
GTP	Guanosine triphosphate
GSG (domain)	GRP33; Sam68; GLD-1
hnRNPs	Heterogeneous nuclear ribonucleoproteins
kDa	Kilodalton
KH (domain)	HnRNP K homology
L (subdomain)	Left subdomain of v5 exon
MAPs	Mitogen-activated protein kinases
MEKs	MAP kinase kinase
RNP-IP	Ribonucleoprotein immunoprecipitation
RT-PCR	Reverse-transcription followed by Polymerase Chain Reaction
Sam68	Src-associated substrate during mitosis (68 kDa)
SELEX	Systematic Evolution of Ligands by Exponential Enrichment
SF1/mBBP	Splicing Factor 1/mammalian Branch-point Binding Protein
SH2 (domain)	Src Homology 2
SH3 (domain)	Src Homology 3
STAR	Signal Transduction and Activation of RNA
TCR	T Cell Receptor
TPA	phorbol ester 12-O-tetradecanoyl-phorbol-13-acetate
U2AF	U2 snRNP Auxiliary Factor
U snRNAs	Uridine-rich small nuclear RNAs
U snRNPs	Uridine-rich small nuclear Ribonucleoproteins
wt	Wild-type
WW (domain)	Related to the two highly conserved tryptophane residues in this domain